JOURNAL OF ENVIRONMENTAL GEOGRAPHY
*Journal of Environmental Geography* 7 (3–4), 1–12.
DOI: 10.2478/jengeo-2014-0007
ISSN: 2060-467X

# PRELIMINARY CONTAMINATION RISK ASSESSMENT OF MINING WASTE USING SPATIAL ANALYSIS AND GEOCHEMICAL CHARACTERIZATION OF ROCK FORMATIONS. CASE STUDY IN HUNGARY

**Ahmed Abdelaal**

Department of Geology, South Valley University, 83523 Qena, Egypt
*Corresponding author, e-mail:ak_elmalt@yahoo.com

Research article, received 10 February 2014, accepted 01 April 2014

**Abstract**

The Mine Waste Directive (2006/21/EC) requires the risk-based inventory of all mine waste sites in Europe. The geochemical documentation concerning inert classification and ranking of the mine wastes requires specific field study and laboratory testing and analyses of waste material to assess the Acid Mine Drainage potential and toxic element mobility. The procedure applied in this study used a multi-level decision support scheme for the inert classification of waste rock material including: 1) expert judgment, 2) data review, 3) representative field sampling and laboratory analysis and testing of rock formations listed in the National Inert Mining Waste List, and 4) requesting available laboratory analysis data from selected operating mines. Based on a preliminary expert judgment, the listed formations were classified into three categories. A: inert B: probably inert, but has to be checked, C: probably not inert, has to be examined. This paper discusses the heavy metal contamination risk assessment (RA) in the Hungarian quarry-mine waste sites. In total 30 waste sites (including both abandoned mines and active quarries) were selected for scientific testing using the EU Pre-selection Protocol. Altogether 93 field samples were collected from the waste sites including andesite, rhyolite, coal (lignite and black coals), peat, alginite, bauxite, clay and limestone. Laboratory analyses of the total toxic element content (aqua regia extraction), the mobile toxic element content (deionized water leaching) carried out according to the Hungarian GKM Decree No. 14/2008. (IV.3) concerning mining waste management. A detailed geochemical study together with spatial analysis and GIS were performed to derive a geochemically sound contamination RA of the mine waste sites. Key parameters such as heavy metals, in addition to the landscape metric parameter such as the distance to the nearest surface and ground water bodies, or to sensitive receptors such as settlements and protected areas calculated and statistically evaluated in order to calibrate the RA methods. Results show that some of the waste rock materials, assumed to be inert, were found non-inert. Thus, regional RA needs more spatial and petrological examination with special care to rock and mineral deposit genetics.

**Keywords**: risk assessment, pre-selection, rock formations, spatial analysis, geochemistry, inert, mining waste

## INTRODUCTION

Mining has severe impacts on the environment, including contamination by toxic metals. In this context, Europe-wide survey identified wide-spread pollution problems caused by mining, abandoned mines in particular (COM, 2003). Since most of the elements used by the society come from mineral extraction (76 out of 90 frequently used elements), mining of mineral resources provide essential raw material for economic development (COM, 2005). Abandoned mines are more of a problem in areas with long historic mining like Europe, because mine closure practices have changed with time and environmental protection has not been considered for closed mines until recently (Jordan, 2004; Navarro et al., 2008). Apart from that abandoned mines are the same as active mines in terms of types of hazard and potential impact on the environment, their major problems are uncertainty in information and lack of control. Direct exposure to acid mine drainage (AMD) and sediments discharged from abandoned metal mines poses a serious hazard to aquatic biota and to humans (Peplow and Edmonds, 2005; Panagopoulos et al., 2009; Lei et al., 2010; Sarmiento et al., 2011). Younger et al. (2002) estimated that about 1,000 to 1,500 km of watercourses are polluted by metal mine discharges in the EU (estimate is for the former EU 15). There are an estimated 3 million potentially contaminated sites in the whole European Union, of which about 250,000 are actually contaminated and in need of remediation (EEA, 2007). Due to great volumes and slow chemical processes, mineralised rock in mine workings and in mine waste can release toxic compounds for a very long time on the scale of centuries and thousands of years (BAT, 2003). Thus, remediation of mine sites, including abandoned mines, has to consider long-term solutions and remediation technologies have to be sustainable for a long time (Sinding, 1999; Panagopoulos et al., 2009). Around the mine site, soils and surface water in the receiving environment are often contaminated with harmful elements or compounds (Puura et al., 2002; Sarmiento et al., 2011). These contaminated sites act as secondary sources for pollution, especially for historic sites (Jordan and D'Alessandro, 2004).

Significance of contamination risk posed by mining is highlighted by mine accidents (Jordan and D'Alessandro, 2004). Examples of such accidents are Wales, UK, in 1966, Stava, Italy, in1985, Aznalcollar, Spain, in 1998, Baia Mare, Romania, in 2000 and most recently the catastrophic release of 850 million cubic meters of alkaline (pH >13) caustic red mud through the failed dam of the Ajka alumina plant depository on October 4, 2010 in Kolontar, Hungary, resulting in loss of lives and contamination of agricultural lands (Jordan et al., 2011). Limited financial resources restrict remediation of sites at regional scale, therefore, there is a strong need to develop methodologies that rank sites based on risk magnitude, rather than to produce absolute estimates of health/ecological impacts, or to prioritize the remediation actions (Long and Fischhoff, 2000; Marcomini et al., 2009). U.S. EPA (2001) gives a detailed description of risk-based assessment of mine sites. The effort required to identify and prioritize contaminated sites in Europe is considerable (EEA, 2005). Moreover, as for the prioritization process, the Soil Thematic Strategy for soil protection (COM, 2006) and the EU Mine Waste Directive (2006/21/EC), point out the need to develop spatial risk-based methodologies for sustainable management of contaminated sites and mining waste sites at regional scale.

The EU MWD Pre-selection Protocol (Stanley et al., 2011) is applied for contamination risk assessment of mine waste sites (Abdaal et al., 2013). The protocol has a 'YES-or-NO' questionnaire and consists of 18 questions using simple criteria available in existing databases readily enabling the preliminary screening of the mine waste sites for environmental risk (Fig. 1). This screening should result in the elimination of those sites which do not cause or have the potential to cause a serious threat to human health and the environment from the inventory of waste sites. Since the pre-selection protocol meant not to involve field sampling or laboratory analysis, any level will be sufficient to pass the test and select the site for further investigation as a precautionary measure. In case of lack of knowledge or information, i.e. in the presence of uncertainty, an 'UNKNOWN' response is entered for the particular parameter which is the same as a YES response and the site is selected for further examination which is a precautionary position. In this study the mine waste sites included inside the rock formations and delineated as polygons' maps.

The geochemical documentation concerning inert classification and ranking of the wastes listed in the Inert Mining Waste List of the Hungarian Office of Mining and Geology involves the following procedures: 1) expert judgment, 2) data review, 3) representative field sampling and laboratory analysis of formations listed in the Inert Mining Waste List, and 4) requesting available laboratory analysis data from selected operating mines. Based on a preliminary expert judgment the listed formations classified into three categories. A: inert B: probably inert, but has to be checked C: probably not inert, has to be examined (Table 1). According to the Hungarian GKM Decree No. 14/2008 (IV.3) the mining waste classified to inert as if the content of substances potentially harmful to the environment or human health in the waste and in particular As, Cd, Co, Cr, Cu, Hg, Mo, Ni, Pb, V and Zn, including in any fine particles alone in the waste, is sufficiently low to be insignificant human and ecological risk, in both the short and long term, in order to be considered as sufficiently low to be of insignificant human and ecological risk, the content of these substances shall not exceed the thresholds values for geological medium and underground waters identified as not contaminated in relevant legal rules.

*Table 1* The inert-not inert classification of the listed rock formations based on preliminary expert judgment. A: inert B: probably inert, but has to be checked C: probably not inert, has to be examined. Number of waste sites and field samples for each rock group are shown.

| Rock group | Rock type | Number of waste sites | Number of samples | Inert-Not Inert ranking |
|---|---|---|---|---|
| Coal | Lignite | 2 | 10 | C |
| | Black Coal | 2 | 7 | C |
| Peat | | 4 | 9 | C |
| Alginite | | 2 | 5 | B |
| Bauxite | | 2 | 6 | B |
| Rhyolite tuffs | | 2 | 6 | B |
| Clay | Clay | 4 | 8 | A-B |
| | Bentonite clay | 1 | 1 | A |
| Andesite | | 10 | 37 | B |
| Limestone | | 1 | 4 | A |

A detailed geochemical study together with spatial analysis and GIS performed to derive a geochemically sound contamination RA of the mine waste sites in order to identify the current geochemical status of sampled rock materials from the 30 mine waste sites and to answer the question, if these waste rock materials (i.e. coal, peat, alginate, bauxite etc.) are still inert or non-inert. Distribution analysis applied to the median values of the elements As, Cd, Co, Cr, Cu, Mo, Ni, Pb, and Zn contents in order to find if there are any significant correlations between these elements to each other and to be compared to the local (country-specific) thresholds values for geological medium and underground waters in Hungary, in addition to the environmental limit values in Europe. The key landscape parameter, the distance from the waste sites (as centroid point of the formation polygon) to the nearest surface and ground water bodies, or to sensitive receptors (such as settlements and protected areas) was statistically calculated in order to evaluate the RA method (MWD Pre-selection Protocol, Fig. 1) and to identify local thresholds (median-based values of the measured distances from waste sites to the nearest pathways and sensitive receptors) more adopted the local conditions in Hungary.

The objective of this paper is to perform a pre-selection RA for selected rock types using the Geological map of Hungary as polygons, to evaluate the EU MWD Pre-selection Protocol (Stanley et al., 2011, Fig. 1) by applying it to real-life cases of 34 mines waste sites in Hungary. Three tests are carried out.

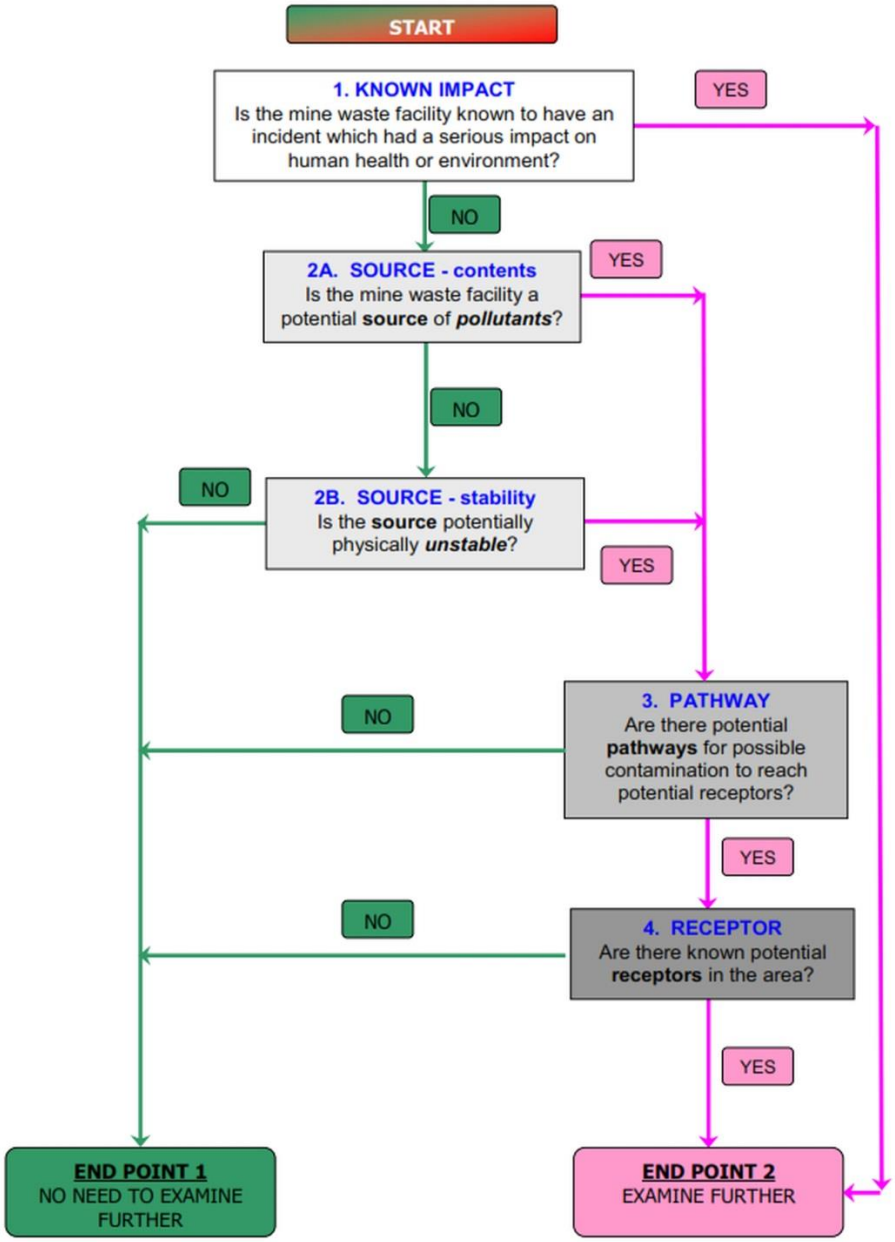


*Fig. 1* The EU MWD Pre-selection Protocol Flowchart (Stanley et al. 2011)

First, a detailed statistical and landscape metric analyses are carried out for the Protocol threshold values (e.g. stream line density inside the polygons, number of patches (settlement, lake, Natura 2000 sites and agricultural areas inside each polygon) and counting the polygon overlap areas between Natura 2000 sites and the rock formation polygons.

Second, altogether 93 field samples of different rock types, collected from the waste sites, were analysed for the total toxic element content (aqua regia extraction), the mobile toxic element content (deionized water leaching) on the base of Hungarian GKM Decree No. 14/2008. (IV.3) concerning mining waste management. This detailed geochemical study together with spatial analysis and GIS were performed to derive a geochemically sound contamination RA of the mine waste sites.

Third, A, B and C inert ranking system based on the expert judgment, has been applied for the rock types in the waste sites, which were compared to a simple risk-based ranking of the mine waste sites based on the specific geochemical analysis results of the waste samples.

## STUDY AREA

Altogether 30 waste sites of both abandoned mines and active quarries have been selected for scientific testing using the EU MWD Pre-selection Protocol (Fig. 2). 93 field samples have been collected from the waste sites including different rock samples such as; andesite, rhyolite tuffs, coal (lignite and black coals), peat, alginite, bauxite, clay and limestone according to the EuroGeoSurveys Geochemistry Expert Group Sampling Protocol (Fig. 3). Various wall rock and waste heap samples were collected for a detailed geochemical characterization.

The alginite mined in Pula site (NW Hungary, Fig. 2) originated from biomass of fossil algae during several millions of years in volcanic craters. Its organic material content is about 5-50% (Szabo, 2004). Gömöryová et al. (2009) reported that tests of alginite from the deposits in Pula and Gerce showed that it can be used in agriculture and forestry to improve soil quality, soil water dynamics and nutrient content, to increase organic matter content, colloid content and to protect soil against acidification, desiccation and leakage of nutrients (Vass et al., 2003).

In the power generation sector, coal is playing a dominant role in the EU with 25% share of the total installed capacity and almost one-third of the power generation (Kavouridis and Koukouzas, 2008). Coal resources in Hungary are in total 3,300 million tons (Mt) with annual production between 9-10 Mt (of which 8 Mt is lignite) (Perger, 2009). At this rate of use the reserves could last for centuries. Three types of coal in Hungary were sampled: 1) black coal in southern Mecsek Mountains (Lower Jurassic- Lias) is Hungary's only black coal reserve, calculated to be 198.8 Mt. Due to the complicated geological circumstances and the high cost of exploitation, production was stopped in 2004. 2) Brown coal was widely mined throughout recent decades through the Transdanubian Mountains with good quality Eocene and Oligocene coal, supplying a significant amount of Hungary's energy needs. Mining has virtually stopped due to economic reasons, with remaining reserves calculated to be 170 Mt. There is only one mine operating and supplying the Vértes Power Plant. Cretaceous coal exploitation in the region ended in 2004, after resources ran out. Poor quality Miocene reserves can be found in Northern Hungary. While all underground mining were ceased, small open-pit mines are still operating and exploitation can be extended. 3) Lignite represents about 90% of the Hungarian coal reserves, which means that lignite is first on the Hungarian conventional energy sources. While some Miocene lignite reserves ran out in the Transdanubian Mountains in 1996, about 3000 Mt of Miocene-Pliocene lignite can be found in Visonta, Bükkábrány (Northern Hungary) and Torony (Western Hungary) (Fig. 2). Recently, the Visonta and Bükkábrány sites were subject to vast open-pit mining supplying the Mátra Power Plant, while the Torony site remains practically untouched by any mining activity (Hamor-Vido, 2004). Peat was used as a fuel from early times in Europe. It was exploited intensively in agriculture and currently there is a renewed interest in the material because of its potential as a general source of hydrocarbons and other more particular organic raw materials used industrially. Peat was invariably found with significant moisture content at the surface of the ground, within a depth of 2-15m (Spedding, 1988). Number of significant articles were published on different aspects of peat and its use (e.g. Del-Rio et al., 1992; Steinmann and Shotyk, 1997; Charman, 2002).

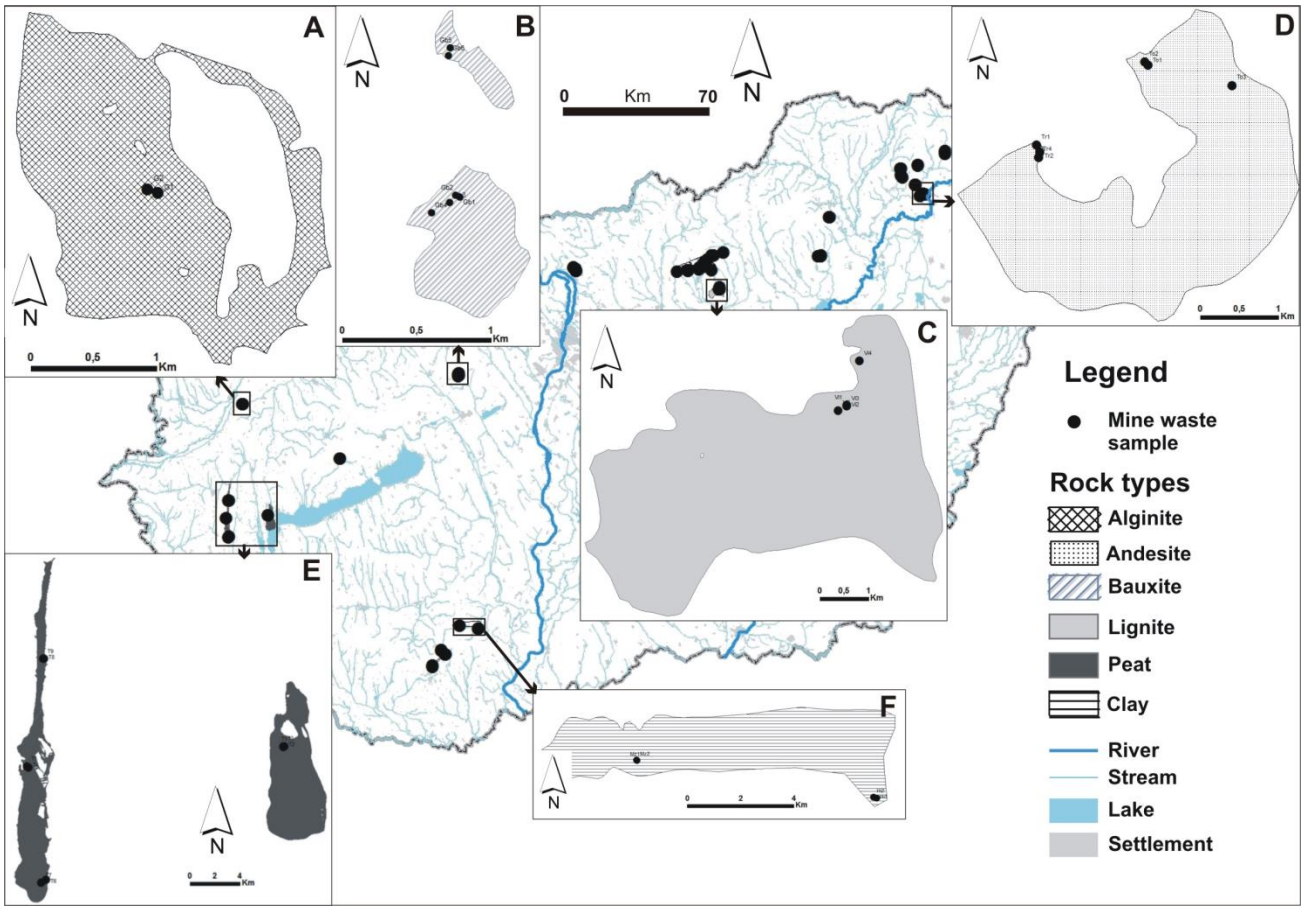


*Fig.2* Examples of rock formations (as polygons) and locations of field sampling from abandoned mines and active quarries in Hungary. A) Pula Alginite Formation, B) Gant Bauxite Formation, C) Lignite Formation at Visonta, D) Andesite Formation in the TokajMts., E) Peat formation at Pölöske, F) Clay Formation at Maza

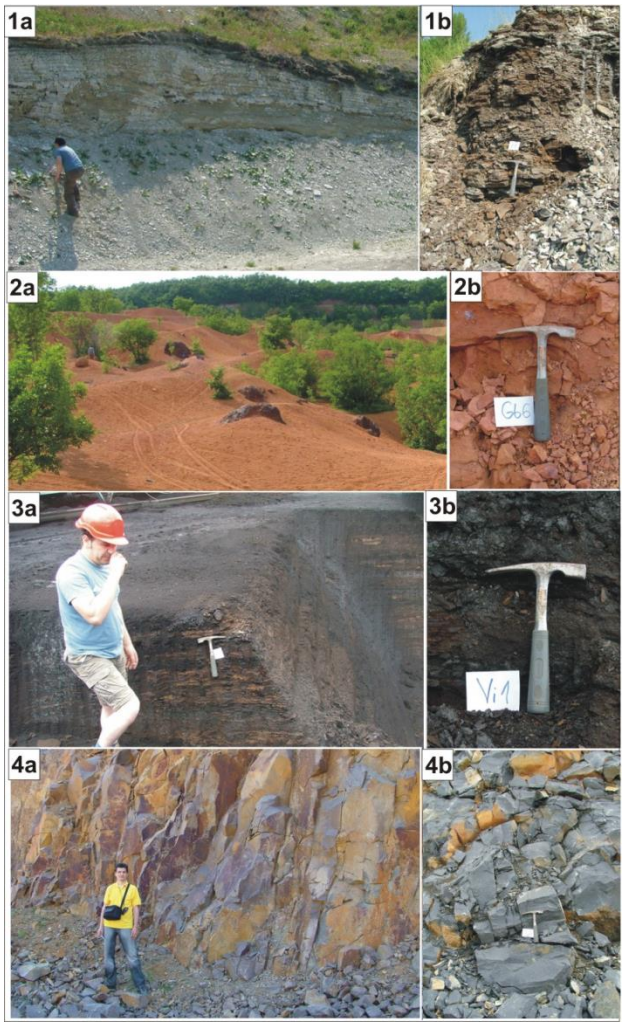


*Fig.3* Field sampling for the EU Mine Waste Directive Inert waste testing and characterization in Hungary
1a and b. Alginite sampling in Pulla; 2a and b. Bauxite sampling in Gant; 3a and b. Lignite sampling in Visonta; 4a and b. Andesite sampling in Tokaj. See Fig.1 for sampling locations

## MATERIALS AND METHODS

### *Sampling*

This study used a multi-level decision support scheme including a representative field sampling and laboratory analysis of formations listed in the Inert Mining Waste List and requesting available laboratory analysis data from selected operating mines. Altogether 93 samples have been collected according to the EuroGeoSurveys Geochemistry Expert Group Sampling Protocol from 30 mine-quarry waste sites along Hungary (Fig. 2). Rock types and locations of samples are as follow: coal (10 lignite samples from Visonta and Bükkábrány sites and 7 black coal samples from Pécs-Vasas mine sites); 9 peat samples from Pölöske, Hahót and Alsopatak sites; 5 alginite samples from Pula and Gérce sites; 6 bauxite samples from Gánt site; 8 clay samples from Máza, Miskolc and Vác sites and one bentonite clay sample from Mád site; 37 andesite samples from Recsk, Tokaj, Komló, Tállya, Sárospatak and Tarcal mine sites; 6 rhyolite tuffs samples from Gyöngyöslymos and Felsoabasár sites and 4 limestone samples from Vác mine site (Fig. 2, Table 1). Selection of the samples at the site depends on the location of each sample, (e.g. lignite includes wall, overburden and waste samples), and on the rock type (mineral composition), (e.g. oxi-andesite and pyrite andesite samples were collected). The collected two kilograms of samples were always composed of three sub-samples located at a minimum of 10m distance and at any sudden change in the color of waste rock, a new sample was collected (Fig. 3).

### *Laboratory analysis*

Laboratory analysis of the collected 93 field samples is carried out for the total toxic element content (aqua regia extraction) and the mobile toxic element content (deionized water leaching) at the Geological and Geophysical Institute of Hungary (MFGI) and 70 samples were selected for the analysis of different forms of sulfur (sulfuric acid potential) are carried on the ISD DUNAFERR laboratory at Dunaujvaros on the base of Hungarian GKM Decree No. 14/2008. (IV.3) concerning mining waste management. Samples were analyzed for total toxic element content (aqua regia extraction), the mobile toxic element content (deionized water leaching) with ICP-OES. Samples were air-dried, crushed in an agate mortar, passed through disposable sieve of 100 mesh, and digested by aqua regia with $HNO_3$, HCL and $H_2O_2$ under the ISO 11466 procedure (International Organization for Standardization 1995). All materials used during analytical determinations were kept in Teflon or other metal-free containers. To check the quality of preparation and analysis, replicate determinations were performed on approximately 25% of samples. Total element content of As, Cd, Co, Cr, Cu, Mo, Ni, Pb, V and Zn was defined by a mixed acid microwave unit digestion while deionized water leaching (pH=7) was performed to estimate the mobility of toxic elements in relative percent of total concentration.

### *Spatial data*

Two types of data were used in this study. Waste site data includes (1) location of mines waste sites as polygons (*Fig. 2*), (2) composition of the mine waste including sulphides, toxic metals, and dangerous processing substances (Q2-Q3), (3) geometry of the waste site area (Q8) and slope of foundation (Q10), and (4) other data such as presence of impermeable layer beneath the waste site (Q12), and if the site is uncovered and thus the waste is exposed to wind or direct contact (Q13-Q14). Information on the mine waste site engineering design was obtained from mine archives, aerial photos and field studies. Spatial data include topographic data of location of settlements as polygons, surface water courses (streams and lakes).

Slope data calculated from the Hungarian national contour based military DDM 50m grid using ArcGIS 10® software (Fig. 4). Then polygons of the rock formations added as overlay layer to the slope map in raster format using Spatial analysis tool in ArcGIS 10®. The slope value for each rock formation polygon (in degrees)

was counted as an average value from all pixels inside the polygon. Census data for 2009 is available from the Hungarian Central Statistical Office. Data on the national protected areas (Natura 2000 sites) and the location and status classification of groundwater bodies in Hungary under the Water Framework Directive (WFD) were obtained from the Hungarian Central Directorate of Water and Environment (VKKI) and from EEA website (Waterbase-Groundwater datasets). Land use/land cover data (LULC) maps at 1:100,000 scale were obtained from the European CORINE Land Cover website.

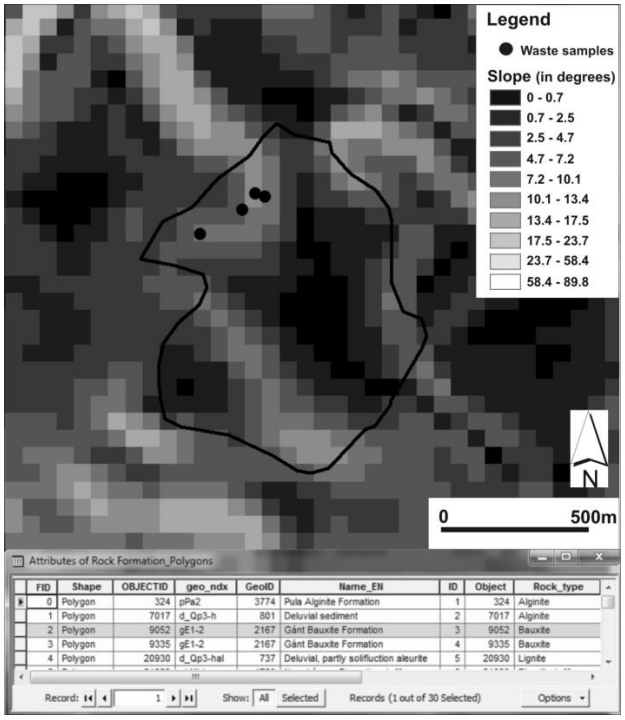


*Fig.4* Calculation of the topographic slope for the sampled rock formations (as polygons) using the national contour-based spline-interpolated military 50m grid DEM. The same DEM is used for question Q10 of the EU Pre-selection protocol on the topographic slope below the mine waste site. Polygon highlighted is this example delineates the Gant Bauxite Formation including Bauxite samples from Gant bauxite mine

In order to identify if there is a high permeable layer beneath the mine waste site (Q12), a surface permeability map for the geological formations of the 1:100,000 surface geological map of Hungary has been constructed using ArcINFO® 10, on the basis of the physical and geochemical characteristics of the uppermost rock units. Three classes were distinguished (Fig. 5). Low-permeability formations (clay and other impermeable rocks), formations with medium-permeability (loess, sand-gravel and fractured metamorphic and volcanic rocks) and with high-permeability (karstified limestones and dolomites belong to this group). An example for the high permeability rock class is the Alginite Formation in Gérce Mining Area, NW Hungary (Fig.5). Polygons of the mines waste sites derived from the CORINE land cover 1:50,000 map (2000) were overlaid by Google Earth® aerial photographs (2013), in order to identify if the material within the mine waste sites is exposed to wind or not (Q13) or covered or not (Q14), (Fig. 6).

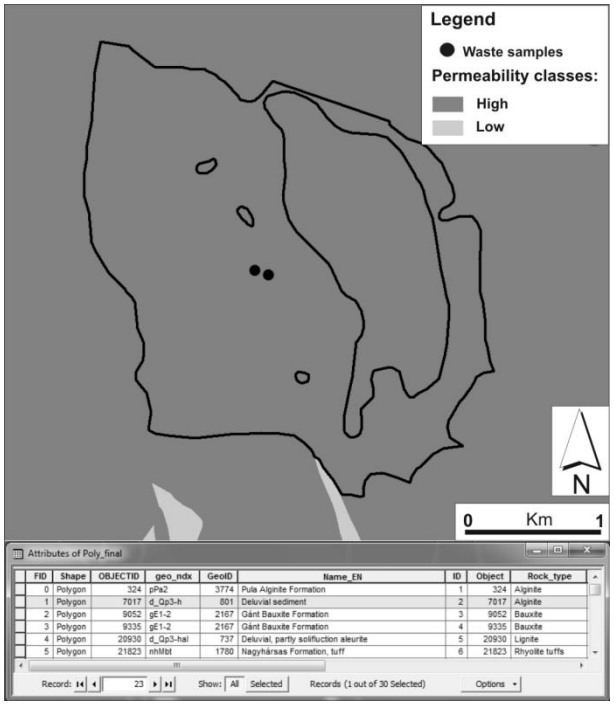


*Fig.5* Surface permeability map developed to answer question Q12 of the EU MWD Pre-selection Protocol if there is a high permeable layer beneath the mine waste site. Ploygon highlighted is an example for the Alginite Formation at the Gérce Mining Area, NW Hungary. See text for details.

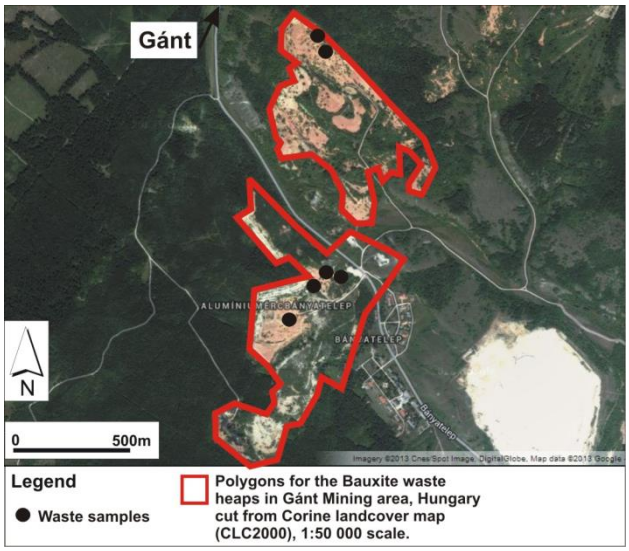


*Fig.6* Polygons of the mine waste sites defined from the CORINE land cover map (CLC 2000) overlaid by Google Earth® aerial photographs (2013) to answer EU Pre-selection Protocol questions Q13 and Q14 on the air and direct contact pathways related to the cover of waste heaps, respectively. An example shows the Bauxite waste heap in Gánt Mining Area, Hungary.

In this study the mine waste sites were included inside the rock formations and delineated as polygons using ArcGIS 10® software (Fig.2). Altogether 30 mine-quarry waste sites both abandoned mines and active quarries, were selected for scientific testing using the EU MWD Pre-selection Protocol (Stanley et al., 2011; Fig. 1). Then, by running the protocol, the number of YES, NO and UNKNOWN responses are registered for each site.

The proportion of the certain to uncertain responses for a site and for the total number of sites may give an insight of specific and overall uncertainty in the data we use (Table 2). The distance from mine-quarry waste sites to the nearest receptors such as human settlements (Q15) is measured using Proximity Analysis tools (Point Distance and Generate Near Table) in ArcINFO® 10 (Fig.2).

*Table 2* Summary statistics of the EU Pre-selection Protocol responses of questions Q1-Q18, showing the number of YES, NO and UNKNOWN responses (U) based on the EU thresholds

| EU Pre-selection Protocol | | Number of sampled sites | EU thresholds | | |
|---|---|---|---|---|---|
| | | | YES | NO | U |
| Impact | Q1 | 30 | 0 | 30 | 0 |
| Source | Q2 | 30 | 12 | 18 | 0 |
| | Q3 | 30 | 14 | 16 | 0 |
| | Q5 | 30 | 0 | 30 | 0 |
| | Q8 | 30 | 30 | 0 | 0 |
| | Q10 | 30 | 21 | 9 | 0 |
| Pathway | Q11 | 30 | 16 | 14 | 0 |
| | Q12 | 30 | 21 | 9 | 0 |
| | Q13 | 30 | 18 | 12 | 0 |
| | Q14 | 30 | 18 | 12 | 0 |
| Receptor | Q15 | 30 | 26 | 4 | 0 |
| | Q16 | 30 | 22 | 8 | 0 |
| | Q17 | 30 | 19 | 11 | 0 |
| | Q18 | 30 | 28 | 2 | 0 |

Statistical analyses were carried out using STATGRAPHICS Centurion XV.II® software (*Table 3*), such as the topographic slope (Q10) and the measured distance to the nearest surface water courses (Q11), settlements (Q15), ground water bodies (poor status) (Q16), protected areas (Natura 2000 sites, Q17) and agricultural areas (Q18). Summary statistics of the analyzed heavy metal concentrations from the mine waste sites (Aqua regia leaching analysis) were compared to the local (country-specific) thresholds values for geological medium and underground waters in Hungary, in addition to the environmental limit values in Europe. Spearman's rank correlation is performed on the total concentrations of the analysed elements to determine the relationships and variance between elements in the studied rock samples. Moreover, the Ficklin Diagram is constructed for the sum of heavy metals Zn, Cr, Cd, Pb, Co and Ni against pH in the deionized water leaching (DW, Fig. 7).

## RESULTS AND DISCUSSION

The contamination RA according to the EU MWD Preselection Protocol is carried out using the EU thresholds (slope $\leq 5^{o}$ and 1 km distance and number of people in the nearest settlement $\geq 100$). The YES, NO and UNKNOWN responses of the EU MWD Pre-selection Protocol (Fig. 1) were registered and calculated for each question in Table 2. In this study each rock formation was treated as a waste site and projected in the map as one or more polygons (Fig. 2). Questions describe if the mine uses any dangerous chemicals in processing minerals (Q4), the geometry of the tailings lagoon height and area (Q6-Q7) and for the waste heap height (Q9) of the Pre-selection Protocol are not fit to the rock waste sites and were skipped in this study (Table 3). Out of 30 mine waste sites, none of sites have a documented incident (Q1, Jordan et al. 2011). In Q2, 12 sites with YES responses were producing waste with sulphide minerals, 18 sites have NO responses. While in Q3, 14 sites were producing minerals with toxic heavy metals. In Q5, all sites are waste heaps and none of sites are tailings la-

*Table 3* Class boundaries of the EU MWD Pre-selection Protocol parameters based on the natural-breaks found in the corresponding cummulative histograms. Class boundaries were used to define thresholds adapted to local conditions in Hungary

| Question | Class boundaries | Class-Range | Median of class | Median of all sites | Number of sites |
|---|---|---|---|---|---|
| Q10 | | Topographic slope below waste site (degree) | | | |
| | 1.-20 | 1.-20 | 10 | 10 | 30 |
| Q11 | | Distance to the nearest surface water course (m) | | | |
| | <1300 | 0-1280 | 188 | | 22 |
| | >1300 | 2219-5376 | 2861 | 631 | 8 |
| Q15 | | Distance to the nearest settlement (m) | | | |
| | 0 | 0 | 0 | | 14 |
| | >0<=1000 | 82-838 | 548 | | 12 |
| | >1000 | 1585-3319 | 2350 | 150 | 4 |
| Q16 | | Distance to the groundwater bodies of 'poor status' (m) | | | |
| | 0 | 0 | 0 | | 18 |
| | >=36 | 36-14717 | 5229 | 0 | 12 |
| Q17 | | Distance to the nearest Natura 2000 sites (m) | | | |
| | 0 | 0 | 0 | | 12 |
| | >0<=1000 | 158-713 | 286 | | 6 |
| | >1000 | 1072-5548 | 2416 | 224 | 11 |
| Q18 | | Distance to the nearest agricultural areas (m) | | | |
| | 0 | 0-861 | 0 | | 24 |
| | 59-2092 | 3688-3976 | 359 | 0 | 6 |

goon. In Q8, all 30 waste heap sites with YES responses are greater than 10,000 $m^2$ in surface area. The slope of the foundation upon which the waste heap rests is of concern with respect to stability. The greater the slope angle the greater the risk of waste heap failure. The EU threshold chosen is 1:12 which equates to 8.3% or a slope angle of almost 5°. Based on the slope values derived from the 50m DEM, 16 waste heap sites with YES responses are greater than or equal 1:12 ($5^o$) in slope (Q10). This shows that most of the sites were located in hilly areas. The use of the surface permeability map (Fig.5) developed to generate answers for Q12, resulted in 21 waste sites with YES responses and underlain by medium and high permeable layer, while 9 sites underlain by low permeable layers. When the mine waste site is covered and the original material is not accessible this means there is no direct contact with receptors. In Q13, 18 sites were exposed to the wind and 12 sites were not. While in Q14, 18 sites were uncovered and 12 sites were covered with water, vegetation, soil and forest (Fig.6).

For Q11, 16 sites are within 1 km distance to the nearest surface water bodies (streams and lakes). In Q15, 26 mine waste sites are within 1 km distance to nearest human settlements with >100 people, indicating that these sites require prime attention if settlement protection is the concern. In Q16, 22 sites are within 1 km distance to the groundwater bodies of less than good status. For Q17, 19 waste sites are within 1 km distance to the national protected Natura 2000 sites. 12 waste sites were located completely inside the Natura 2000 sites), this calls for immediate special attention if landscape protection is a priority. Moreover, in Q18, 28 waste sites are within 1 km distance to the agricultural areas including arable lands, pastures, heterogeneous and permanent crops, 24 sites are completely located inside the agricultural lands (Table 2).

Distribution analysis performed on the heavy metals (Table 3) identified various sub-groups in the parameter thresholds of the EU Pre-selection Protocol. For example, in Q10, altogether 30 waste sites have one class of topographic slope ranges from 1-$20^o$. This result suggests the median slope value of all waste sites $10^o$ as a natural threshold reflecting the local Hungarian conditions, instead of the original $5^o$ slope threshold. In Q11, 22 waste sites were located within distance 0-1280m to the nearest surface water bodies and 8 sites are within distance 2,219–5,376m. This shows that almost 73% of the mine waste sites are significantly (at the 90% confidence) closer (≤1280m) to receiving streams than the other sites, thus the 631m (medial value of all sites) threshold may better reflect the local topographic conditions for this question. In Q15, 14 waste sites were located directly inside the nearest settlement (distance=0), indicating that these sites require prime attention if settlement protection is the concern, 12 sites are within distance 82-838m to the nearest settlement and 2 sites are within distance 1,585-3,319m to the nearest settlement. This result suggests the distance 150m (medial value of all sites) as a local threshold for this question in Hungary. It is interesting that 18 waste sites lie directly above the groundwater bodies with 'poor status' (Q16) and 12 sites are located inside the protected Natura 2000 sites (Q17). While in Q18, 24 waste sites are located inside the agricultural areas (Table 3).

A preliminary risk-based site ranking is possible based on the EU thresholds (slope of almost $5^o$ and 1km distance) by counting and ranking the YES responses of the Pre-selection Protocol, and ranging in scores from 5 to 10. Obviously, if there is more than one hazardous material at the source or there are multiple contamination pathways and receptors the site has a higher risk. A simple risk ranking of the rock formations based on the YES responses in descending order as follows: black coal and peat (10 YES), alginite (9 YES), lignite and clay (8 YES), bauxite (7 YES), bentonite-clay (6 YES) and andesite and rhyolite tuffs (5 YES). In summary, after the existing pre-screening risk assessment of the mine waste sites in Hungary, 28 sites were directed to EXAMINE FURTHER based on the EU thresholds and two sites with no risk (one Bauxite site has no pathway and one Andesite site has no sensitive receptor).

Table 4 summarizes the estimated heavy metal concentrations from the mine waste sites (aqua regia extraction) with respect to the environmental limit values in Hungary and Europe. In case of central tendency expressed by the Median, the analyzed heavy metals are in descending order; Zn>V>Cu>Cr>Pb>Co>Ni>As>Mo>Cd. This result shows that Zn has the highest median (24.6 mg/kg) and Cd has the lowest Median (0.11 mg/kg). In case of spread expressed by IQR/Med (Interquartile range/Median), the heavy metals are in descending order; Ni>As>Cr>V>Pb>Co>Cd>Zn>Cu. It is obvious that Ni has the highest spread (5.11) and Cu has the lowest (1.11). While spread expressed by Range/Median, the heavy metals are in descending order; Ni>Cr>Mo>Co>Zn>Pb>As>Cd>Cu>V. Ni still has the highest spread (327.6) but in this case V has the lowest spread (8.42).

Total concentrations of heavy metals as defined by aqua regia extraction were compared to the environmental limit values in Hungary and to the European environmental geochemical background values based on the FOREGS European Geochemical Atlas (Table 4) as follow: the Mean of As (18.17 mg/kg) exceeds the tolerated limit in Hungarian soils (15 mg/kg) and exceeds the Mean value of EU FOREGS geochemical background value (10 mg/kg). At the same time, the Mean of Cd (0.33 mg/kg) is less than the tolerated limit in Hungarian soils (1 mg/kg) and exceeds the Mean of EU FOREGS (0.3 mg/kg). The Mean of Ni (61) exceeds the tolerated limit in Hungarian soils (40) and exceeds Mean of EU FOREGS (31). Moreover, the median of Cu (12.3) exceeds the median of EU FOREGS (12).

The Spearman's rank correlations depicted in Tables 5 and 6 were performed between each pair of the analysed heavy metals from the waste sites by aqua regia and deionized water leaching analyses, respectively. In contrast to the more common Pearson correlations, the Spearman coefficients are computed from the ranks of the data values rather than from the values themselves.

*Table 4* Summary statistics of heavy metal concentrations from the mine waste sites (aqua regia extraction in mg/kg) in respect to the environmental limit values in Hungary and the European Top Soil Baseline Values. Minimum (MIN), maximum (MAX), median (MED) and spread expressed as median absolute deviation (MAD), lower quartile (LQ), upper quartile (UQ), Interquartile range (IQR), Standard deviation (SD). Bold figures show those heavy metal concentrations higher than the environmental standard limits (i.e. the tolerated limit in Hungarian soils or EU FOREGS Geochemical Atlas baseline value for top soils).

| | As | Cd | Co | Cr | Cu | Mo | Ni | Pb | V | Zn |
|---|---|---|---|---|---|---|---|---|---|---|
| Min | **0.6** | **0.06** | 0.018 | 0.537 | 0.766 | **0.2** | 0.4 | 1.15 | 3 | 0.1 |
| LQ | 1.54 | 0.073 | 2.92 | 2.58 | 6.8 | 0.2 | 1.88 | 4.56 | 5.48 | 14.4 |
| Med | 3.93 | 0.117 | 5.12 | 8.11 | **12.3** | 0.2 | 4.79 | 7.08 | 18.4 | 24.6 |
| UQ | 14.3 | 0.22 | 9.98 | 21 | 20.5 | 0.2 | 26.4 | 14.3 | 38 | 46.1 |
| IQR | 12.76 | 0.152 | 7.06 | 18.42 | 13.7 | 0 | 24.52 | 9.74 | 32.52 | 31.7 |
| Max | **247** | 6.07 | **416** | 1185 | **573** | **24.3** | 1570 | 468 | 158 | 1690 |
| Mean | **18.17** | **0.33** | **19.92** | **56.24** | **34.16** | **1.08** | **60.89** | 23.4 | 28.91 | **84.28** |
| Range | 246.4 | 6.01 | 415.9 | 1184.4 | 572.2 | 24.1 | 1569.6 | 466.8 | 155 | 1689.9 |
| SD | 43.31 | 0.87 | 63.67 | 170.09 | 92.44 | 2.96 | 223.3 | 68.72 | 31.64 | 255.83 |
| MAD | 3.07 | 0.057 | 3.52 | 6.34 | 5.7 | 0 | 4.25 | 3.84 | 13.94 | 15.8 |
| Mode | 0.6 | 0.06 | 11.5 | | 13.9 | 0.2 | 0.4 | | 3 | 0.1 |
| Range/Med | 62.69 | 51.36 | 81.24 | 146.04 | 46.52 | 120.5 | 327.68 | 65.93 | 8.42 | 68.69 |
| IQR/Med | 3.24 | 1.29 | 1.37 | 2.27 | 1.11 | 0 | 5.119 | 1.37 | 1.76 | 1.28 |
| MAD/Med | 0.78 | 0.48 | 0.68 | 0.78 | 0.46 | 0 | 0.88 | 0.54 | 0.75 | 0.64 |
| Environmental standard values in Hungary and the European Top Soil Baseline Values (FOREGS Atlas) | | | | | | | | | | |
| Tolerated limit in Soils, Hungary | 15 | 1 | 30 | 75 | 75 | 7 | 40 | 100 | | 200 |
| EU FOREGS Min | <0.5 | <0.01 | <1 | 1 | 1 | <0.1 | <2 | <3 | | 4 |
| EU FOREGS Max | 220 | 14.1 | 255 | 2340 | 239 | 21.3 | 2560 | 886 | | 2270 |
| EU FOREGS Med | 6 | 0.145 | 7 | 22 | 12 | 0.62 | 14 | 15 | | 48 |
| EU FOREGS Mean | 9.88 | 0.28 | 8.91 | 32.6 | 16.4 | 0.94 | 30.7 | 23.9 | | 60.9 |

Thus they are less sensitive to outliers than the Pearson coefficients. Table 5 shows that all the elemental pairs of Aqua regia leaching (with bold figures) have strong correlations with each other which $P < 0.05$, for example Pb and Zn($r = 0.63$, $df = 93$, $P < 0.05$), and Ni and Pb ($r = 0.71$, $df = 93$, $P < 0.05$) etc. However, pairs such as Co/Mo, Cr/Mo, Cu/Mo, Mo/Ni, Mo/Pb and Mo/Zn show a weak correlation with each other ($P>0.05$). Table 6 shows that all the elemental pairs of deionized water leaching (with bold figures) have strong correlations with each other, for example between Co and Ni ($r= 0.8$). Moreover, pairs such as As and Cd, As and Pb, Cd and Cu, Cd and Pb, Co and Mo, Cr and Zn, Cu and Pb, Mo and Pb and Mo and Zn show a weak but significant correlation with each other ($p>0.05$). Strong correlations signify that each pair of elements may have common contamination sources. Further detailed studies of physico-chemical properties and metal associations are needed to ascertain these results.

*Table 5* The Spearman's rank correlation coefficients between concentrations of heavy metals from the waste sites (aqua regia extraction). Significant correlation coefficients are in bold; $\rho < 0.05$.

| | As | Cd | Co | Cr | Cu | Mo | Ni | Pb | Zn |
|---|---|---|---|---|---|---|---|---|---|
| As | | | | | | | | | |
| Cd | **0.45** | | | | | | | | |
| Co | **0.41** | **0.34** | | | | | | | |
| Cr | **0.37** | **0.39** | **0.72** | | | | | | |
| Cu | **0.42** | **0.42** | **0.77** | **0.66** | | | | | |
| Mo | **0.35** | **0.22** | -0.13 | -0.12 | 0.06 | | | | |
| Ni | **0.57** | **0.5** | **0.72** | **0.81** | **0.7** | 0.19 | | | |
| Pb | **0.5** | **0.58** | **0.61** | **0.57** | **0.6** | 0.09 | **0.71** | | |
| Zn | **0.31** | **0.39** | **0.86** | **0.61** | **0.71** | -0.17 | **0.57** | **0.63** | |

The Ficklin Diagram (adapted after Plumlee et al., 1999) showing the sum of heavy metals Zn, Cr, Cd, Pb, Co and Ni from deionized water leaching (DW) analysis is plotted against pH (*Fig.7*). Differences in the sum of the previous base metals have proven the most diagnostic in differentiating between different geologic controls. This diagram shows two groups as follow.(1) Coal, Lignite, Peat and Bauxite samples are distributed from acid-high acid to near-neutral environments, with low to extreme concentrations of dissolved metals. (2) Alginate, Andesite, Clay, Rhyolite tuffs and Limestone samples are distributed in near-neutral environments, with low to high concentrations of dissolved metals.

Multivariate analysis such as CA and PCA using the analysed trace elements could not identify significant groups of samples. This is not unexpected due to the heterogeneity of the sampled rock types. It seems that specific rock formations with ore minerals content, including pyrite with acid generation potential, such as some andesites and coals are distinct from the non-mineralised as shown by the Ficklin Diagram (Fig.7).

The relative mobility of heavy metals in the various sampled rock formations was calculated as the percentage of the mobile element content (deionized water leaching) to the total element content (Aqua regia extraction) for the 93 samples. Then the median value of these mobility percentages was calculated for each rock type (*Fig.8*). Results show in Black Coal samples, the relative mobility of the heavy metals reduced in the following order: Zn (30.7) > Co (29.5) > Ni (26) > V (11.2) > Cd (4.6) > Cu (2.3) > Pb (0.3) > As (0.27) > Mo (0.26). In Lignite samples, Mo (5) > V (4.6) > As (1.4) > Cd (1.2) > Zn (0.8) > Pb (0.5) > Co (0.3) > Ni (0.2) > Cu (0.16) > Cr (0.1). In Peat samples, Zn (31) > V (16) > Mo (6) > Cd (3) > As (2.5) > Co (1.3) > Pb (0.8) > Cu (0.7) > Cr (0.4) > Ni (0.3). In Bauxite samples, Mo (5) > Cd (0.7) > V (0.4) > As (0.3) > Co (0.11) > Pb (0.1) > Zn (0.06) > Cu (0.05) > Ni (0.03) > Cr (0.01). In Alginite samples, Mo (175) > V (2.1) > Cd (0.6) > As (0.2) > Pb (0.08) > Cu (0.04) > Ni (0.03) > Zn (0.025) > Co (0.02) > Cr (0.01). In Clay samples, Mo (8.7) > V (2.3) > Cd (1.8) > Zn (0.5) > As (0.4) > Pb (0.2) > Co (0.1) > Ni (0.07) > Cu (0.05) > Cr (0.04). In Andesite samples, Mo (5) > Cd

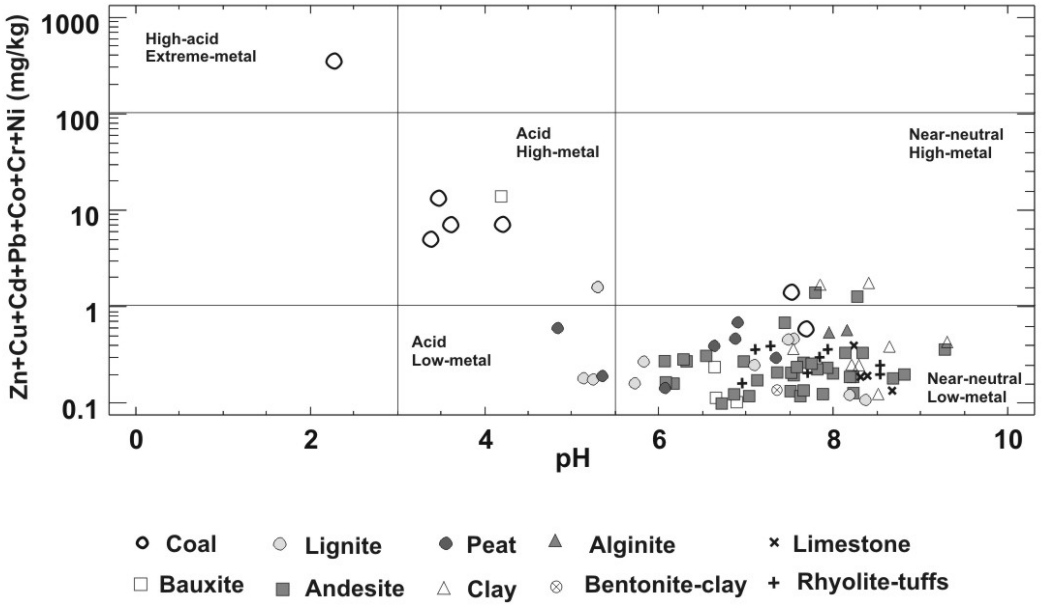


*Fig.7* Ficklin Diagram showing the sum of heavy metals Zn, Cr, Cd, Pb, Co and Ni plotted against pH in the deionized water leaching (DW). Note that acid generation potential (pH<5.5) is for coal, lignite and peat rocks, in addition to a bauxite sample. Elevated mobile heavy metal content is associated with coal, andesite and some clay and a bauxite samples. See text for details.

*Table 6* The Spearman's rank correlation coefficients between concentrations of heavy metals from the waste sites (deionized water leaching). Significant correlation coefficients are in bold; $\rho < 0.05$.

| | As | Cd | Co | Cr | Cu | Mo | Ni | Pb | Zn |
|---|---|---|---|---|---|---|---|---|---|
| As | | | | | | | | | |
| Cd | 0.12 | | | | | | | | |
| Co | **0.22** | **0.27** | | | | | | | |
| Cr | 0.03 | **0.25** | **0.26** | | | | | | |
| Cu | 0.17 | 0.16 | **0.35** | 0.18 | | | | | |
| Mo | **0.28** | 0.08 | -0.04 | 0.1 | **0.27** | | | | |
| Ni | **0.21** | **0.3** | **0.8** | **0.28** | **0.47** | 0.16 | | | |
| Pb | -0.04 | 0.14 | **0.31** | **0.24** | 0.14 | 0.01 | **0.26** | | |
| Zn | 0.14 | 0.02 | **0.27** | -0.04 | **0.47** | 0.11 | **0.35** | 0.12 | |

(4) > As (2.5) > V (1.6) > Ni (0.7) > Pb (0.6) > Zn (0.4) > Co (0.2) > Cu (0.15) > Cr (0.14). While in Rhyolite tuffs samples, V (16.6) > Mo (5) > Ni (4) > Cd (3) > As (2.3) > Co (2) > Zn (1.2) > Cr (0.8) > Cu (0.7) > Pb (0.2). It is obvious that Mo had the highest mobility in Lignite, Bauxite, Alginite, Clay and Andesite rock samples and Zn had the highest mobility in Black coal and Peat samples. While, V had the highest mobility in Rhyolite tuffs samples (Fig. 8).

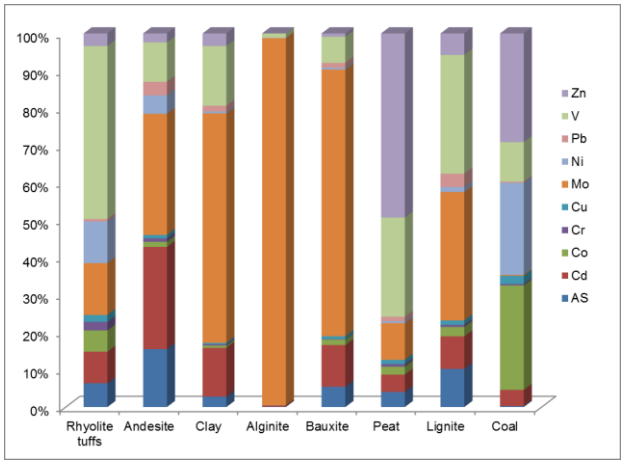


*Fig. 8* Distribution of the relative mobility (%) of heavy metals in the various sampled rock formations

Based on the expert judgment, the listed rock formations were classified into three preliminary categories. A: inert B: probably inert, but has to be checked C: probably not inert, has to be examined (Table 1). According to the geochemical analysis results in this study, coal (black coal and lignite) and peat samples are not inert and classified into group C which matches with the preliminary expert judgment. While alginite, bauxite, rhyolite tuffs and clay samples are probably inert and classified into B group which also matches with the preliminary expert judgment. Moreover limestone and clay samples are inert (A group). It is interesting to report that andesite samples are probably inert (B group) and according to our geochemical analyses, it was found that 5 andesite samples contain higher concentrations of the heavy metals Ni, Zn Cu, Cr and Co than the minimum, median and mean values of the Hungarian standards. While As is even higher than the maximum values of the national environmental standards. These results may suggest that those 5 andesite samples with higher heavy metal concentrations could classify the andesite rock formation into the B or C groups.

## CONCLUSIONS

This paper discusses the heavy metal contamination risk assessment (RA) in a selected group of the mine waste sites in Hungary. A detailed geochemical study together with spatial analysis using GIS was performed to derive a geochemically sound contamination RA of the mine waste sites. Key parameters such as heavy metals, in addition to the landscape parameter such as the distance to the nearest surface and ground water bodies, or to sensitive receptors such as settlements and protected areas are calculated and statistically evaluated in order to calibrate the RA methods.

In deionized water leaching, coal, lignite, peat and bauxite samples were located in one distinct group in the Ficklin diagram and distributed from acid to near-neutral region in the graph with low to extreme concentrations of dissolved metals. While alginate, andesite, clay, rhyolite tuffs and limestone samples were located in one group and distributed in the near-neutral region, with low to high concentrations of dissolved metals.

A simple risk ranking of the waste rock materials based on the YES responses to risk factor questions in descending order of risk resulted as follows: black coal and peat (10 YES), alginite (9 YES), lignite and clay (8 YES), bauxite (7 YES), bentonite-clay (6 YES) and andesite and rhyolite tuffs (5 YES). After the existing prescreening risk assessment of the studied waste sites in Hungary, 28 sites were directed to EXAMINE FURTHER based on the EU thresholds and two sites with no risk.

Results show that some of the waste rock materials, assumed to be inert such as the 5 andesite sites that contain higher concentrations of the heavy metals As, Ni, Zn Cu, Cr and Co than the minimum, median and mean values of the Hungarian standards. These results may suggest that those 5 andesite samples with higher heavy metal concentrations could reclassify the andesite rock formation into the B and C groups. Thus, regional RA needs further spatial and petrological examination with special care to rock and mineral deposit genetics.

### Acknowledgment

The Hungarian Scholarship Board (MOB-Grant) is gratefully acknowledged. A special thank is given to the reviewers for their useful comments. It is noted that this study has no relationship to the reported national inventory by any means and the site data used for this scientific study is not based on the reported inventory.

### References

Abdaal, A., Jordan, G., Szilassi, P. 2013. Testing Contamination Risk Assessment Methods for Mine Waste Sites. *Water, Air, & Soil Pollution* 224,1416. DOI: 10.1007/s11270-012-1416-x

BAT, 2003. Draft Reference Document on Best Available Techniques for Management of Tailings and Waste-Rock in Mining Activities, 2003. European IPPC Bureau, Joint Research Centre of the European Commission, Seville.

Charman, D. 2002. Peatlands and environmental change. J. Wiley & Sons, London & New York, 301 p.

COM 2003, 319 final. Proposal for a Directive of the European Parliament and of the Council on the Management of Waste from the Extractive Industries. COM(2003) 319 final, 2003/0107 (COD), Commission of the European Communities, Brussels.

COM 2005, 670 final. Communication from the Commission to the Council, the European Parliament, the European Economic and Social Committee and the Committee of the Regions - Thematic Strategy on the sustainable use of natural resources.

COM 2006, 231 final. Communication from the Commission to the Council, the European Parliament, the European Economic and Social Committee and the Committee of the Regions - Thematic Strategy for Soil Protection [SEC(2006)620] [SEC(2006)1165]. http://eur-lex.europa.eu/LexUriServ/LexUriServ.do?uri=CELEX:52006DC0231:EN:NOT

Del-Rio, J.C., Gonzalez-Vila, F.J., Martin, F. 1992. Variation in the content and distribution of biomarkers in two closely situated

peat and lignite deposits. *Organic Geochemistry*. 18(1), 67–78. DOI: 10.1016/0146-6380(92)90144-M

Directive 2006/21/EC the European Parliament and of the Council on the management of waste from extractive industries and amending Directive 2004/35/EC. Commission of the European Communities, Brussels.http://eur-lex.europa.eu/LexUriServ/LexUriServ.do?uri=CONSLEG:2006L0021:20090807:EN:PDF

EEA, European Environment Agency. 2007. Progress in the management of contaminated sites (CSI 015) - assessment published in August 2007.

EEA, European Environment Agency. 2005. Towards an EEA Europe-wide assessment of areas under risk for soil contamination, Vol. 2. Review and analysis of existing methodologies for preliminary risk assessment. http://sia.eionet.europa.eu/activities/reportste/PRAMS2

Gömöryová, E., Vass, D., Pichler, V., Gömöry, D. 2009. Effect of alginite amendment on microbial activity and soil water content in forest soils. Biologia 64(3), 585–588. DOI: 10.2478/s11756-009-0081-z

Hamor-Vido, M. 2004. Coal facies studies in Hungary: a historical review. International *Journal of Coal Geology* 58, 91–97. DOI:10.1016/j.coal.2003.05.003

Hungarian GKM Decree No. 14/2008. (IV. 3) concerning mining waste management. http://www.mbfh.hu/gcpdocs/201107/gkm_ministry_of_economy_and_transport_decree_no_14_2008_iv_3_on_minig_waste_management.pdf

International Organization for Standardization 1995. ISO 11466 International standard Soil quality –extraction of trace elements soluble in aqua regia. 03-01.

Jordan, G. 2004. Mining and mining waste: pressures, impacts and responses in the enlarged European Union. In: Jordan G, D'Alessandro M. (eds) Mining, mining waste and related environmental issues: problems and solutions in the Central and Eastern European candidate countries. Joint Research Centre of the European Commission, Ispra. LB-NA-20868-EN-C, 13-34.

Jordan, G., D'Alessandro, M. (eds). 2004. Mining, mining waste and related environmental issues: problems and solutions in the Central and Eastern European candidate countries. Joint Research Centre of the European Commission, Ispra. LB-NA-20868-EN-C.

Jordan, G., Fügedi, U., Bartha, A., Vatai, J., Tóth, G., Murati, J., Szentpéteri, I., Konya, P., Gaburi, I., Tolmács, D., Müller, T. 2011. The red mud catastrophe in Kolontár Hungary: applying geology. *European Geologist* 32, 9–13.

Kavouridis. K., Koukouzas, N. 2008. Coal and sustainable energy supply challenges and barriers. *Energy Policy* 36, 693–703. DOI:10.1016/j.enpol.2007.10.013

Lei, L.., Song, C.., Xie, X.., Li, Y., Wang, F,. 2010. Acid mine drainage and heavy metal contamination in groundwater of metal sulfide mine at arid territory (BS mine, Western Australia). Transactions of Nonferrous Metals Society of China 20, 1488–1493.

Long, J., Fischhoff, B. 2000. Setting risk priorities: a formal model. *Risk Analysis* 20, 339–352. DOI: 10.1111/0272-4332.203033

Luo, W., Lu, Y., Zhang, Y., Fu, W.,Wang, B., Jiao, W.,Wang, G.,Tong, X.,Giesy, J. P. 2010. Watershed-scale assessment of arsenic and metal contamination in the surface soils surrounding Miyun Reservoir, Beijing, China. *Journal of Environmental Management* 91, 2599–2607. DOI:10.1016/j.jenvman.2010.07.023

Marcomini, A., Suter II, G. W., Critto, A. 2009. Decision support systems for risk based management of contaminated sites. New York: Springer Verlag.

Navarro, M. C., Pérez-Sirvent, C., Martínez-Sánchez, M. J., Vidal, J., Tovar, P. J., Bech, J. 2008. Abandoned mine sites as a source of contamination by heavy metals: A case study in a semi-arid zone. *Journal of Geochemical Exploration* 96, 183–193. DOI:10.1016/j.gexplo.2007.04.011

Panagopoulos, I., Karayannis, A., Adamb, K., Aravossis, K. 2009. Application of risk management techniques for the remediation of an old mining site in Greece. *Waste Management* 29, 1739–1746. DOI: 10.1016/j.wasman.2008.11.017

Peplow, D., Edmonds, R. 2005. The effects of mine waste contamination at multiple levels of biological organization. *Ecological Engineering* 24, 101–119. DOI:10.1016/j.ecoleng.2004.12.011

Perger A. 2009. The role of coal in the Hungarian electricity sector. Short overview on the use of coal in the electricity sector. Energiaklub. http://energiaklub.hu/en/publication/the-role-of-coal-in-the-hungarian-electricity-sector

Plumlee, G.S., Smith, K.S., Montour, M.R., Ficklin, W.H., and E.L. Mosier, 1999. Geologic Controls on the Composition of Natural Waters and Mine Waters Draining Diverse Mineral-Deposit Types. In: L.H. Filipek and G.S. Plumlee (Eds.), The Environmental Geochemistry of Mineral Deposits, Part B: Case Studies and Research Topics, Reviews in Economic Geology Vol. 6B, Society of Economic Geologists, 373–432.

Puura E., Marmo L. and D'Alessandro M. (eds), 2002. Proceedings of the Workshop on Mine and Quarry Waste - the Burden from the Past. Joint Research Centre of the European Commission, Ispra.

Szabo, L.P. 2004. Characterization of alginite humic acid content. *Desalination*, 163, 85–91. DOI: 10.1016/S0011-9164(04)90180-4

Sarmiento, A. M., DelValls, A., Nieto, J. M., Salamanca, M. J., Caraballo, M.A. 2011. Toxicity and potential risk assessment of a river polluted by acid mine drainage in the Iberian Pyrite Belt (SW Spain). *Science of the Total Environment* 409, 4763–4771. DOI: 10.1016/j.scitotenv.2011.07.043

Sinding K., 1999. Environmental impact assessment and management in the mining industry. *Natural Resources Forum*, 23, 57–63. DOI: 10.1111/j.1477-8947.1999.tb00238.x

Spedding, P.J. 1988. Peat, review. *Fuel* 67, 883–900. DOI: 10.1016/0016-2361(88)90087-7

Stanley, G., Jordan, G., Hamor, T., Sponar, M. 2011. Guidance Document for A Risk-Based Selection Protocol for the Inventory of Closed Waste Facilities as required by Article 20 of Directive 2006/21/EC. February, 2011. http://www.geofond.cz/rroum/dokument/2011_GUIDANCE_DOCUMENT_PRE_SELECTION.pdf

Steinmann, P., Shotyk, W. 1997. Geochemistry, mineralogy, and geochemical mass balance on major elements in two peat bog profiles (Jura Mountains, Switzerland). *Chemical Geology* 138, 25–53. DOI:10.1016/S0009-2541(96)00171-4

Szabo, L.P. 2004. Characterization of alginite humic acid content. *Desalination* 163, 85–91. DOI:10.1016/S0011-9164(04)90180-4

U.S. EPA. 2001. Abandoned mine site characterisation and cleanup handbook. Denver. EPA530-C-01-001. http://www.epa.gov/superfund/policy/remedy/pdfs/amscch.pdf

Vass, D., Bublinec, E., Halás, L., Beláček, B. 2003. Overview of Pinciná alginite fertility. *Földtani Kutatás* 15, 75–80.

Younger P. L., Banwart S. A. and Hedin R. S., 2002. Mine Water. Hydrology, Pollution, Remediation. Kluwer Academic Publishers, Dodrecht.

Websites:

Hungarian Central Statistical Office. www.ksh.hu

Hungarian Central Directorate of Water and Environment (VKKI). http://www.vkki.hu

EEA website/ Data and maps/ Datasets/ Waterbase-Groundwater. http://www.eea.europa.eu/data-and-maps/data/waterbase-groundwater-6

CORINE Land Cover datasets. http://www.eea.europa.eu/publications/COR0-landcover

JOURNAL OF ENVIRONMENTAL GEOGRAPHY
*Journal of Environmental Geography* 7 (3–4), 13–19.
DOI: 10.2478/jengeo-2014-0008
ISSN: 2060-467X

# MAPPING FRESHWATER CARBONATE DEPOSITS BY USING GROUND-PENETRATING RADAR AT LAKE KOLON, HUNGARY

**Eszter Pécsi[1*], Orsolya Katona[1], Károly Barta[1], György Sipos[1], Csaba Biró[2]**

[1]Department of Physical Geography and Geoinformatics, University of Szeged, Egyetem u. 2-6, H-6722 Szeged, Hungary
[2]Directorate of Kiskunság National Park, Liszt F. u. 19, H-6000 Kecskemét, Hungary
*Corresponding author, e-mail: pecsi.eszter18@gmail.com

Research article, received 02 March 2014, accepted 13 May 2014

**Abstract**

Freshwater carbonate deposit, as a special phenomenon in the Danube-Tisza Interfluve, located in the centre of Hungary, is a significant geological heritage in the Carpathian Basin. At present there is not any applicable method to investigate the presence of carbonate layers in an undisturbed way, as neither vegetation nor morphological characteristics indicate unambiguously these formations. Ground-penetrating radar technology is widely used in various earth science related researches, and the number of applications is steadily increasing. The aim of the study was to determine the spatial extension of freshwater limestone using geophysical methods near Lake Kolon, Hungary. The lake, which is now a protected wetland area with opened water surfaces, was formed in the paleo-channel of the River Danube. Measurements were performed with the help of ground-penetrating radar, the results were calibrated by high spatial resolution drillings. Investigations have been made since 2012, and freshwater limestone was detected at several locations determining the more exact extension of the formation. Ground-penetrating radar proved to be an appropriate method to detect the compact and fragmented freshwater limestone layers in such an environment. However, based on the results the method can be best applied under dry soil or sediment conditions while the uncertainty of the results increases significantly as a matter of higher soil moisture. Further control measurements are necessary verified by several drillings in order to give an exact method to determine freshwater limestone.

**Keywords**: freshwater limestone, ground-penetrating radar, Lake Kolon, drilling

## INTRODUCTION

Freshwater limestone is a significant but unique geological formation (Philip, 1987) in the arid and semiarid areas around the World. It can be found in California, where besides geological research it is also used for building purposes (Goodfriend and Stipp, 1983). In Australia a vast amount of freshwater limestone has been formed, here wine is being cultivated on the surface (Johns, 1963). Similar formations have evolved in Iran and in Inner-Anatolia (Thomas et al., 1981; Gail et al., 2014).

In Hungary it has been mined since the Arpad era, it has been used for building purposes, which is being neglected nowadays. The reason may be the artificial improvement of building material, as well as the delivery made easier with the improvement of technology and logistics. Tálasi (1946) pointed out the usage of freshwater limestone during his ethnographical research in Danube-Tisza Interfluve. He emphasized in his study that freshwater limestone is being mined and made use of the same way as two centuries before. Since the 1970's environment protection has been given more emphasis, and the unique nature of freshwater limestone has been largely recognized as well. As a result, more and more people think that it is essential to gain thorough knowledge of this geological formation, because, it being a unique formation, it is part of our geographical heritage, and by studying it, we are able to understand the details of its formation process (Sümegi et al., 2013).

Despite the fact that the appearance of freshwater limestone is known in Danube-Tisza Interfluve, there is not any applicable method which would be able to prove its presence from either ecological or morphological characteristics.

The aim of this research is to border both the solid, compact and scattered freshwater limestone with help of ground-penetrating radar on two study areas. It was tried to determine the presence and deepness of freshwater limestone both with boreholes and with ground-penetrating radar. The results received by the ground-penetrating radar were calibrated with the drilling data, so it was able to border the extension of freshwater limestone on the study areas.

In order to find out the spatial extension of freshwater limestone, measurements with the help of ground-penetrating radar have previously taken place in Turkey (Selma, 2008). The main aim of this study was to determine the thickness of freshwater limestone with ground-penetrating radar on Turkish study areas, as well as to map the caves and joints in the limestone.

During the research several fissures and caves were located, and an accurate estimate was given about the deepness of freshwater dolomite.

Further ground-penetrating radar research took place in Denmark, but not on freshwater dolomite (Nielsen et al., 2004). During the measurements the geometrical characteristics of limestone structure were mapped. That way it is possible to forecast the possible behaviour of limestone layers, in case of seismic events. As a result, an important evaluation came to existence about contingencies concerning reservoirs on limestone surfaces.

A similar study took place in Germany; it's about to map limestone's structure (Asprion et al., 2000). The measurements proved that the ground-penetrating radar is particularly suitable for analyzing limestone, defining its geomorphological structure, and it provides help in defining the individual facies in the limestone structure.

The aim of this study is to prove that ground-penetrating radar is suitable to determine where this geological formation can be found and regardless of whether the freshwater limestone is compact or fragmented.

*Dolomite formation in the Danube-Tisza Interfluve*

The process of dolomite formation is probably most thoroughly described by Morrow (1982). The formation process is the thermodynamical transformation of dolomite, lasting from calcite to dolomite (Morrow, 1982; Jenei, 2007). It is pointed out that the two main influencing factors are the velocity of crystallization and the proportion of Ca/Mg. This lattest one can help the process if it is higher than 1.

Carbonates in the Danube-Tisza Interfluve have been given attention since the 1930's (Faragó, 1938). Formations and sedimentary rocks from the ice age and from the Holocene have been studied in the area and as part of these geological researches freshwater limestone has also been examined (Miháltz, 1938, Miháltz and Faragó, 1945). Besides the formation process the spatial extension of this phenomenon has also been pointed out. It was stated that carbonate rocks had been formed in loess and in small patterns near blown sand forms and in lakes' deeper carbonate sludge layers (Mucsi, 1963). It was also pointed out that the water level of several lakes is found lower than the groundwater level of the neighbouring territories, so the groundwater with different solute minerals inside is leaking towards the lakes helping the carbonate accumulation (Miháltz and Mucsi, 1964).

Later geochemical, paleontological and sedimentological research was made on this formation (Molnár and Kuti, 1978a). During the research the evolution conditions of freshwater limestone have been defined, the environmental conditions determining the evolution of freshwater limestone have been presented, the time interval, during which under the given environmental conditions this significant geological formation evolved, was restricted. Besides, they proved that during the evolution process evaporation is of immense importance, as the solute minerals can move closer to the surface of the soil (Molnár and Kuti, 1978b). They stated that sodic lakes include a vast amount of calcium, so the conditions are given to the formation of freshwater limestone. Via collected water samples it has been established that the proportion of $CO_3$/Ca is always higher than one, therefore the formation of dolomite can take place in the investigated area (Molnár and Jenei, 2006).

Several further publications can be found about pollen analytical, malacological, and sedimentological researches about the Kiskunság (Sümegi et al., 1991; Molnár and Botz 1996; Sümegi et al., 2005; Jenei et al., 2007; Sümegi et al., 2011).

These publications also mention several aspects of freshwater limestone around Lake Kolon. During these researches the picture about environmental conditions and their changes has been clarified as well. At the end of the ice age, a significant climate change took place, which induced several further changes, and thus enabled the formation of freshwater limestone in Kiskunság. The local accumulation of blown sand started at this period as well, this is today's bedrock level in Kiskunság (Sümegi et al., 2013). Eolic forms like hummocks, and parabolic dunes evolved in this period. Besides, they stated that the accumulation of chemical components necessary for the formation on freshwater limestone, like Ca and Mg, took place in sedimentary basins, and hollows between hills (Iványosi, 2013). The accumulation of carbonate sludge is very typical in the soils of the Danube-Tisza Interfluve and several carbonate resources are worth mentioning in this area (Fügedi et al., 2008; Molnár, 1980). One of them is the organic resource originated from fossil remains like snails and shells, which plays a significant part during formation. Another carbonate resource determining process is the changing ground water level and the capillary water lifting that is also an influential factor. In warm periods, the salts in the groundwater approach the surface with the steaming water, then they are evaporated. The rock hardening takes place in this period, along with the cementation of the accumulated carbonate sludge, which in this case, is a fast process, in which the periodical water cover is a determining factor. If there is a permanent water cover, then there is no possibility to dry surface and subsurface layers, so compact freshwater limestone is unable to be formed, only uncompacted carbonate sludge remains in the area (Sümegi et al., 2013).

## STUDY AREA

Lake Kolon is located in the middle of Hungary, in the Danube-Tisza Interfluve (Fig.1); it is the greatest and most significant freshwater swamp of the region. It is situated in north-western direction from the settlement Izsák, it is approximately 7 kilometers long and it is found 5-6 kilometers eastwards from the western border of Kiskunság Sand Back.

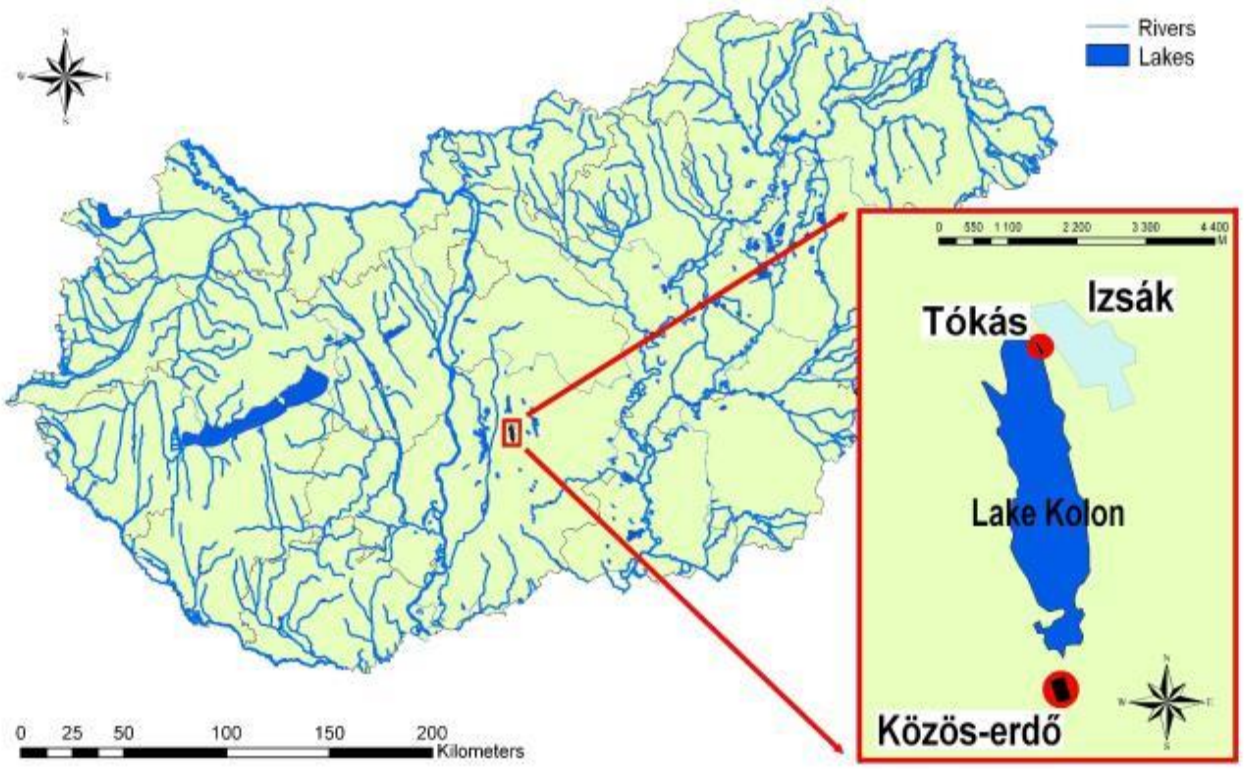


*Fig. 1* Location of Lake Kolon in Danube-Tisza Interfluve and the two sample sites

The lake and its environment are found in an excessively fragmented area. The area is divided into three geomorphological units:

- Bikatorok Hill and its environment (W from the lake) were formed by aeolian processes, elder fluvial sediments are buried by sand. The highest point of this area is Revecke Hill with height 120 m.
- Lake Kolon and its near environment are in the ancient Danube riverbed. Its shape's direction is north-south, the bed is gradually rising from west to the east.
- Sandy loess back near Izsák is a little bit higher surface formed by wind but with lower relief than Bikatorok.

Lake Kolon is part of the Kiskunság National Park and the marshlands and surrounding areas are strictly protected. The extension of the National Park exceeds 48.000 hectares, the lake itself is 2962 hectares from it.

Two sample sites have been appointed in the lake basin. The northern one so called "Tókás" (Fig. 1.) is located in the direct neighbourhood of Izsák, in the south-western direction, the north-eastern shore of Lake Kolon; as a natural meadow. The height difference between the highest and lowest points is 1.2 meter.

The second study area is situated on the southern part of Lake Kolon, near the ash-oak bog forest called "Közös-erdő". The study area is located on its margin as a swamp meadow with variable hydrological and ecological conditions from permanent water cover until steppe-like grasslands.

## MATERIALS AND METHODS

In order to map the freshwater limestone on the sample sites, first hand drill and the Pürkhauer sticking rod was applied. When it has reached the freshwater limestone, its deepness was measured from the surface, as well as its appearance (hooked, compact, etc.). Guessing from the occurrence of freshwater limestone based on its formation process, it was mapped with denser drilling network, but at the same time there were several control points on higher surfaces as well; so altogether on the northern area was made more than 100, while at Gulya-kút about 140 boreholes.

The digital elevation model (DEM) of the study areas was prepared in ArcGIS. With the help of DEMs it was possible to locate the territories more effectively, where freshwater limestone might have been formed with more probability. It can be found in lower relief, closed hollows, and under their concave slopes. That way it is possible to make impoundment on both sample sites, with combining drilling data with the ground-penetrating radar results.

In the sections between the point-like drillings it's possible to map freshwater limestone with the help of ground-penetrating radar. Ground-penetrating radar consists of a transmitter, a receiver and a control unit (Katona et al., 2013). Its operation is based on the transmitter emitting electromagnetic impulses, which has strong reflection from even surfaces and depending on electromagnetic characteristic of the investigated surface diffraction can occur (Jol, 2009). Electrical permittivity, magnetic permeability and electrical con-

ductivity determine the reflection of electromagnetic waves from objects in the investigated material. The reflected wave is being received by the receiver, after the registration the data, stored in digital form (Cardimona et al., 2000). Because of the measurement area of the ground-penetrating radar, it is not possible to give the locality with absolute precision, because the ground-penetrating radar transmits electromagnetic impulses in the subsurface layers forwards and backwards in 60° angle, sideward in 90° (Casa et al., 2000). The differences in the measured material can be determined based on the reflected signal amplitudes, frequency and phase.

The measurements were completed with 400 MHz antenna, in central frequency. On the northern shore of Lake Kolon altogether 7 ground-penetrating radar cross sections were registered and 6 ones on the southern sample site. Ground-penetrating radar segments were planned mainly through points, where during the previous drillings freshwater limestone has been found. Recording these points has been important because of the calibration with ground-penetrating radar.

First static correction was applied on the registered segments. After that, band pass filter was applied to remove noise. Migration steps were used to determine the velocity of electromagnetic wave in the different part of the investigation area. By analyzing the magnitude and frequency, it was possible to allocate the presence of freshwater limestone on the ground-penetrating radar map.

Ground-penetrating radar was used for the determination of limestone amounts on the previously allocated points based on samples taken from the soil. Altogether 5 segments and 25 soil samples have been collected. The carbonate content in the samples was determined with Scheibler calcimeter. In light of the results it is possible to border the territories where there is a high carbonate capacity in the soil. That way the ground-penetrating radar measurements can be calibrated with pedological properties, because both soil conditions and its physical characteristics influence the results of ground-penetrating radar measurements.

## RESULTS AND DISCUSSION

At "Tókás" freshwater limestone was found in 45 cases between 35 and 100 cm deep in the soil, while at 60 boreholes the presence of the formation is not detected. Besides at "Gulya-kút" freshwater limestone was found at 64 points, between 60 and 120 cm deep; at 55 points it was not detected the presence of freshwater limestone with drilling. Where its presence was not obvious, in these cases it is due to the soil being full of pieces of limestone and this condition inflicts same received signal like dolomite on the ground-penetrating radar map. These cases occurred 5 times on the north, and 10 times on the south. Based on the drillings, one can state that freshwater dolomite is not a continuous strata, but a fragmented phenomenon on the study areas (Fig. 2).

In order to eliminate the uncertainty, ground-penetrating radar measurements were calibrated with drilling results. On the deeper reliefs the drilling results unanimously proved, how the freshwater limestone might have been formed; this has been supported by the ground-penetrating radar research, according to which a more dominant signal can be detected on these points. Here the signal is stronger on the ground-penetrating radar map, but probably not because of the

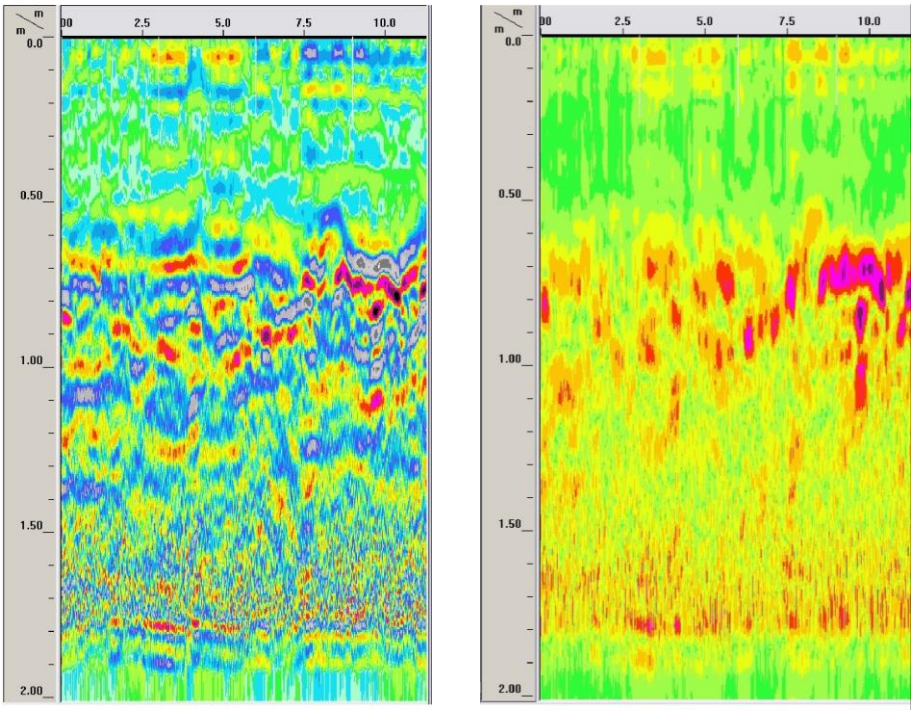


*Fig. 2* Ideal case: detection of freshwater limestone's presence based on the electromagnetic wave magnitude Left: compact limestone, right: fragmented limestone (2012)

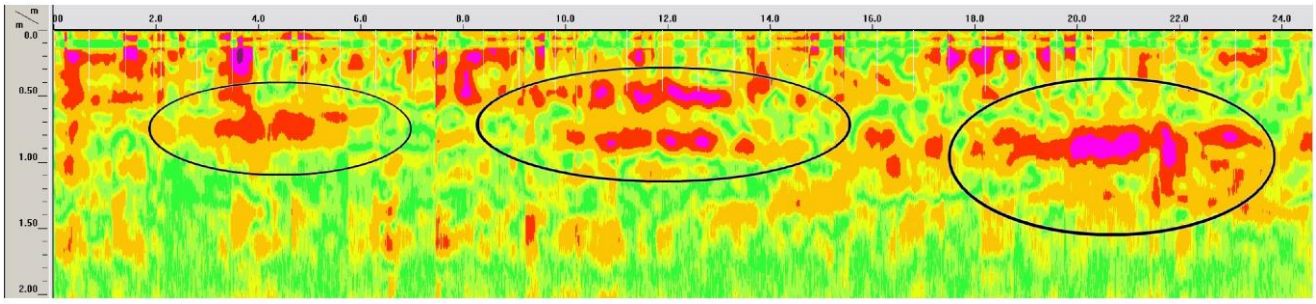

*Fig. 3* Calibrated on the basis of drilling data, ground-penetrating radar cross section recorded in dry period. There is fragmented formed limestone between compact layers (marked in black) (2012)

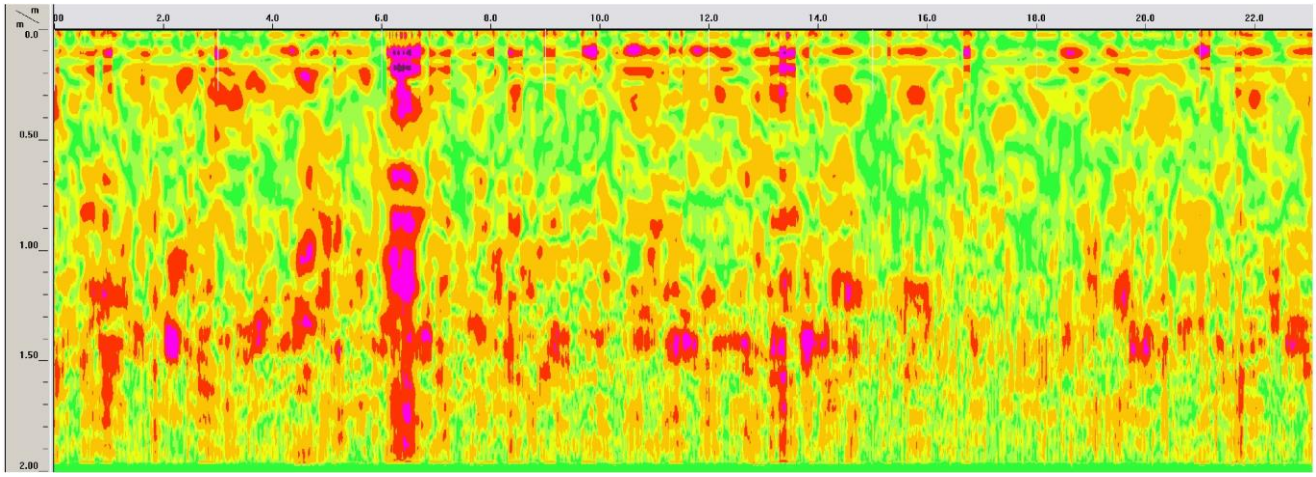

*Fig. 4* A ground-penetrating radar image received after rainfall in October 2013. Existence of freshwater limestone is not clear

physical characteristics caused by the high amount of limestone in the soil, but because of the presence of freshwater limestone. Nevertheless, on points, where based on the drillings, no dolomite can be found, the ground-penetrating radar still measured under surface discrepancies, this is due to the fragmented nature of the formation, along with the aforementioned high amount of carbonate, which on the northern sample ground collected from the given deepness, is 28,8%, while on the southern sample grounds 53%.

Previously, in autumn 2012 ground-penetrating radar research was conducted. This year it was examined after a long dry period, with deep groundwater. At this time it was possible to unequivocally determine the compact and fragmented limestone, it was not necessary to take into consideration the disturbing effect of high carbonate-content of the soil on the ground-penetrating radar maps (*Fig. 3*).

A year later measurements were made after a rainfall period with high groundwater (Autumn 2013). Although the high soil moisture content enhances the amplitude of the electromagnetic waves, it causes signal loss. Due to the signal loss interpreting the ground-penetrating radar segments proved to be difficult, therefore it wasn't possible unequivocally to determine the presence of limestone. In the deeper layer, during the set fortifications in the measurements the formations close to the surface are not reflected, so it is not possible to unequivocally border the freshwater limestone (*Fig. 4*).

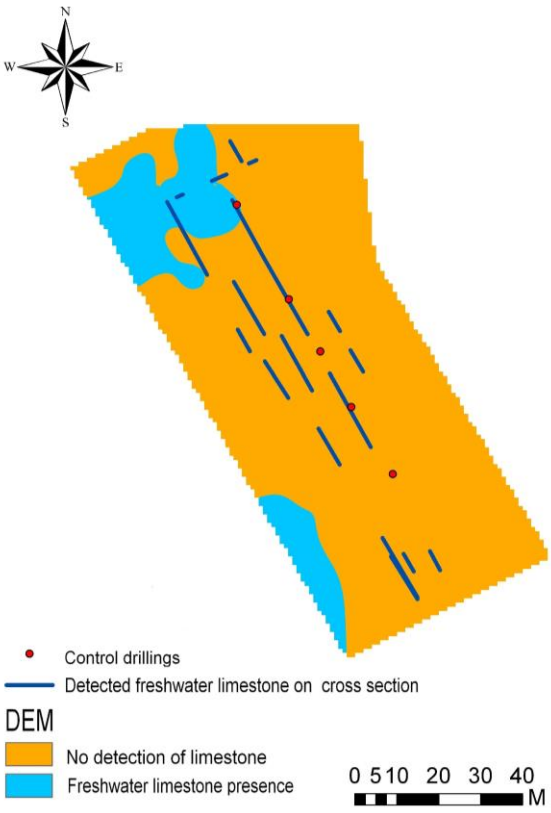


*Fig. 5* Results of the investigation in the northern study area (Tókás)

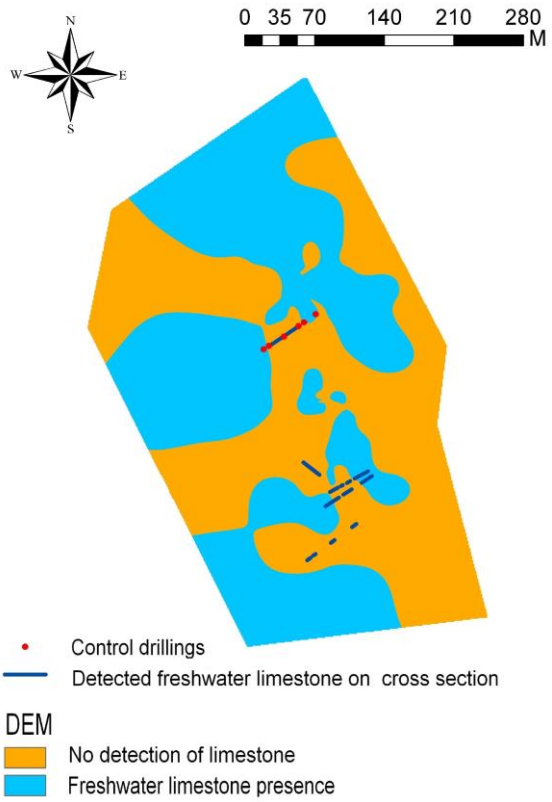


*Fig. 6* Results of the investigation in the southern study area (Gulya-kút)

## CONCLUSIONS

Ground-penetrating radar can be used to map freshwater limestone. It was established that high soil moisture content is not optimal environment for taking measurements; therefore it is worth taking into consideration the given environmental factors. The electromagnetic wave applied by the ground-penetrating radar, due to its characteristics, easily shows freshwater limestone on records on dry soil. The moisture content of the environment largely influences the measurements made by ground-penetrating radar. The moisture content reduces the penetrating deepness, as well as enhances value of the reflected electromagnetic wave's amplitude. Accordingly, although the reflected electromagnetic wave's amplitude is higher, it cannot be applied with such soil conditions, due to the quick absorption of the sign. Dry weather and deep ground water are preferable when making measurements. Therefore, it is advisable to conduct research in early autumn, or in summer, after a long rainfall free period, in order to avoid signal loss. In case of wet, clayey soil the signal loss might be significant.

With the help of ground-penetrating radar both compact and fragmented freshwater limestone can be traced, if the measurement took place during a dry period. Otherwise the ground-penetrating radar cannot clearly distinguish between freshwater limestone and high carbonated soil because of its characteristics. In this case it is worth combining research data with other methods, in order to specify the final results. It means that ground-penetrating radar can open new perspectives for mapping freshwaters limestone: the former point based mapping can be changed to linear mapping (*Fig. 5-6*) that gives us more adequate and faster method for determining its spatial extension.

## References

Asprion, U., Aigner, H., Aigner, T. 2000. An initial Attempt to Map Carbonate Buildups Using Ground-Penetrating Radar: an Example from the Upper Jurassic of SW-Germany. Erlangen (2000) 42, 245–252.

Cardimona, S., Webb, D. J., Lippincott, T. 2000. Ground Penetrating Radar. Department of Geology and Geophysics, University of Missouri-Rolla, Rolla, MO., 2–9.

Casa, A., Pinto, V., Rivero, L. 2000. Fundamentals of ground penetrating radar in enviromental and engineering applications. Annali di Geofisica, Vol. 43, N. 6, December 2000. Department of Chemistry, Petrology, and Geologycal Prospecting, Faculty of Geology, Univerity of Barcelona, Spain, 1091–1097.

Faragó, M. 1938. Nagykőrös környékének felszíni képződményei. *Földtani Közlöny* 68, 144–167.

Fügedi, U., Pocsai, T., Kuti, L., Horváth, I., Vatai J., 2008. A mészfelhalmozódás földtani okai Közép-Magyarország talajaiban. *Agrokémia és talajtan* 57/2, 239–260.

Gail, M. A., Carol, B., Manuel, D-R., Alyssa, M.K., Theresa, M.O., Rodinell, B. 2014. Freshwater Limestone In An Arid Rift Basin: A Goldilocks Effect. *Journal of Sedimentary Research* 84, 988–1004. DOI: 10.2110/jsr.2014.80

Goodfriend, G.A., Stipp, J.J. 1983. Limestone and the problem of Radiocarbon Dating of Land Snail Shell Carbonate. *Geology* 11, 575–577.

Iványosi Szabó, A. 2013. Csólyospálosi Földtani Feltárás Természetvédelmi Terület. In: Kustár, R., Balázs, R. (eds.) Talpalatnyi kő - elveszett emlékeink nyomában. A darázskő. Kiskunsági Nemzeti Park Igazgatóság, 13–22.

Jenei, M. 2007. Tavi karbonátképződés a Duna-Tisza közén. Doctoral (PhD) Theses. Szegedi Tudományegyetem Földtani és Őslénytani Tanszék

Jenei, M., Gulyás, S., Sümegi, P., Molnár, M. 2007 Holocene lacustrine carbonate formation: old ideas in the light of new radiocarbon data from a single site in Central Hungary. Radiocarbon 49/2, 1017–1021.

Johns, R.K., 1963. Limestone, dolomite and magnesite resources of South Australia. South Australia. *Geological Survey. Bulletin*, 38.

Jol, H. M., 2009. Ground Penetrating Radar Theory and Applications. *Elsevier Science*, 13–24.

Katona, O., Sipos, Gy., Fiala, K., Mezősi, G. 2013. A georadar működése és felhasználási területei, különös tekintettel a vízügyi gyakorlatra I. rész: működési elv, fontosabb alkalmazások. *Hidrológiai Közlemények* 93/ 4, 4–7.

Miháltz, I., Mucsi, M. 1964. A kiskunhalasi Kunfehértó hidrogeológiája. *Hidrológiai Közlöny* 44, 463–471.

Molnár, B. 1980. Hiperszalin tavi dolomitképződés a Duna-Tisza közén. *Földtani Közlöny* 120/1, 45–64.

Molnár, B., Botz, R. 1996. Geochemistry and stable isotope ratio of modern carbonates in natron lakes of the Danube–Tisza Interfluve, Hungary. *Acta Geologica Hungarica* 39, 153–174.

Molnár, B., Jenei, M. 2006. A Kiskunsági Nemzeti Park talaj- és felszíni vizek hidrodinamikai és hidrokémiai változásainak összefüggése a tavi karbonát képződéssel. *Hidrológiai Tájékoztató* 45, 57–59.

Molnár, B., Kuti L. 1978a. A Kiskunsági Nemzeti Park III. sz. területén található Kisréti-, Zabszék- és Kelemenszék-tavak keletkezése és limnogeológiai története. *Hidrológiai Közlöny* 58/ 5, 216–228.

Molnár, B., Kuti L. 1978b. A Kiskunsági Nemzeti Park III. sz. területén található Kisréti-, Zabszék- és Kelemenszék-tavak keletkezése és limnogeológiai története. *Hidrológiai Közlöny* 58/ 8, 347–355.

Morrow, D.W. 1982. Diagenesis I. Dolomite – Part 1. The geochemistry of dolomitisation and dolomite precipitation. *Geoscinece Canada* 9, 5–13.

Mucsi, M. 1963. Finomrétegtani vizsgálatok a kiskunsági édesvízi karbonát-képződményeken. *Földtani Közlöny* 93, 373–386.

Nielsen, L., Boldreel, L.O., Surlyk, F. 2004. Ground-penetrating radar imaging of carbonate mound structures and implications for interpretation of marine seismic data. American Association of Petroleum Geologists, *Bulletin* 88, 1069–1082.

Philip, D. ,Gingerich ,1987. Early Eocene Bats (Mammalia, Chiroptera) and other Vertebrates in Freshwater Limestones of the Willwood Formation, Clark's Fork Basin, Wyoming. Contributions from the Museum of Paleontology. The University of Michigan, 27/11, 275–320.

Selma, K. 2008. Photographing layer thicknesses and discontinuities in a marble quarry with 3D GPR visualisation. *Journal of Applied Geophysics* 64, 109–114. DOI:10.1016/j.jappgeo.2008.01.001

Sümegi, P., Gulyás, S., Törőcsik, T. 2013. A kiskunsági édesvízi mészkő és dolomitképződés folyamata a geológiai, a geokémiai és a környezettörténeti elemzések tükrében. In: Kustár, R., Balázs, R. (eds.) Talpalatnyi kő - elveszett emlékeink nyomában. A darázskő. Kiskunsági Nemzeti Park Igazgatóság, 25–86.

Sümegi, P., Molnár, M., Jakab, G., Persaits, G., Majkut, P., Páll, D. G., Gulyás, S., Jull, A.J.,T., Törőcsik, T. 2011 Radiocarbon-dated paleoenvironmental changes on a lake and peat sediment sequence from the central part of the Great Hungarian Plains (Central Europe) during the last 25.000 years. Radiocarbon 52, 85–97.

Sümegi, P., Mucsi, M., Fényes, J., Gulyás, S. 2005. First radiocarbon dates from the freshwater carbonates of the Danube–Tisza Interfluve. In: Hum, L., Gulyás, S., Sümegi, P. (eds.): Environmental Historical Studies from the Late Tertiary and Quaternary of Hungary. University of Szeged. 103–117. Szeged

Sümegi, P., Szöőr, Gy., Hertelendi, E. 1991. Palaeoenviromental reconstruction of the last period of the Upper Würm in Hungary, based on malacological and radiocarbon data. Soosiana, 19, 5–12.

Tálasi, I. 1946. Az Alföld néprajzi kutatásának kérdései és problémái In: Bartucz L. (ed) *Az Alföldi Tudományos Intézet Évkönyve* 1/1944-45, 1–35.

Thomas N. T., Robert M. O., Bruce H. W. 1981. Sr/Ca and Mg/Ca ratio sin polygenetic carbonate allochems from a Michigan marl lake. *Geochimica et Cosmochimica Acta* 45, 439-445. DOI: 10.1016/0016-7037(81)90252-0

JOURNAL OF ENVIRONMENTAL GEOGRAPHY
*Journal of Environmental Geography* 7 (3–4), 21–30.
DOI: 10.2478/jengeo-2014-0009
ISSN: 2060-467X

# GRAIN SIZE DISTRIBUTION OF STABILISED AEOLIAN DUNE SEDIMENTS IN INNER SOMOGY, HUNGARY

**Katalin Györgyövics*, Tímea Kiss, György Sipos**

Department of Physical Geography and Geoinformatics, University of Szeged, Egyetem u. 2-6, H-6722 Szeged, Hungary
*Corresponding author, e-mail: katalingy87@gmail.com

Research article, received 24 July 2014, accepted 15 September 2014

**Abstract**
In Inner Somogy the former researches concluded that the grain size of stabilised aeolian dunes decreases from north to south fitting to grain size distribution of the alluvial fan the dunes were built of and to the prevailing wind. However, the trend is not so evident, if considering the dune types and sand moving periods. The aim of this paper is to analyse the grain size distribution trends from the point of view of (1) different dune classes, (2) OSL age and (3) general morphological characteristics of the region. During the analysis the grain size distribution of 345 samples from 17 cores (120-300 cm in depth) was determined, and 15 OSL samples were dated. According to the results, the material of simple forms and level 1 dunes (these are the lowest dunes on the surface of the alluvial fan) becomes finer southward, in accordance with the structure of the alluvial fan and prevailing wind direction. Similar trend applies for level 2 dunes (which were formed on the top of level 1 dunes), but it does not apply for level 3 dunes, which are situated on the top of other dunes. It seems that the grain size is inversely proportional to the size of a dune and its age, thus younger and smaller dunes have coarser and less well sorted material. The sediments of the oldest, large parabolic dunes are the finest, younger, medium size parabolic forms have fine material, and the youngest hummocks contain the coarsest sand. The decreasing grain size towards south is the most apparent along longitudinal residual ridges, while within parabolic dunes the wings contain finer material than their elevated head.

**Keywords:** Inner Somogy, grain size distribution, aeolian sediment, parabolic dunes, sorting process

## INTRODUCTION

Grain size distribution analysis is one of the most commonly used methods in aeolian sand research (Bagnold, 1937; Lancaster, 1995; Zhu et al., 2014), therefore several techniques and scales were developed (Sahu, 1964; Wang et al., 2003; Blott and Pye, 2012). Aeolian sands are well sorted; the dominant grain size varies between 125-500 μm (Bagnold, 1937; Borsy, 1961). On dune heads, sediment is better sorted and finer than in interdune areas, the largest grains remain in deflation hollows (Zhu et al., 2014). On a sand area evolved by reworking an alluvial fan, the characteristics of the source material control the grain size, prevailing wind barely can modify it (Liu et al., 2014; Zhu et al., 2014); only sorting is improved through transportation (Zhu and Yu, 2014). Based on surface sediments from northern China, Nottebaum et al. (2014) determined that coarser aeolian grains appear more likely in lower elevations while finer sediments in higher elevations above sea level. Dunes of various ages in India show similar grain size distribution and consist mainly of fine sand (120-250 μm, Reddy et al., 2013).

Inner Somogy (southwest Hungary) was an alluvial fan of the Danube and its tributary, and the alluvial material was reworked by wind during the Neogene. Earlier researches investigated the grain size distribution of the alluvial sediments and aeolian sands too. Marosi (1970) separated fluvial and aeolian sands based on fauna remnants, cross-bedded sediment structure and surface characteristics of the single grains. According to his research, fluvial sediments of East Inner Somogy become finer from east to west and also from north to south (in accordance with the construction mechanism of alluvial fans). Thus, in the northern part 11% of the aeolian sediment is ≥1400 μm, while in the southern part its proportion is only around 2%. Also the distribution curve mode gradually shifted to the finer fractions towards the southern region (320-630 μm in north and 60-100 μm in south). Separating fluvial and aeolian sands applying electron microscope studies Lóki (1981) showed similar results. He noted that fluvial sediments of the northern region are coarser, as samples contain 50-60% of medium and coarse sand (>300-200 μm), and grains above 3000 μm were also found. In East Inner Somogy towards south, the proportion of the fine and very fine sand fraction (200-50 μm) gradually increases to 80%. The most common grain size is 320-100 μm, and 200-100 μm.

Increased proportion of fine particles towards south can also be detected in aeolian sands, as during the aeolian transport the sediment became sorted and

refined (Marosi, 1970). In northern areas, the proportion of fine sand fraction (60-100 µm) decreased in the aeolian sediments compared to alluvial fan material, since wind presumably blown it southward. In south, loessy sediments (≤60 µm) accumulated, the predominant fraction remained 100-200 µm, its proportion even increased from approx. 30% to approx. 50% (Marosi, 1970). In East Inner Somogy in the sand dunes the proportion of fine sand is larger than of medium sand (Lóki, 1981). During a sedimentological research Marosi (1970) derived results from regional average values and did not investigate grain size distribution differences of dune types. Lóki (1981) did not study the grain size distribution differences between different aeolian forms, however he described dunes on the leeward side of Marcali Loess Ridge covered by loessy-sand (20-50 µm: 15-25%), and therefore, concluded that sand movement was not continuous.

This research aimed (1) to study the sedimentological characteristics of dune classes identified in the region by Györgyövics and Kiss (2013); (2) to evaluate the grain size distribution changes within the whole sand dune area and within a single dune, and (3) to analyse the connection between aeolian material and OSL age of dunes.

## STUDY AREA

The most western sand dune area in the Carpathian Basin is Inner Somogy (3000 km2), situated on the south-western part of the basin between Lake Balaton and River Dráva (Fig. 1). During the Pliocene, the Danube and its tributaries flowed into the remnant of Pannonian Lake (Slavonian or Paludina Lake) and built an extensive alluvial fan (Ádám et al., 1981). Then as north of Inner Somogy, the Keszthely-Gleichenberg divide uplifted in the Late Pliocene (Pécsi, 1959) or Early Pleistocene (Ruszkiczay-Rüdiger et al., 2011), the Danube shifted northward and occupied its current west-east flow direction between Bratislava and Budapest (Borsy et al., 1969). Later even the smaller rivers abandoned the alluvial fan, thus aeolian processes reworked the surface during the Weichselian (Marosi, 1970). Throughout the more humid Holocene, sheetwash, gully and valley formation were widespread (Marosi, 1970). In the development of the area Sebe et al. (2010) emphasised the role of wind erosion and described the landscape as a complex yardang system, yet the age and process of sand dune formation and their possible Holocene modification was not studied in their work.

In the early twentieth century, Cholnoky (n.d.) described the area as a single, large blowout – residual ridge – hummock form. Later Marosi (1967, 1970) mapped several smaller blowout – residual ridge – hummock systems and identified superimposed dune generations. Lóki (1981) edited a large scale (1:100,000) geomorphologic map of the region, indicating complex dune systems, longitudinal ridges and blowouts. The latest research (Györgyövics and Kiss, 2013) identified large- and medium-size parabolic dunes with different degree of infilling, hummocks and wing fragments. The described forms occur as single dunes or as part of a three-level superimposed hierarchy system. From periglacial perturbation exposures inside the stabilised dunes, earlier researches (Pécsi, 1962; Marosi, 1870; Lóki, 1981) presumed widespread aeolian sand formation since Early Wechselian until Upper Pleniglacial. However, recent OSL measurements (Kiss et al., 2012) indicate to Late Glacial Dryas phases as the main active aeolian period, and local deflation events during the Preboreal and Boreal Phases, and human induced sand movements in the Subboreal Phase and in the 17$^{th}$-18$^{th}$ centuries.

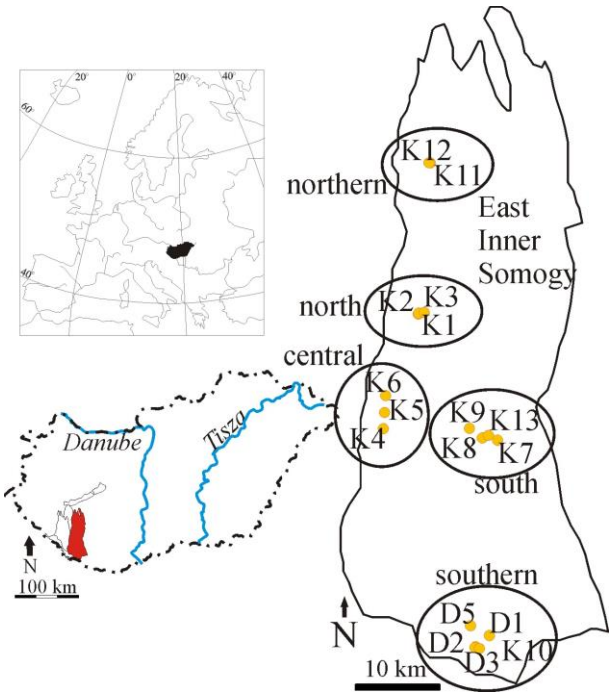


*Fig. 1* The study area is located in southwest Hungary, in East Inner Somogy. The sampling sites (K and D) were grouped based on their location within the region.

Nowadays the mean annual temperature is 10-11°C (TJan= -1°C, TJul= 20-21°C, Dövényi, 2010). The annual precipitation is 700-800 mm, 150-200 mm higher than in the other large sand dune areas on the Great Hungarian Plain. Prevailing wind direction is northwardly, however, south-westerly winds are also abundant. The predominant wind speed is 2.5-3.5 m/s which is not sufficient to trigger recent aeolian activity (Marosi and Somogyi, 1990). Human impacts date back to the Iron Age since the area has been populated (Zatykó et al., 2007). The natural hydrography has been severely modified by draining swamps, building canals and constructing fish-ponds. Only remote depressions are occupied by interdune lakes, marshes and alder-swamps. The natural vegetation of the area is hornbeam-oak forests with juniper, however on large areas agricultural activity dates back to centuries (Iványi and Lehmann, 2002).

## METHODS

Altogether 17 boreholes (120-300 cm deep) were drilled in Inner Somogy mainly on the heads of parabolic dunes. Samples were collected from every 10 cm for grain size distribution analysis. The sampling sites were chosen to include superimposed and simple dunes from each morphological class, and three boreholes from a single residual ridge. Meanwhile, to date the age of the aeolian forms samples were collected for optically stimulated luminescence (OSL) dating from the bottom of boreholes or at each 1.0 meter.

Grain size distribution analysis of the 345 collected samples was carried out by Analysette 22 MicroTec plus laser diffraction analyser. As the measurement range of the equipment is 0.008-2000 µm, particles larger than 2000 µm where removed by sieving, and percentage values were modified in accordance with fraction weight. Combined Udden-Wenthworth scale was used for classification (Blott and Pye, 2012). Profile figures were created in Tilia Graph where cluster analysis was also applied to facilitate the identification of zones and layers. The following statistical parameters were calculated according to the method of Folk and Ward (1957) in Gradistat (Blott and Pye, 2001):

- mode, which is the local maximum of the grain size distribution curve;
- mean (Mz), which is the arithmetic mean of the three thirds of the grain size distribution curve (Folk and Ward, 1957);
- grain size values at different cumulative percentages:
- $d_{25}$ is the lower quartile of the grain size distribution curve, thus it is the diameter which separates the finer 25% of the grain population from the coarser 75%.
- $d_{75}$ is upper quartile of the grain size distribution curve.
- $d_{90}$ is the diameter size from which 90% of all sizes are smaller and 10% is larger.

Based on the difference of the values of $d_{75}$ and $d_{25}$, the degree of sorting could be estimated. However, it is important to note, that this is not equal with sorting calculated as statistical standard deviation. In this case, the smaller difference between the values of lower and upper quartiles refers to better sorting.

In this research, grain size distribution variances of dunes in different hierarchy levels and morphometric classes were analysed. Based on mean (Mz) values the coarsest samples were chosen from each profile and only these were included in the regional comparison.

## RESULTS

The studied borehole profiles were classified according to the morphometric class of the dune they were deepened in. The most typical profile of each class is presented here in details, first the largest thus the oldest dunes will be introduced, and then the smaller and younger forms.

*Large parabolic dunes*

These are the largest dunes of the region; therefore they form the base of the dune association. They are 1-10 km long along the crest, located in the accumulational zones and sometimes superimposed on each other. Based on the degree of infilling (sediment supply) unfilled and partially filled subclasses were identified. They consist of several different sediment layers which indicate that these dunes were formed during more than one aeolian period. For example in the profiles of dune heads (D3, K12, K13) a coarser sand layer is intercalated by two finer sand layers, while on the windward slope (K8) and wing (D5) the finest grain size is at the bottom of the profile, and the grain size distribution gradually becomes coarser towards the surface.

The profile D3 was made in a head of a large parabolic dune. The samples contain 77% sand in average (Fig. 2), within the sand fraction the predominant grain size class is fine sand (34-56%). Based on grain size variation three zones were identified. The bottom zone I. (210-155 cm) contains some coarse sand (0.5-1.1%), the proportion of medium sand gradually decreases (from 41% to 14%), while fine sand increases from 34% to 56% ($d_{90mean}$ = 336 µm). Within this zone two layers of higher sand proportion were also defined. The grain size distribution of zone II. (155-65 cm) is relatively homogenous ($d_{90mean}$ = 335 µm), a peak (38%) in medium sand proportion (85-95 cm) divides it to three layers. In zone III. (65-30 cm) probably due to soil development processes, the silt and clay content increased (32-36%, $d_{90mean}$ = 280 µm), but well distinguishable layers were not found. Two OSL samples were dated from this profile. The age of the sample from 200-210 cm is 17.42±2.77 ka indicating Late Pleistocene sand movement when coarse grained sand was deposited ($d_{90mean}$ = 349 µm). The age of the upper sample (100-110 cm: 13.43±2.08 ka) indicates Late Glacial aeolian activity. The finer layers (I/2-4) between the two dated samples are probably paleosols developed in the Bølling and/or Allerød interstadials between the two dated stadials. The upmost zone was deposited during a younger aeolian phase; its homogeneity refers to fast sedimentation within a short aeolian activity period. The grain size distribution of profile K13 is slightly different, as it was dissected to three zones: the middle zone (95-175 cm) contains the coarsest sand ($d_{90mean}$ = 363 µm), the lower zone I. ($d_{90mean}$ = 332 µm) and upper zone III. ($d_{90mean}$ = 343 µm) are only slightly finer. This form is younger than the other dated large parabolic dunes, as its OSL age (K13/200-210 cm) indicates Preboreal aeolian activity (10.77±0.71 ka).

The D5 coring represents the material of the wing of a large parabolic dune. The sediment samples get coarser towards the surface (190 cm: $d_{90}$ = 218 µm, 70 cm: $d_{90}$ = 312 µm). OSL sample from 180-190 cm indicates 17.76±4.07 ka old sand movement, similar to the OSL sample of D3 profile at 200-210 cm. However this wing profile is much finer grained (D5/180-190 cm: $d_{90}$ = 218 µm, D3/200-210 cm: $d_{90,}$ =

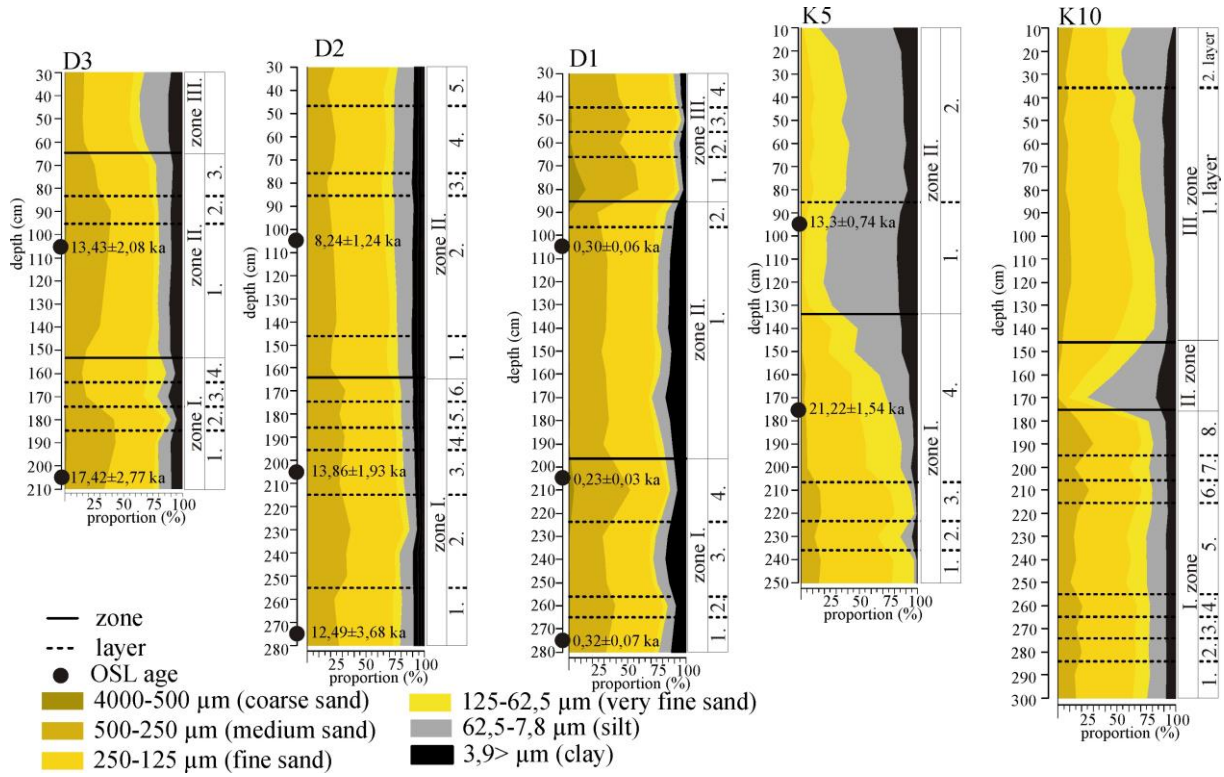


*Fig. 2* Grain size distribution of profiles from each morphometric class, where D3 represents the head of a large parabolic dune, D2 represents a medium-size parabolic dune, D1 is a head of a hummock, K5 represents a residual ridge and K10 a deflation hollow

349 µm). The material of the windward slope of a large parabolic dune (profile K8) also becomes coarser towards the surface (zone I. $d_{90mean}$ = 174 µm, zone II. $d_{90mean}$ = 243µm), similarly to profile K12 where medium sand proportion in zone I. is 4-13%, but in zone II. it rises to 17-39%. However, here a significant sand peak was also defined.

*Medium-size parabolic dunes*

Medium-size parabolic dunes are an order of magnitude smaller than the large parabolic dunes, as the length of their crest varies between 1.0 and 0.16 km. Some are located in the accumulational zones superimposed on the heads of large parabolic dunes; others are in the transportational-erosional matrix and often form a row of dunes perpendicular to the prevailing wind direction. Their degree of infilling (filled, partially filled, unfilled) indicates various amount of sand supply during their formation. Their material is more homogenous, as the profiles show less variation than of the large parabolic dune profiles. The minor differences among the samples refer to repeated aeolian activity. The fine-grained layers of some profiles (K7 and K11) possibly refer to weathering caused by ground water or to soil development processes. These forms are simple dunes without large elevation differences, thus the lack of superimposition allowed the ground water variations to have an effect on sediments. However, similar weathering processes cannot be detected in the material of the superimposed level 2 or level 3 dunes (profiles D2, K1 and K2) located in the accumulational zones.

D2 coring deepened into a filled medium-size parabolic dune in hierarchy level 3. The sand proportion of the samples is over 70% (Fig. 2), where fine sand fraction is the predominant (≥ 40%). Based on the variations of fine and medium sand proportions, two zones were defined. In zone I. (280-165 cm) the samples contains 25-36% ($d_{90mean}$ = 336 µm) medium sand fraction, while in zone II. (165-0 cm) only 17-25% ($d_{90mean}$ = 302 µm). Within the two zones, finer and coarser layers can be found. Three OSL samples were dated from this profile. Samples from 270-280 cm and 200-210 cm date back to the Late Pleistocene (12.49±3.68 ka and 13.86±1.93 ka). As all along zone I. the grain size characteristics are similar, all layers were probably deposited during Late Glacial sand movements. The D3/100-110 cm OSL sample revealed similar age (13.43±2.08 ka). The grain size distributions of the dated samples of the two profiles are similar (D2/200-210 cm: $d_{90}$ = 339 µm, D2/270-280 cm: $d_{90}$ = 321 µm, and D3/200-210 cm / $d_{90}$ = 349 µm), indicating identical wind regime and similar environmental conditions at the time of their formation. The uppermost OSL sample from D2 profile (D2/100-110 cm) refers to Boreal sand movement (8.24±1.24 ka). As this zone has relatively homogenous fine-grained samples, presumably all the 160 cm deep layer of the zone I. was deposited within a short period.

K1 drilling represents an unfilled medium-size parabolic dune from hierarchy level 3. All along the profile the sand content is higher (80-92%) than in profile D2. Here three zones were identified, as the sandy materials were intercalated by a fine-grain layer, where the silt and clay content increases 15-20%.

However, the profile of K2 was made in a filled medium-size parabolic dune in hierarchy level 2, it is similar to the material of the large parabolic dunes. The lower zone I. is finer grained ($d_{90mean}$ = 316 μm) than zone II. ($d_{90mean}$ = 362 μm). The proportion of the medium sand varies considerably therefore 8 and 7 layers were defined respectively. In I/6-8. layers the silt and clay content was high, indicating soil development processes, thus they refer to a possible paleo-surface. An OSL sample taken from K2/260-270 cm refers to Subboreal aeolian activity at 2.99±0.19 ka. From other blown sand territories of Hungary similar age of sand movement was identified (Danube Tisza Interfluve: Sipos et al., 2009; Kiss et al., 2008; and Nyírség: Kiss and Sipos, 2008), and related to Bronze Age anthropogenic activity.

Unlike earlier profiles presented here, the profile K7 is extremely rich in silt and clay. It was drilled in the head of a simple, partially filled medium-size parabolic dune. However, in zone I. sand content is relatively large (63-74%), then it is reduced to 44-67% in zone II., finally it increases to 69-81% in zone III. where silt-rich (32% and 43%) layers were intercalated between the sand layers. The Preboreal age (11.11±0.64 ka) of the OSL sample from K7/200-210 cm is very close to the age of profile K13/200-210 cm (10.77±0.71 ka).

Similarly to Profile K7, the middle zone of Profile K11 is also rich in silt (52-77%) framed by sandy lower and upper zones. K11 core was deppened in the head of a simple, filled medium-size dune. The increased silt and clay content might refer to soil development or caused by the effects of ground water variations.

*Hummocks*

Hummocks are the smallest crescentic forms (crest length is less than 160 m). They are generally elevated and located in groups superimposed on larger forms. Their material is relatively homogenous, thus it was probably accumulated within a short time. These dunes are very young, anthropogenic activity in historical times triggered their formation.

The D1 coring was made on the head of a hummock superimposed in hierarchy level 3. Its sand content is high (71-96%) with the predominance of medium and fine sand (24-51% and 32-50% respectively; Figure 2). The profile was dissected to three zones and within the zones 2-4 layers were identified. In zone I. (280-195 cm) the medium and fine sand grain size classes are the most common ($d_{90mean}$ = 362 μm). This zone contains two coarser sand layers (sand proportion is 85% and 87%), and two finer grained layers (sand content is 75% and 71%). In the middle zone II (195-85 cm) the clay content slightly increases (from 4-9% to 7-10%), therefore the mean grain size is considerably finer ($d_{90mean}$ = 342 μm). The bottom of the zone is nearly homogenous as sand proportions are between 71-76%, while in the upper part (105-95 cm) the proportion of sand abruptly rises to 83%. In the topmost zone III. (85-30 cm) the coarsest sandy layers were deposited ($d_{90mean}$ = 425 μm). The largest grains were found in the lowermost layer ($d_{90mean}$ = 504 μm), which was then covered by a finer ($d_{90mean}$ = 386 μm), then a coarser ($d_{90mean}$ = 412 μm), and another finer ($d_{90mean}$ = 371 μm) layer. Three OSL samples were dated from this profile which all gave a very young age: 0.30±0.07 ka, 0.30±0.06 ka and 0.23±0.03 ka. North from the windward slope of the dune, a well-defined blowout is located. Presumably, this is the source area of the sediment deposited in the hummock. Probably the deflation was the result of human influence (grazing or bush burning). The three grain size zones refer to at least three deposition periods, but due to the measurement range and available error levels of OSL dating, the exact time of the sand movement phases cannot be specified. Three aeolian periods within approximately 130 years, during the 17$^{th}$ and 18$^{th}$ centuries can only be concluded.

*Longitudinal form*

Longitudinal ridges are elongated, quazi-linear forms which appear in various sizes (length: 35-5600 m). Numerous ridges are scattered all over the study area, some are simple dunes, but many are superimposed on large or medium-size parabolic dunes. Wing fragments or residual ridges could only be identified by their individual stratigraphic characteristics and age. On the western part of the region a longitudinal form stretching from north to south was sampled at three boreholes along the longitudinal axis. The studied form is covered by sandy silt and silty sand, and this sandy material becomes coarser and thinner downwind. The topmost layer of the sandy zones at the bottom of each profile has the coarsest grain size, referring to the existence of a paleo-surface where larger grains remained as the result of aeolian deflation. This stratigraphic characteristic is typical of residual ridges.

In the middle part of the residual ridge, at the K5 profile two sediment zones were identified. The lower zone contains high proportion of sand fraction, and it is divided by a sharp boundary from the upper, silt- and clay-rich zone (Fig. 2). In the bottom zone (250-135 cm) the proportion of sand fraction gradually decreases from 97% to 49%, meanwhile the medium-sized sand fraction completely disappears ($d_{90mean}$ = 235 μm). The proportion of silt and clay abruptly increases to 14% at 235-225 cm, then decreases (3%) again, and only gradually rises up to 51%. These variations define four layers in zone I. In the upper zone II. (135-0 cm) the silt fraction dominates (53-73%, $d_{90mean}$ = 110 μm), however, in the topmost layer the proportion of the sand fraction slightly increases (35-41%). For OSL dating the sandy I/4 layer (170-180 cm) and the loess-like II/1 layer (90-100 cm) were sampled. The sandy sample revealed the oldest age (21.22±1.54 ka) dated in the region. These data support our assumption that this form is a residual ridge formed during the deflation of the previously stable surface while in the central part of the region large parabolic dunes developed (e.g. D3: 17.76±4.07 ka). The age of the approxi-

mately 130 cm thick loess-like cover is 13.3±0.74 ka, determining the same age as D2/200-210 cm, D2/270-280 cm samples and D3/100-110 cm. It suggests that at time, when in the southern part of East Inner Somogy medium size parabolic dunes formed, simultaneously at the margins aeolian dust (loess) covered the residual ridge. Similar loess accumulation was also identified at the margins of other large aeolian areas in Hungary (Borsy, 1987).

*Deflation hollows*

Deflation hollows are located in the northern foreground of accumulational zones, which are the largest negative landforms here (area: >8 ha). They are built of alternating sandy and silty sedimentary layers. In the hollows after the aeolian activity the groundwater level increased, thus swamps and wetlands evolved, which were covered by varying thickness of sand during further aeolian phases. At the northern sampling site (K3) greater number of sandy and finer sediment layers was found than in south, while in the southern sampling site (K10) the sand layers are thicker.

Unlike previous profiles, at the K10 sampling site (Fig. 2) gray-coloured sand was found, which presumes dissimilar processes and the role of diverse post-sedimentation influences. The zone I. (300-175 cm) contains 75-81% sand ($d_{90mean}$ = 287 µm), within the zone four sandy layers indicate repeated aeolian activity. In the zone II. (175-145 cm) fine grained layer was deposited ($d_{90mean}$ = 166 µm) with high silt proportion (44-66%). In the topmost zone III. (145-0 cm) the proportion of fine and very fine sand is higher than in the bottom zone ($d_{90mean}$ = 244 µm), while its silt proportion gradually increases towards the current surface (from 16% to 46%). Probably, the silty layers of zone II. and zone III/2 deposited in a swamp, where intensive weathering facilitated concentration of silt. The coarsest layers are I/6-8 which could represent the maximum deflation level. Later, a swamp was covered by blown sand layers which facilitated soil development and weathering processes took place. The only OSL samples collected at the bottom of the profile (280-290 cm) is currently under laboratory analysis.

## DISCUSSION

*Regional analysis*

Earlier researches (Marosi, 1970, Lóki, 1981) found that the fluvial sediments of the alluvial fan and consequently the reworked aeolian material become finer southward. For the regional analysis the coarsest samples of each profile were chosen (based on mean values) and their $d_{90}$ values were used. The samples were collected from five well recognisable regions, therefore they were examined in five (from northern to southern) location groups (Fig. 1). Besides the variance in these location groups, grain size distribution of hierarchy levels and morphometric classes were also studied.

On higher elevation the deposition of fine material is more common, while coarser sediments are more abundant on less elevated areas. However, data derived from the 17 study sites are not significantly different, as fine samples were also found in lower laying areas (Fig. 3).

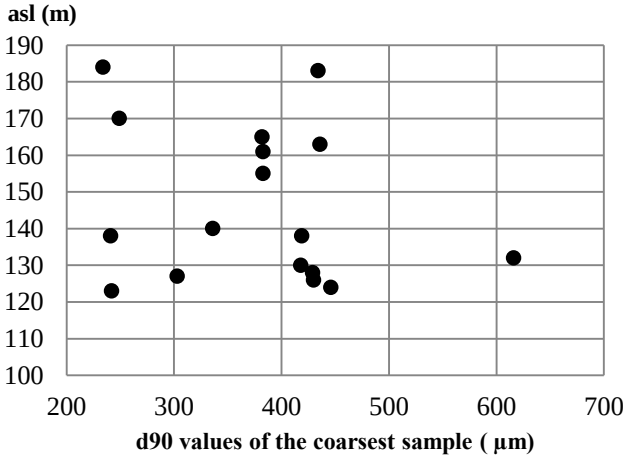


*Fig.3* The $d_{90}$ values of the coarsest samples from each profile plotted against elevation above sea level of the sampling site

Clear trend cannot be identified either by plotting the elevation of the coarsest samples against the first mode values of their grain size distribution curves (Fig. 4), however only six different first mode values are present. This presumes that the sediments deposited during at least six aeolian erosional-accumulational periods each characterised by different energy conditions.

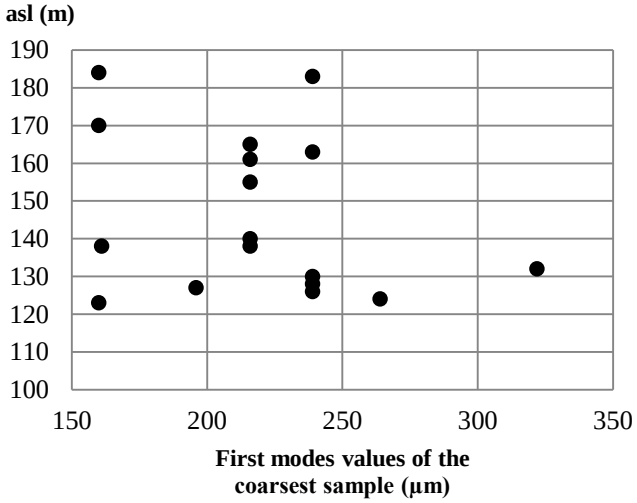


*Fig. 4* The first modes of the grain size distribution curves of the coarsest samples from each sampling site plotted against elevation above sea level

As forms were grouped based on their hierarchy levels and morphometric classes, the grain size distribution analysis was also carried out on both classes. Within the accumulational zones grain size variation trends cannot be examined, because (1) most of the

sampled dunes are in the southernmost part of each accumulational zones, and (2) the sampling sites are only 1-2 km apart, therefore a lack of representativity within each accumulational zone is a concern. Therefore only changes in the whole region and within single forms were analysed.

Considering the grain size distribution of the whole region (Fig. 5), the material in the northern part of the region is coarser ($d_{90}$=382-446 µm), then grain size decreases considerably towards the middle part ($d_{90}$=243-419 µm), while it rises again in the southernmost areas ($d_{90}$=242-616 µm). This contradicts the previous results, which described continuous refinement towards south. However, the coarse sandy material in south could be explained by the diverse ages and morphometric characteristics of the sampled forms. The southernmost accumulation zone is the highest containing the greatest amount of blown-out material, thus deeper layers were blown out, which were probably coarser due to the texture of alluvial fan sediments coarsening downward.

Within hierarchy levels, the grain size of simple dunes and level 1 forms become explicitly finer downwind. The $d_{90}$ values of simple dunes decreases southward from 446 µm to 242 µm, while of hierarchy level 1 from 429 µm to 249 µm. This is probably the result of grain size trends in the original material, as fluvial sediments in the substrate also getting finer from north to south. In case of hierarchy level 2 dunes the $d_{90}$ grain size values also decrease downwind (from 436 µm to 430 µm and then to 303 µm). However, the trend reverses in case of the elevated hierarchy level 3 dunes, where the $d_{90}$ value in north is 382 µm, and it increases towards south to 616 µm. It could be explained by the development of hierarchy level 3 forms: they are mostly hummocks formed as the result of local deflation. The developed small blowouts acted as wind-tunnels where even the coarser sand fraction could be transported, and it became the building material of the hummocks. Also, these are the youngest dunes, therefore fine sediments of the surface were probably removed during earlier aeolian phases, thus the source of hierarchy level 3 dunes was the lower layers of the alluvial fan substrate, where coarser material was deposited.

Considering the average values of each hierarchy levels, the material of simple dunes is the finest ($d_{90mean}$ = 313 µm), while of hierarchy level 1 dunes slightly coarser ($d_{90mean}$ = 354 µm). The average values of hierarchy level 2 dunes become even coarser ($d_{90mean}$ = 390 µm), and the coarsest forms are in hierarchy level 3 ($d_{90mean}$ = 472 µm). So the more elevated a form is, the coarser $d_{90}$ values is characteristic, as the source material was blown from deeper and deeper, thus coarser and coarser layers of the alluvial fan substrate. Thus, the aeolian deflation and accumulation reversed the original stratigraphy of the alluvial fan's surface.

Among the members of the large parabolic dune morphometric class, coarser and finer samples were both found, regardless of their spatial distribution (Fig. 1), thus downwind refinement cannot be determined in case of the oldest forms (Fig. 5). The material of medium-size parabolic dunes becomes finer southward, as their $d_{90}$ values decrease from 446 µm to 246 µm. However, the southernmost sample does not fit into this trend ($d_{90}$= 418 µm). In case of the studied members of the hummock morphometric class, the material of the southern studied hummock is coarser than of the northern. During the formation of hummocks, the sediment was probably transported just for a very short distance, from the open sand

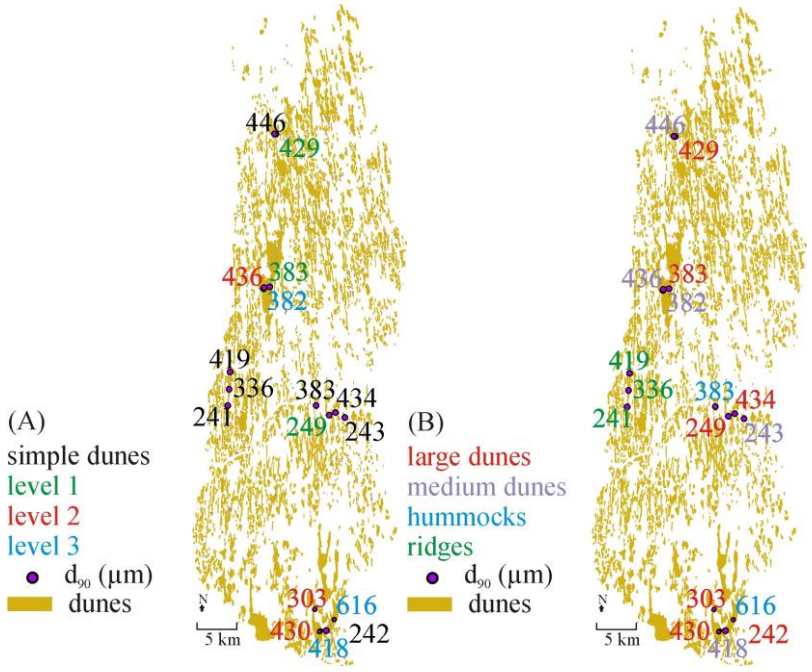


*Fig. 5* The $d_{90}$ values of the coarsest samples of the sampling sites according to the hierarchy level (A) and morphometric class (B) of the sampled dune

patches created by human disturbance, thus the source material of that location determined the grain size characteristics of the forms.

Average values of the morphometric classes become gradually coarser from the large parabolic dunes ($d_{90mean}$ = 353 µm) through the medium-size ones ($d_{90mean}$ = 385 µm) to the hummocks ($d_{90mean}$ = 499 µm). Therefore as the size of the form decreases, their grain size increases, referring to limited sand supply and simultaneously denser vegetation, which restrict the spatial distribution of aeolian activity.

Within single forms, north to south refinement is the most emphasised in the sediments of the residual ridge sampled at three points, as here $d_{90}$ values decrease from 419 µm to 336 µm and then to 241 µm. (Fig. 5). Considering the grain size distribution within a large parabolic dune it seems that finer material characterises the wings ($d_{90}$=303 µm) and coarser sand was found in the head ($d_{90}$=430 µm). It could be explained by the elevation of these sampling sites: the wing is lower, thus richer in moisture; therefore here the developed vegetation could act as effective sediment trap, resulting in finer sediment deposition due to the increased friction.

*Correspondence of grain size analysis and OSL ages*

Based on OSL ages and grain size distribution analysis data, grain size characteristics of the transported sediments during the different aeolian phases could be compared. Previous researches (Marosi, 1970, Lóki, 1981) argue that since Late Glacial wind velocity gradually declined, thus the extent of sand movement and also the grain size of deflated material decreased as well. In contrary, plotting OSL ages and $d_{90}$ values of the samples (Fig. 6) shows that older forms are characterised by finer grain size distribution, however, the statistical relation of the two variables is not explicit (R2=0,198).

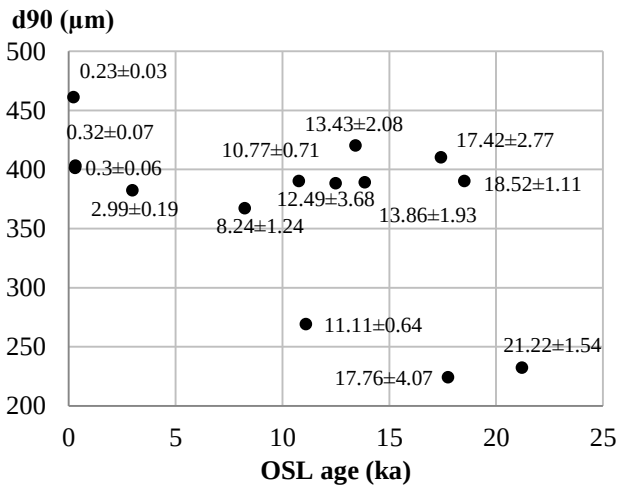


*Fig. 6* Connection between OSL age and $d_{90}$ values of grain size distribution curves of the same OSL samples

The youngest (0.23±0.03 ka, 0.30±0.06 ka and 0.32±0.07 ka) samples have very coarse grain size distribution ($d_{90}$ values are 461 µm, 401 µm and 403 µm, respectively), thus these are even coarser than Late Glacial (17-18 ka old) sands. The formation of the 17th-18th c. hummocks is probably due to human activity. At the time of the first military mapping, the area was a pasture, therefore, possibly as a result of overgrazing the closed vegetation opened and the wind started to deflate the available sand. Probably, due to wind-tunnel effect the wind speed was high, thus coarse material could also be eroded and transported. However, it was transported only a very short distance and deposited soon forming hummocks.

It could be concluded, that if conditions are suitable – dry, open sand surface – the wind is capable of transporting the coarse fraction of sand, despite of the more humid climate since the Last Glacial that allowed the development of a dense vegetation cover (Járainé-Komlódi, 2000). However, in case of disappearing vegetation cover, coarse sand could be transported due to wind-tunnel effect.

The grain size of a sample could also be characterised by the mode of its grain size distribution curve. The plot of modes and OSL ages show a similar trend as $d_{90}$ values and OSL age plots (Fig. 7). Modes of the grain size distribution curves of younger forms gradually increase from 150 µm to 300 µm, suggesting that the younger forms have higher first mode values. However, the statistical relation of the two variables is ambiguous, as correlation coefficient for the dataset is only R=-0.67. This is partly because samples with similar age show varying mode values as during an aeolian phase in different parts of the region sediments was deposited under different energy conditions and various sand availability.

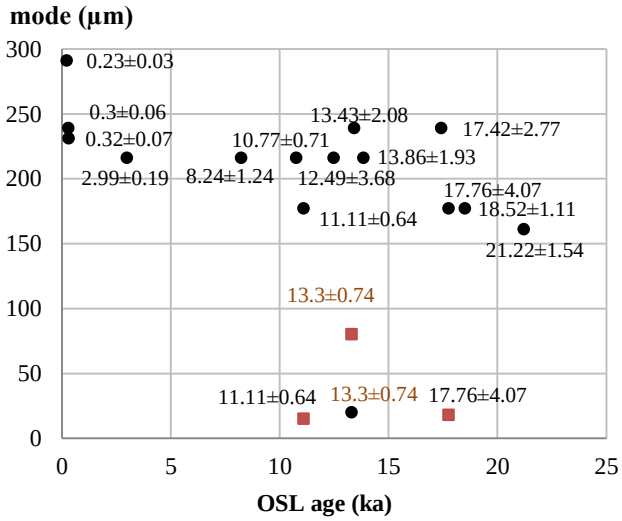


*Fig. 7* Connection between OSL ages of the samples and their grain size distribution curve's mode values (black – first mode; red – second mode)

Second modes of the samples refer to secondary processes besides aeolian activity. For example on stabilised aeolian sand surfaces soils can develop, winnowed fine sand in dust can accumulate in leeward areas or variations in ground water level can locally concentrate fine particles and intensify weathering (Profile D5, K7 and K5).

Sorting of a sample was expressed by the difference of $d_{75}$ and $d_{25}$ values, where smaller sorting value refers to better sorted sediment. The correlation between OSL ages and sorting was also examined (R2=0.742, Fig. 8). The younger samples are less sorted than older ones. It refers to extensive and probably longer sand movement periods (Báldi, 1978) during older, climate induced aeolian activity phases. In contrary, during human induced, young sand movement periods the locally disturbance enabled just limited sorting process, as the material was transported within a very short distance which was not sufficient for sorting the sediment.

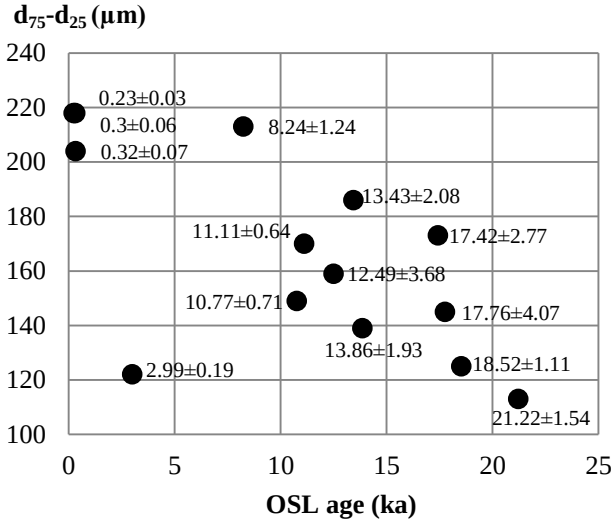


*Fig. 8* Connection between OSL age and sorting value of the samples

## CONCLUSIONS

In the studied profiles sandy and finer grained layers alternated. Probably during aeolian activity sandy material was deposited, whilst during humid phases finer material was formed due to increased weathering in swamps and soils. OSL data proved several sand movement periods when the finer layers were covered by sand.

The material of large parabolic dunes, simple dunes and hierarchy level 1 dunes is getting finer towards south, in accordance with the grain size changes of the alluvial fan. The grain size distribution of smaller, elevated and younger dunes is determined predominantly by local factors, such as grain size characteristics of source material and wind-tunnel effect. Similar results were found in North China, where the grain size distribution of sand dunes also became finer in the deposition direction of alluvial fan in the substrate (Zhu and Yu, 2014). Liu et al. (2014) and Zhu et al. (2014) concluded that sediment characteristics are predominantly determined by the source material, therefore sand reworked from deeper layers of the alluvial fan can form small in size but coarse in grain dunes. This phenomenon was also observed in Inner Somogy.

The $d_{90}$ values show that the grain size is not finer in younger forms, as it was suggested in earlier studies (Marosi, 1970), on the contrary, it is coarser. Mode values of the grain size distribution curves also prove coarser sand in younger dunes. This can be a result of increased wind energy due to wind-tunnel effect, or of coarser source material. Similarly increasing grain size distribution was described in the Carpathian Basin on the Maros alluvial fan by Sümeghy (2014), where Pleistocene fluvial sands are finer grained than Holocene sediments, which is a result of increased energy of the river and therefore coarser sediment load. This indicates that during Holocene not only in fluvial, but also in aeolian environment the transport capacity increased. Moreover, in Inner Somogy based on $d_{75}$-$d_{25}$ values, younger samples are poorly sorted, presuming short aeolian periods.

**Acknowledgements**

This research was supported by the OTKA 83561; and European Union and the State of Hungary, co-financed by the European Social Fund in the framework of TÁMOP-4.2.4.A/ 2-11/1-2012-0001 'National Excellence Program'.

**References**

Ádám, L., Marosi, S., Szilárd, J. 1981. A Dunántúli-dombság: Dél-Dunántúl. Akadémiai Kiadó, Budapest, 704 p.

Bagnold, R.A. 1937. The size-grading of sand by wind. Proc. R. Soc. London A *Math. Phys. Sci.* 163 (9), 250–264.

Báldi, T. 1978. A történeti földtan alapjai. Tankönyvkiadó. Budapest. 308.

Blott, S. J., Pye, K. 2012. Particle size scales and classification of sediment types based on particle size distributions: Review and recommended procedures. *Sedimentology* 59, 2071–2096. DOI: 10.1111/j.1365-3091.2012.01335.x

Borsy, Z. 1961. A Nyírség természeti földrajza. Akadémiai Kiadó. Budapest. 227 p.

Borsy, Z. 1987. Paleogeography of blown-sand in Hungary. In: Pécsi, M., Velichko. A.A. (eds.) Paleogeography and Loess. Akadémiai Kiadó. Budapest. pp. 75–87.

Borsy, Z., Molnár, B., Somogyi, S. 1969. Az alluviális medencesíkok morfológiai fejlődéstörténete. *Földrajzi Közlemények* 17, 237–254.

Cholnoky, J. n.d. Somogy vármegye természeti viszonyai. Magyarország vármegyéi és városai, Somogy vármegye. Budapest.

Dövényi, Z. (ed.) 2010. Magyarország kistájainak katasztere, Budapest, MTA FKI, 2010. 876 p.

Farrell, E.J., Sherman, D.J., Ellis, J.T., Li, B. 2012. Vertical distribution of grain size for wind blown sand. *Aeolian Res.* 7, 51–61. DOI:10.1016/j.aeolia.2012.03.003

Folk, R.L., Ward, W.C. 1957. Brazos river bar: a study in the significance of grain size parameters. *J. Sediment. Petrol.* 27 (1), 3–26.

Györgyövics, K., Kiss, T. 2013. Dune hierarchy and morphometric classes of the parabolic sand dune association of Inner Somogy, Hungary. *Studia Geomorphologica Carpatho-Balcanica* VOL. XLVII, 31–48.

Iványi, I., Lehmann, A. 2002. Duna-Dráva Nemzeti Park . Mezőgazda Kiadó, Budapest, 406 p.

Járainé-Komlódi, M. 2000. A Kárpát-medence növényzetének kialakulása. *Tilia* 9, 5–59.

Kiss, T., Györgyövics, K., Sipos, Gy. 2012. Homokformák morfometriai tulajdonságainak és korának vizsgálata Belső-Somogy területén. *Földrajzi Közlemények* 136 (4), 361–375.

Lancaster, N. 1995. Geomorphology of Desert Dunes. Routledge, London, 290 p.

Liu, B., Qu, J., Ning, D., Gao, Y., Zu, R., An, Z. 2014. Grain-size study of aeolian sediments found east of Kumtagh Desert. *Aeolian Research* 13, 1–6. DOI:10.1016/j.aeolia.2014.01.001

Lóki, J. 1981, Belső-Somogy futóhomok területeinek kialakulása és formái. *Közlemények a Debreceni Kossuth Lajos Tudományegyetem Földrajzi Intézetéből* 139, 81–107.

Marosi, S. 1967. Kovárványrétegek és periglaciális jelenségek összefüggésének kérdései a belső-somogyi futóhomokban. *Földrajzi Értesítő* 15 (1), 27–40.

Marosi, S. 1970, Belső-Somogy kialakulása és felszínalaktana. Akadémiai Kiadó, Budapest, 169 p.

Marosi, S., Somogyi, S. (eds.) 1990. Magyarország kistájainak katasztere 1-2. kötet. MTA Földrajztudományi Kutató Intézet. Budapest.

Nottebaum, V., Lehmkuhl, F., Stauch, G., Hartmann, K., Wünnemann, B., Schimpf, S. and Lu H. 2014. Regional grain size variations in aeolian sediments along the transition between Tibetan highlands and north-western Chinese deserts – the influence of geomorphological settings on aeolian transport pathways. *Earth Surf. Process. Landforms*. DOI: 10.1002/esp.3590

Pécsi, M. 1997. Szerkezeti és váztalajképződés Magyarországon. MTA FKI, Budapest, 296 p.

Pécsi, M. 1959. A magyarországi Duna-völgy kialakulása és felszínalaktana. Akadémiai Kiadó, Budapest, 346 p.

Reddy, D. V., Singaraju, V., Mishra, R., Kumar, D., Thomas, P. J., Rao, K. K., Singhvi, A. K. 2013. Luminescence chronology of the inland sand dunes from SE India. *Quaternary Research* 80 265–273. DOI: 10.1016/j.yqres.2013.06.003

Ruszkiczay-Rüdiger, Zs, Braucher, R., Csillag, G., Fodor, L., Dunai, T.J., Bada, G.,Bourlés, D., Müller, P. 2011. Dating Pleistocene aeolian landforms in Hungary,Central Europe, using in situ produced cosmogenic 10Be. *Quaternary Geochronology* 6, 515-529. DOI: 10.1016/j.quageo.2011.06.001

Sahu, B. K. 1964. Depositional mechanisms from the size analysis of clastic sediments. *J. Sediment. Petrol*. 34 (1), 73–78.

Sebe, K., Csillag, G., Ruszkiczay - Rüdiger, Zs., Fodor, L., Thamó – Bozsó, E., Müller, P., Braucher, R. 2011. Wind erosion under cold climate: A Pleistocene periglacial mega-yardang system in Central Europe (Western Pannonian Basin, Hungary). *Geomorphology* 134, 470–482. DOI:10.1016/j.geomorph.2011.08.003

Sümeghy, B. 2014. A Maros hordalékkúp fejlődéstörténeti rekonstrukciója. Doktoral (PhD) thesis, Szeged.

Wang, X., Dong, Z., Zhang, J., Qu, J., Zhao, A. 2003. Grain size characteristics of dune sands in the central Taklimakan Sand Sea. *Sediment. Geol*. 161 (1–2), 1–14. DOI: 10.1016/S0037-0738(02)00380-9

Zatykó, Cs., Juhász, I., Sümegi, P. (eds.) 2007. Environmental Archaeology in Transdanubia (Hungary). Budapest, *Varia Archaeologica Hungarica* 20, 239–241.

Zhu, B., Yu, J. 2014. Aeolian sorting processes in the Ejina desert basin (China) and their response to depositional environment. *Aeolian Research* 12, 111–120. DOI : 10.1016/j.aeolia.2013.12.004

Zhu, B., Yu, J., Rioual R., Ren X. 2014. Particle size variation of aeolian dune deposits in the lower reaches of the Heihe River basin, China. *Sedimentary Geology* 301, 54–69. DOI:10.1016/j.sedgeo.2013.12.006

JOURNAL OF ENVIRONMENTAL GEOGRAPHY
*Journal of Environmental Geography* 7 (3–4), 31–42.
DOI: 10.2478/jengeo-2014-0010
ISSN: 2060-467X

# THE ROLE OF HABITAT TYPES AND SOIL PHYSICOCHEMICAL PROPERTIES IN THE SPREAD OF A NON NATIVE SHRUB *LANTANA CAMARA* IN THE DOON VALLEY, WESTERN HIMALAYA, INDIA

**Gautam Mandal*, Shambhu Prasad Joshi**

*Ecology Research Laboratory, Department of Botany, DAV (PG) College, HNB Garhwal Central University, Dehradun–248001, Uttarakhand, India
*Corresponding author, e-mail: gautam231@gmail.com

Research article, received 23June 2014, accepted 20 October 2014

**Abstract**

Invasive alien species colonize very aggressively and forcefully, menacing native biodiversity. The success of invasive alien plants is due to their opportunistic exploitation of anthropogenic disturbances, the absence of natural enemies, free from herbivory and frequently their allelopathic competition. Invasive species can have a significant impact on development, affecting sustainability of livelihood, food security and essential ecosystem services and dynamics. *Lantana camara* is a documented weed of worldwide significance; it is indigestible due to its toxic chemicals and highly competitive. In this study physicochemical properties of soil were analysed from different high and low *Lantana* infested areas. Significant site effect was frequently observed than effect due to invasion status. The present study tested the impact of soil properties in the measured and calculated attributes of *Lantana* by randomly sampling soil from the highly invaded and less invaded sites in different habitats using the Modified Whittaker plot design. Results indicated that edaphic factors such as soil pH, total nitrogen, soil organic carbon, phosphorus and potassium content positively influenced the growth of *Lantana* and helped in its own further invasion process. These factors were also positively influencing the measured and calculated attributes of *Lantana* such as canopy coverage, average crown diameter, shrub canopy area, phytovolume and biomass from all sites. However some attributes like shrub height and stem diameter were negatively influenced by these soil factors. The present results show that *Lantana* invasion can significantly improve the soil nutrient level but also positively increasing the chances of its further invasion with more copious plant attributes.

**Keywords**: invasive alien plants, soil physicochemical properties, biomass of shrub, geomorphology, principal component analysis

## INTRODUCTION

The invasive alien species are well thought-out to be the second principal cause of biodiversity loss after habitat destruction (Schwartz et al., 1996; Shinwari et al., 2012). The negative impact of such plant species on native biodiversity has been well documented (D'Antonio and Mahall, 1991; Ridenour and Callaway, 2001). Invasive alien plants have been found to change the structure and composition of native communities and been associated with reduced native plant diversity (Bone et al., 1997; Ferreira and Marques, 1998; Shinwari and Qaisar, 2011).

Introduced species severely threaten some native flora and fauna communities, either directly or by modifying ecosystem process and functions (Gordon, 1998; Hulme, 2006; Vitousek et al., 1997). The introduction of non-native plants or animals has usually been deliberately facilitated by humans, and although most introduced species do not deleteriously affect ecosystems, a small proportion become invasive (Hulme, 2006). Traits that enable introduced species to persist or spread successfully include high fecundity, good defence mechanisms, high survival rates, adaptability and a lack of natural enemies such as predators and diseases (Cheal et al., 2006). Introduced species that become invasive can have catastrophic effects on native biodiversity assets and ecological processes by altering nutrient levels, hydrological cycles, fire regimes and community composition, including the removal of keystone species (Brooks et al., 2004; D'Antonio and Vitousek 1992; Le Maitre et al., 1996; Vitousek and Walker 1989; Yurkonis et al., 2005). For conservation strategies to be successful, it is essential that the introduced species, both plant and animal, that pose major threats, be identified and the mechanism through which they threaten biodiversity assets be understood.

India is suffering from the impacts of invasive alien species in many ways. Recently it was reported that the alien flora of India accounts for 1599 species, belonging to 842 genera in 161 families and constituting 8.5% of the total vascular flora found in the country (Khuroo et al., 2012). The negative impacts have been felt through losses of grazing, agricultural production and for some species, human health (Kohli et al., 2006). The Himalayas on the other hand is well recognized for its ecosystem services to the Asian region as well as to the world at large for maintaining slope stability, regulating hydrological integrity, sustaining high levels of biodiversity and human wellbeing. Mountains, due to their exclusive and inimitable biodiversity, are recently receiving priori-

ty for biodiversity conservation in global agendas. The western Himalayan part is a dynamic landscape with a rich and remarkable biodiversity (Guangwei, 2002). The western Himalayan region is endowed with a rich variety of gene pools and species, and ecosystems of global importance. The region, with its varied landscapes and soil formation, and variety of vegetation types and climatic conditions, is well known for its unique flora and fauna, and has a high level of endemism (Myers et al., 2000) and numerous critical eco regions of global importance (Olson et al., 2001; Olson and Dinerstein, 2002).

Total forest cover of the country is 697,898 sq. km (69.79 million ha) which is 21.23% of the geographical area of the country. The total tree cover of the country is estimated to be 91,266 sq.km (9.13 million ha) which is 2.78% of the total geographical area. The present study site Doon valley is a part of Uttarakhand state which is situated in the western Himalaya. The state of Uttarakhand has a geographical area of 53,483 sq. km, of which 4785 sq. km area is covered by very dense forest (VDF), 14,111 sq. km area is covered by moderately dense forest (MDF) and 5612 sq. km area comes under open forest (OF) giving a total forest cover of 24,508 sq. km which is 45.82% of the total geographical area (ISFR, 2013). The Doon valley is surrounded by sal (*Shorea robusta* Gaertn. f.) hereafter, *Shorea robusta* forest, where number of tree species are co-dominant such as *Syzygium cumini, Mallotus philippensis, Terminalia alata, Tectona grandis, Ficus benghalensis, Cassia fistula, Ehretialaevis, Adina cordifolia, Bauhinia variegate, Flacourtia indica.* These forests are invaded by number of exotic species. A large number of exotics have become naturalized in India and have affected the distribution of native flora to some extent, only a few have conspicuously altered the vegetation patterns of the country. *Lantana camara, Cytisus scoparius, Chromolaena odorata, Eupatorium adenophorum, Mikania micrantha, Mimosa invisa, Parthenium hysterophorus* and *Prosopis juliflora* are important among terrestrial exotics and are heavily distributed in the Doon valley forests.

*Lantana* is one of the most obnoxious weeds that has encroached most of the areas under community and reserve forestlands of western Himalaya. The outer fragile Himalayas are almost completely enraptured by this rapidly spreading weed. This weed, not only ruins common agricultural and forestlands but also makes shade as well as alellopathy impacts on the regeneration of important forestry species. Due to spread of *Lantana*, the yields of crops and pastures get reduced. The harvesting costs have increased manifolds. Heavy expenditure is incurred for afforestation of lands infested with this weed which requires frequent weeding so as to avoid suppression of young seedlings of planted species. Apart from its popularity as a garden plant, *Lantana* is said to form a useful hedge and to provide a good preparation for crops, covering the ground with fine leaf mulch. It improves the fertility of rocky, grave, or hard laterite soils, enriches the soil, and serves to retain humus in deforested areas and checks soil erosion. It can serve to nurse the parasitic sandalwood seedlings and in the Pacific islands has been used as a support for yam vines. *Lantana* leaves and twigs are often used in India as green mulch. The plant is not readily eaten by cattle unless pasturage is very scarce. In tropical countries, the ripe blue black berries are eaten, but ingestion of the green berry has led to human fatalities (Ross, 1999). *Lantana* has been introduced in India through one of the human orchestrated movement of plants which has often been found responsible for movement of plants from their native areasto other countries as introduced ornamental plants (Fig. 1).

There is much evidence that invasive plant species can modify physical or chemical attributes of soil, including inputs and cycling of nitrogen and other elements (Ehrenfeld, 2003; Haubensak et al., 2004; Hawkes

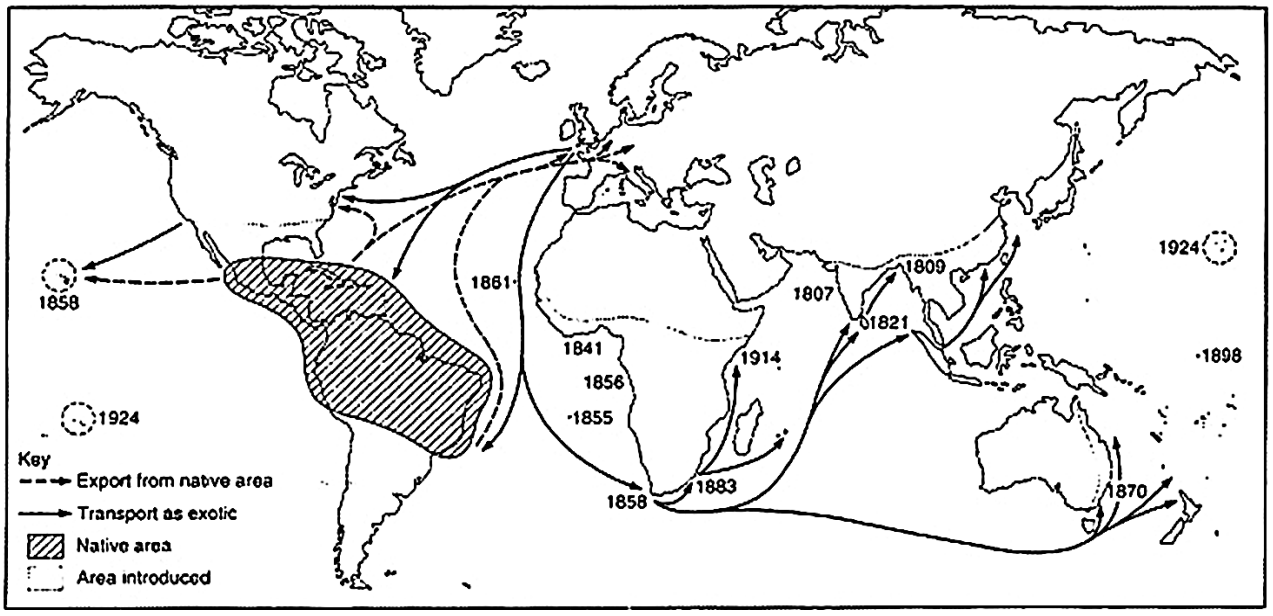


*Fig.1* Map showing years of transport and introduction of the woody shrub *Lantana camara*, across the world, from its native countries. Adopted with modification from Cronk and Fuller (1995)

et al., 2005), pH (Kourtev, 2002a), and soil organic matter and aggregation (Saggar et al., 1999). There is also evidence of direct modification of various components of the biotic composition of invaded soil, e.g., affecting a soil food web (Duda et al., 2003) total soil microbial communities (Kourtev et al., 2003) and mutualistic fungi (Hawkes et al., 2005). As noted, these effects will enable plant invasion by positive feedback with soil attributes only if invasive species are benefited, and indeed there are clear indications of such benefits. In temperate old-field communities, modification of soil micro biota by common invasive species typically had beneficial or neutral effects on growth of these species (Agrawal et al., 2005) and micro biota associated with roots of several invasive woody species have increased growth of these species (Bray et al., 2003).

Most changes in species composition reflect changes in soil water nutrient availability and changes in availability of essential plant resources such as light, nutrients and water may result in a change in vegetation community composition (Clegg, 1999). According to the review given by Chatanga, 2007 nutrient dynamics may become altered as a result of changes in the physical properties of the soil caused by the introduction of an alien species such as *Lantana* but it is not always the case that soil properties will be altered following alien species invasion. *Lantana* population persistence also occurs through processes unrelated to allelopathy such as edaphic effects and changes in ecosystem functioning (Gentle and Duggin, 1997a, Chatanga, 2007). These processes may facilitate ongoing suppression of indigenous species by altering nutrient cycles and modifying microenvironments and disturbance regimes (Van Wilgen and Richardson, 1985). *Lantana* also has negative effect on soil water supply (Hieramath and Sundaram, 2005, Chatanga, 2007).The dense stands of this shrub vegetation and the capacity of the soil beneath to absorb rain which could potentially increase the amount of runoff and the subsequent risk of soil erosion in areas infested with this shrub (Day et al., 2003). Increase in the soil nitrate following *Lantana* invasion to the benefit of this shrub and to the detriment of some native species and decline in other nutrients. In Australia, the moisture content and pH were not significantly affected by *Lantana*. The allelochemicals produced by this woody shrub could alter the populations of soil microbial symbionts necessary for the early establishment of certain seedlings (Vranjic et al., 2000). Few study sites investigated in the present study were heavily forested with northern subtropical moist deciduous forest having an admixture of a variety of species in four tier structures (Top canopy, middle strata, understory shrub and herb strata) with *Shorea robusta* as predominant tree species and understory heavily covered by *Lantana camara* and *Chromolaena odorata*.

The studies in different vegetation communities of Indian subcontinent and Australia, which were based on infertile sandstone derived soils, nutrient enrichment was found to be the key factor that facilitates exotic species invasion (King and Buckney, 2002; Lake and Leishman, 2004; Leishman et al., 2004; Leishman and Thomson, 2005; Hill et al., 2005). This was also consistent with the intermittent resource hypothesis of invasibility proposed by Davis et al. (2000). Davis et al. (2000) suggested that a plant community is more susceptible to invasion when there is an increase in the amount of unused resources, such as nutrients. In above mentioned studies it was found that invasion success of plants like *Lantana* in sandstone-based vegetation depends on nutrient enrichment, which occurs mainly through nutrient rich storm water runoff from impervious surfaces, such as roads within a developed catchment, entering the bushland and flowing into the bay systems (Hill et al., 2005). These same anthropogenic influences, roads and nutrient enriched runoff, as well other factors associated with agricultural production, occur in areas of the Doon valley in western Himalaya (Fig. 2). Thus, we might hypothesize that invasion by exotic plants may be facilitated by nutrient enrichment in the valley's vegetation communities also. Alternatively, the naturally more fertile shale derived soil of Doon valley may make it less vulnerable to nutrient facilitated exotic plant invasion.

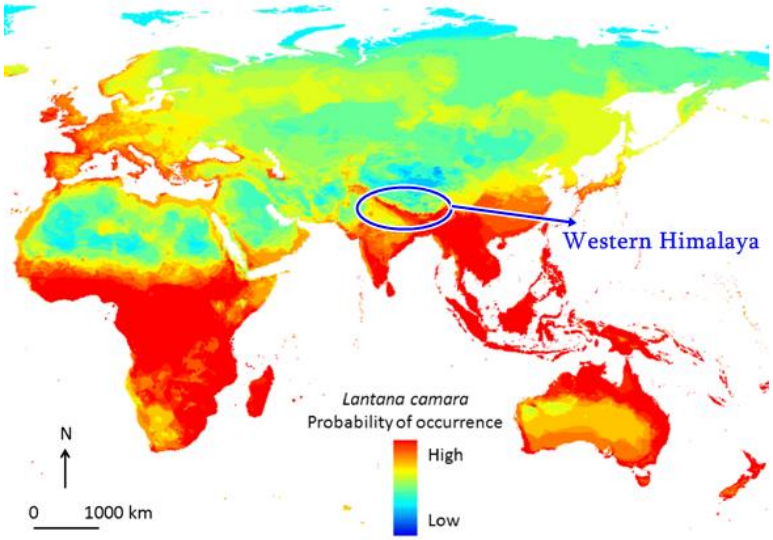


*Fig. 2* Bioclimatic niche model of probable *Lantana camara* occurrence generated by automated open Modeller algorithm, adopted and modified from Bhagwat et al. (2012)

The aims of this study were to determine the relative effect of different anthropogenic disturbances in Doon valley on vegetation composition and soil characteristics and to investigate whether there are significant correlations between various soil attributes and the success of exotic woody shrub species *Lantana*. We selected six study sites comprising of three habitat types such as (i) forest (ii) riparian areas (iii) shrub grassland. We measured a range of soil characteristics that are likely to be affected by the invasion of *Lantana* from different habitat types and also the vegetation of these habitats which are likely to be affected due to the infestation of this woody shrub. These were pH, total phosphorus, total potassium, calcium, magnesium, manganese, nitrogen, water retention capacity, organic matter content and electrical conductivity. The specific questions addressed were:

1. What is the effect of *Lantana* invasion on vegetation and soil characteristics from the valley?

2. What is the relative importance of the three habitat types (Forest, riparian area and shrub grassland) for exotic species invasion?

3. Are there consistent relationships between soil characteristics and success of exotic invasives among the disturbance types?

## MATERIALS AND METHODS

*Study sites*

The present study was carried out in the Doon valley, a part of western Himalaya, India. The Doon valley is surrounded by hills on all the sides and has a varied range of subtropical deciduous forests mainly dominated by *Shorea robusta*, *Syzygium spp.*, *Terminalia spp.*, *Ehretia spp.*, and *Litsea spp.* It is lying between latitudes $29^0 55'$ and $30^0 30'$ N and longitudes $77^0 35'$ and $78^0 24'$ E. It is a saucer shaped valley about 20km wide and 80km long with a geographical area of about 2100km$^2$. The Doon valley falls under the sub-tropical to temperate climate due to its variable elevation and is a part of western Himalaya (Fig. 3). The average maximum temperature for the Doon valley was 27.65$^0$C and the average minimum temperature was 13.8$^0$C with average maxima in June (40$^0$C) and average minima in January (1.80$^0$C). The area receives an average annual rainfall of 2025.43 mm. The region receives most of the annual rainfall during June to September; the maximum rainfall was recorded in July and August. We selected six sampling sites covering all parts of the valley and divided into three habitat types *i.e.*, forest, riparian, shrub grassland (Table 1). To see the level of differences in soil properties we categorised each site into 3 types (i) control (un-invaded site), (ii) moderately invaded sites and (ii) heavily invaded sites of *Lantana*.

*Research Methods*

Soil was randomly sampled from the centre of the four small (1 m$^2$) subplots near the centre and at the centre of the middle plot measuring 100 m$^2$ after litter was removed. A hand held push probe measuring 2.5 cm diameter was used to collect soil from a depth of 15 cm below the ground surface to ensure sufficient quantity of soil was collected for subsequent analysis. Ten samples were collected at non invaded, moderately invaded and highly invaded sites, which were obtained and analysed. The soil samples from moderate and highly invaded sites were collected within the *Lantana* thickets for consistency in data capture. Each soil sample was packed in a separate labelled plastic bag and transported to the laboratory for analysis. The soil samples were oven dried at 55°C for 24 h to reduce the moisture content and increase the concentration of the nutrients prior to chemical analysis. Then, they were passed through a 2 mm pore sieve for homogenization before they were analyzed for various contents.

*Soil chemical analysis*

Air dried 2 mm sieve soil samples collected from the two studies were subjected to routine chemical analysis. Total N was determined by micro Kjeldahl approach and available P was determined by molybdenum blue colorimetry. Exchangeable K, Ca and Mg were extracted using ammonium acetate, K was determined on flame photometer while Ca and Mg by atomic absorption spectrophotometer

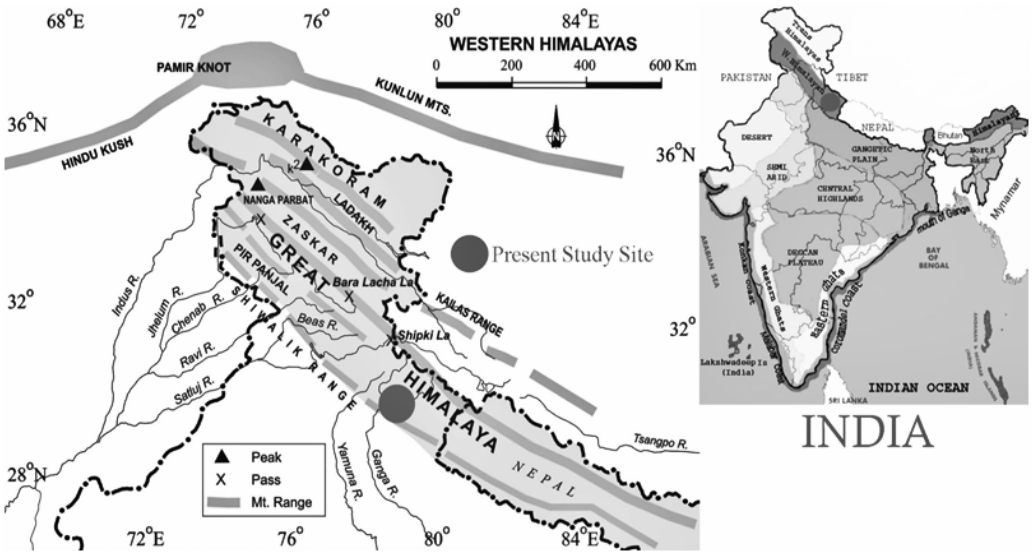


*Fig. 3* Map showing western Himalayan part and present study areas (Doon valley) in India

*Table 1* Site characteristics of Doon valley with dominant invasive species

| Name of the Sites | Dominant species | Point Coordinates | Elevation (m) | Habitat Type |
|---|---|---|---|---|
| Sahastradhara | *Lantana camara* L.<br>*Adhatoda zeylanica* L.<br>*Parthenium hysterophorus* L. | $30^0$ 23′ 08.17″ N,<br>$78^0$ 07′ 53.81″ E | 889 | Riparian areas |
| Asarori riparian area | *Parthenium hysterophorus* L.<br>*Lantana camara* L.<br>*Ageratum conyzoides* L. | $30^0$ 17′ 10.40″ N,<br>$78^0$ 03′ 22.27″E | 629 | Riparian areas |
| Chandrabani Forest Periphery | *Lantana camara* L.<br>*Opuntia dillenii* Ker Gawl.<br>*Adhatoda zeylanica* L. | $30^0$ 15′ 26.03″ N,<br>$78^0$ 00′ 29.45″ E | 893 | Dense forest |
| Rajpur Forest Periphery | *Lantana camara* L.<br>*Murraya koenigii* (L.) Spreng.<br>*Parthenium hysterophorus* L. | $30^0$ 23′ 02.83″N,<br>$78^0$ 05′ 09.93″ E | 952 | Dense forest |
| Mothronwala | *Parthenium hysterophorus* L.<br>*Lantana camara* L.<br>*Ageratum conyzoides* L<br>*Chromolaena odorata* L. | $30^0$ 15′ 22.81″ N,<br>$78^0$ 01′ 42.46″ E | 532 | Shrub Grassland |
| Jolly Grant | *Lantana camara* L.<br>*Arundinella spicata* Dalzell.<br>*Ageratum conyzoides* L<br>*Parthenium hysterophorus* L. | $30^0$ 11′ 17.16″ N,<br>$78^0$ 11′ 17.91″ E | 561 | Shrub Grassland |

(Okalebo et al., 1993), pH and electrical conductivity of the soil (soil: water, 1:5) was determined by the help of water analysis Kit (Systronics India Ltd, Gujarat, India). The organic carbon of the soil was determined by Walkley and Black (1934) rapid titration methodas given by Piper (1944). Pearson's correlation matrix, students''t' test and one way ANOVA was calculated to establish the relation between the soil parameters and the measured attributes of lantana. Statistical analysis was done using XLSTAT *V.* 2011 (Addinsoft, Rue Damremont, Paris – 75018, France) for Microsoft Windows.

*Biomass calculation*

Above ground and fine root biomass (Kg per sq. m.) of large colonies of lantana was recorded, for which plant roots were carefully collected using a 25×25×40 cm soil monolith within the $1m^2$ quadrat. Plant materials such as green material (leaves), dead residues (mulch), and roots collected were oven dried at 60 °C for 72 h and weighed. The location of each site was recorded using a Global positioning system (GPS) device (Garmin 72, Garmin, Olathe, KS, USA).

## RESULTS

All the *Lantana* invaded sites including the moderate and high, showed considerable increase in the mean pH value. The maximum range of pH was between 7.12 (±0.40) to 7.22 (±0.24), recorded from shrub grassland type habitat and was about 1.40 % high from other moderately invaded sites of all habitat, minimum pH range was between 5.53 (±0.45) to 6.13 (±0.62), recorded from forest periphery type habitat and was about 10.84 % higher than the other moderately invaded areas ($P<0.01$). The moderately invaded and highly invaded areas of all the habitats recorded high pH values than the control or non invaded sites of all the habitats (Table 2). The forest peripheries were situated at a comparatively higher altitude than other habitats and were found more acidic than the other two; this was explained perhaps due to fewer disturbances, free from herbivory and high altitude (952 m). The increase in pH value did not show any positive relation with the measured attributes of *Lantana* (ANOVA, $P < 0.001$). However, both increases and decreases in pH following plant invasion have been equally reported in the literature (Ehrenfeld, 2003). It is not clear whether *Lantana* prefers microsites with elevated soil pH or, in fact, it was responsible for the increase observed in this study. Thus the precise soils require further study, including the contribution of its biomass parts and associated chemical contents to the change. Under the *Lantana* patch only, availability of soil base ions of Ca, P, as well as carbon and EC correlated significantly and positively with increasing pH ($r=0.74, 0.69, 0.78, 0.84$, respectively; $P<0.05$, $N=30$), while S and Fe showed the opposite pattern ($r=-0.89, -0.73$, respectively; $P<0.05$, $N= 30$).

Macronutrients measured in this study (Mg, Ca, K, P and N) showed significant differences between the moderately invaded, highly invaded and un-invaded sites (ANOVA, $P < 0.05$), except carbon concentrations which did not differ between all sites (ANOVA, $P = 0.673$) (Table 1). The macronutrients among the different habitat types such as the forest, riverine and shrub grassland habitats also strongly and significantly differed (ANOVA, $P < 0.001$) except carbon concentrations which did not show significant variations across habitats (ANOVA, $P = 0.376$). Further, when the possible relationship between the habitat type and invasion pattern was analysed (Si × Ha level interaction), the Ca, K, N and P concentrations were found highly significant (ANOVA, $P < 0.001$) while Mg and S was found less

*Table 2* Mean soil chemical and physical properties by site type. P-values are from t-tests comparing the properties by site type (C.V. stands for coefficient of variation, and is provided as a percentage, SD: standard deviation, NS = Non significant,* P<0.05, *** P≤0.001)

| Soil property | Control (Non invaded) | | | Moderately invaded | | | Heavily invaded | | | p value | Site | Habitat type | Si × Ha (interaction level) |
|---|---|---|---|---|---|---|---|---|---|---|---|---|---|
| | Mean | SD | C.V. | Mean | SD | C.V. | Mean | SD | C.V. | | | | |
| Bulk Density ($gm/cm^3$) | 0.97 | 0.16 | 16.5 | 1.1 | 0.15 | 13.6 | 1.6 | 0.23 | 14.2 | < 0.001 | *** | * | *** |
| CEC ($meq/100cm^3$) | 4.9 | 1.28 | 26.1 | 7.8 | 2.8 | 35.9 | 8.1 | 1.3 | 34.7 | < 0.001 | *** | *** | *** |
| Base Saturation (%) | 58 | 14.52 | 25 | 84 | 11.96 | 14.2 | 87 | 10.22 | 13.9 | < 0.001 | *** | NS | NS |
| pH | 6.19 | 0.37 | 7.4 | 6.34 | 0.61 | 10.3 | 6.78 | 0.61 | 10.3 | < 0.001 | *** | *** | *** |
| P ($mg/dm^3$) | 8.7 | 2.6 | 29.9 | 14.9 | 7.25 | 54.12 | 16.34 | 8.21 | 55.1 | < 0.001 | *** | *** | * |
| Ca ($mg/dm^3$) | 383 | 219.68 | 57.4 | 936 | 457.12 | 45.21 | 1044 | 481.88 | 41 | < 0.001 | *** | *** | * |
| Mg ($mg/dm^3$) | 162 | 77.74 | 48 | 102 | 43.44 | 42.6 | 100 | 72.13 | 44.21 | < 0.001 | *** | *** | NS |
| Zn ($mg/dm^3$) | 2.8 | 1.51 | 53.9 | 13.24 | 15.23 | 97.6 | 15.6 | 16.23 | 96.33 | < 0.001 | *** | *** | NS |
| Cu ($mg/dm^3$) | 1.1 | 0.38 | 34.5 | 3.8 | 2.68 | 70.5 | 3.98 | 2.78 | 73.21 | < 0.001 | *** | *** | NS |
| Fe ($mg/dm^3$) | 703 | 3.12 | 24.5 | 531 | 3.66 | 28.8 | 459 | 3.68 | 28.8 | < 0.001 | *** | *** | NS |
| Na ($mg/dm^3$) | 19 | 4.03 | 26.9 | 17 | 4.23 | 42.2 | 16 | 3.21 | 42.2 | < 0.001 | *** | *** | *** |
| Mn ($mg/dm^3$) | 52.4 | 27.08 | 51.7 | 42.18 | 15.33 | 37.43 | 38.7 | 14.15 | 36.6 | < 0.001 | *** | *** | *** |
| Humic Matter (%) | 0.38 | 0.11 | 28.9 | 0.32 | 0.21 | 65.6 | 0.32 | 0.21 | 65.6 | < 0.001 | *** | *** | * |
| Weight per volume ($g/cm^3$) | 1.02 | 0.07 | 6.9 | 1.04 | 0.1 | 9.6 | 1.04 | 0.1 | 9.6 | < 0.001 | *** | NS | NS |
| K ($mg/dm^3$) | 62 | 24.29 | 39.2 | 66 | 25.75 | 39 | 66 | 25.75 | 39 | < 0.001 | *** | *** | * |
| S ($mg/dm^3$) | 18 | 3.75 | 26.8 | 15 | 2.67 | 67.9 | 13 | 2.06 | 67.9 | < 0.001 | *** | * | NS |
| Clay (%) | 17.12 | 4.49 | 44.9 | 16.33 | 5.86 | 53.3 | 15.88 | 5.86 | 53.3 | < 0.001 | *** | NS | NS |
| Sand (%) | 46.12 | 9.65 | 13.1 | 48.11 | 12.08 | 16.7 | 49.21 | 12.08 | 16.7 | < 0.001 | *** | NS | NS |
| Silt (%) | 37.13 | 6.78 | 40.01 | 35.79 | 8.21 | 48.6 | 35.34 | 8.21 | 48.6 | < 0.001 | *** | *** | NS |
| *Lantana* cover (%) | 0 (± 2.92) | | | 35 (± 2.01) | | | 85 (±3.01) | | | < 0.001 | | | |

significantly different (ANOVA, P = 0.028; P = 0.039, respectively). Carbon concentration was not significantly different (ANOVA, P=0.395) with regard to the interaction level of site and habitat (Si × Ha) interaction. Except for silt which was not significantly different between highly invaded, moderate and un-invaded sites (ANOVA, P=0.966), the values of pH, conductivity, sand and clay recorded significant differences at site level interaction (ANOVA, P < 0.05) but they were non significant when calculated for both site versus habitat level interaction (ANOVA, P=0.452) (*Table 2*). On the other hand, pH, conductivity, sand and silt recorded strong significant variations across the forest, riparian and shrub grassland habitats (ANOVA, P < 0.001) while clay recorded less significant difference (ANOVA, P=0.237). At the invasion verses habitat interaction level (Si × Ha level interaction), significant differences were recorded in pH (ANOVA, P≤ 0.05) while across sites, conductivity, sand, silt and clay did not vary significantly (ANOVA, P > 0.05). The macronutrient concentrations of Mg, Mn, P, N Ca and K measured in this study were also found to be higher in heavy invaded sites than moderate and un-invaded ones (Table 2). The ANOVA results also supported this findings that plots from where the neighbouring plants were removed and only left with *Lantana*, nitrogen availability significantly increased, indicating that the neighbouring plants reduce the nitrogen availability and by the result it is clearly indicated that exotic and invasive plant like *Lantana* increases the total Nitrogen content in the adjoining soil where they grow (ANOVA, P < 0.001) (Table 3). Species diversity and richness varied significantly among the three levels of *Lantana* infestation as revealed by the Shanon Wiener Index of diversity (H') and species richness (S) [F=9.982, P<0.05, F=24.33, P<0.05 respectively]. The un-invaded category had the highest species diversity and species richness followed by the moderately invaded and highly invaded.

The Principal Component Analysis (PCA) of all the soil parameters and the calculated attributes of *Lantana* are shown in (Fig. 4) respectively. In PCA 1 for soil parameters the Eigen values for both F1 and F2 axes were 34.13 and 30.93 respectively, representing 65.05% of the cumulative variance of soil data. The first principal component was related to K, N, Ca, pH and sand while the second principal component was mainly related to conductivity, silt and soil pH. The PCA shows that soil parameters like pH, available P and K, represent ne-

*Table 3* Two way ANOVA results for the vegetation characters, disturbance types and soil properties. ( df = Degrees of freedom, F = Fisher's statistic value , P value = null hypothesis)

| Factor | Variables | d.f. | F | P value |
|---|---|---|---|---|
| Habitat type | Native species richness | 3, 32 | 22.45 | <0.001 |
| | Exotic species richness | 3, 32 | 63.98 | <0.001 |
| | percentage cover of native species | 3, 32 | 55.38 | <0.031 |
| | Percentage cover of *Lantana* | 3, 32 | 23.33 | <0.001 |
| | *Lantana* density ($ha^{-1}$) | 3, 32 | 19.46 | <0.001 |
| | *Lantana* height | 3, 32 | 18.55 | <0.001 |
| Disturbance type | Native species richness | 3, 32 | 4.89 | <0.013 |
| | Exotic species richness | 3, 32 | 13.55 | <0.001 |
| | percentage cover of native species | 3, 32 | 5.89 | <0.001 |
| | Percentage cover of *Lantana* | 3, 32 | 30.12 | <0.021 |
| | *Lantana* density ($ha^{-1}$) | 3, 32 | 23.34 | <0.001 |
| | *Lantana* height | 3, 32 | 20.03 | <0.005 |
| Soil properties | Native species richness | 3, 32 | 34.22 | <0.001 |
| | Exotic species richness | 3, 32 | 56.34 | <0.001 |
| | percentage cover of native species | 3, 32 | 49.56 | <0.001 |
| | Percentage cover of *Lantana* | 3, 32 | 31.24 | <0.002 |
| | *Lantana* density ($ha^{-1}$) | 3, 32 | 23.22 | <0.001 |
| | *Lantana* height | 3, 32 | 15.35 | <0.001 |

gative correlation with other soil parameters (r = –0.042 with P, 0.109 with K, –0.009 with N and 0.0624 with C). The analysis revealed that the principal components were sufficient in explaining the variation of the soil properties between the highly invaded, moderate and un-invaded sites in Doon valley. After correlation, the results were subjected to an ordination biplot, which revealed that the sites separated into clusters based on the sites and their measured properties. Many of the macro nutrients ratio were showing negative correlation with different calculated attributes but total nitrogen and carbon contents were represented as the key factor for deciding the different shrub attributes and thereby contributing strongly in the total shrub level biomass calculation.

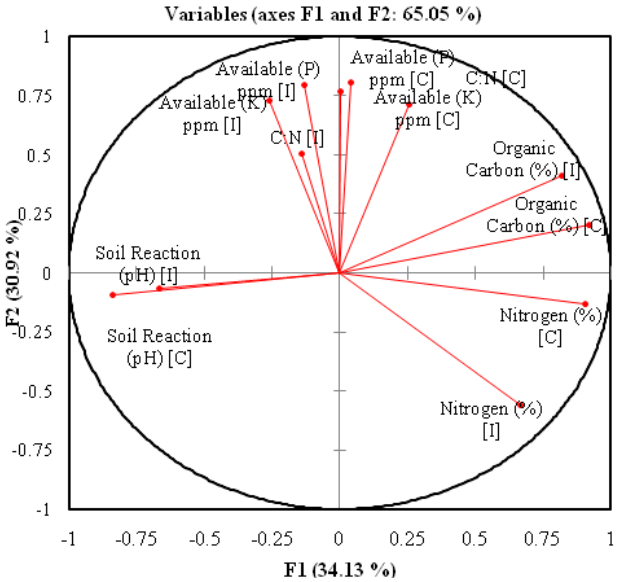


*Fig. 4* PCA ordination for soil properties from different habitats (I = invaded sites, C = control or un-invaded sites)

## DISCUSSION

The moderately invaded plots and the highly invaded plots were located close to the selected invaded patches, being separated only by a few meters. Moreover, preliminary field observations and samples analyse (e.g., texture and cationic exchange capacity) showed that soils of moderate and no invasion areas differ significantly from the highly invaded areas except few. It should also be noted that *Lantana* patches are incessantly escalating in Doon valley but other opportunistic species such as *Chromolaena odorata, Parthenium hysterophorus, Cassia tora, Cassia occidentalis, Urena lobata, Ipomoea carnea, Sida acuta* and *Solanum torvum* and their growth is still restricted to some specific areas and specific geographical conditions. The pH amongst other parameters was found to be a significant factor deciding only the coverage of *Lantana*. In shrub grassland and riverine areas, we found that pH is slightly less acidic to neutral and recorded a little difference between moderate invasion and high invaded sites. However, the less acidic condition favoured *Lantana* to grow better in these habitats than the forest (site data of this study). The density of *Lantana* in shrub grassland was found highest (21,800 $ha^{-1}$) with a maximum biomass of (1.356 Kg $m^{-2}$) followed by another highly disturbed area the riparian zone where the pH was slightly changed from less invaded areas to invaded areas *i.e.*, from 7.12 (±0.40) to 7.22 (±0.24) which was again a neutral to basic condition and found favouring the *Lantana* growth with a density of 20,340 $ha^{-1}$ and biomass (1.296 Kg $m^{-2}$). The increased pH from all the highly invaded sites and even from the moderately invaded sites were found to have a strong positive correlation with the coverage and total shrub density (r= 0.89). The similar change had been recorded from a dry deciduous forest of India (Sharma and Raghubanshi, 2011).

All the moderate and highly invaded areas showed the elevation in soil macronutrients including N, P, K, Ca, Mg, Mn, and took up about twice as much of these macronutrients per unit area as the native plants. This may explain the higher proportion of these above mentioned soil macronutrients fraction in invaded patches. The availability of these macronutrients in the highly invaded soil was recorded much higher than their control *i.e.*, non invaded sites, this clearly indicates that *Lantana* invaded areas have more N, P, K, Ca, Mg, Mn, than less invaded or the places where *Lantana* infestation is negligible and surely this increased level of these macronutrients strongly favoured in increasing their coverage and biomass.

Different attributes like plant height, stem diameter, canopy area and phytovolume were also found directly related to the availability of SOC and total N. Soil organic carbon (SOC) and the total Nitrogen (N) had a direct impact in determining the coverage of *Lantana* and biomass (Table 4). An increase in soil organic carbon (SOC) content under stands of invasive plants had been reported in many previous studies (Fickbohm and Zhu, 2006; Heneghan et al., 2006), and had also been attributed to increase biomass production and litter fall (Yelenik et al., 2004) or to reduce litter decomposition rates (Ogle et al., 2004).The SOC and total N was considerably increased in all the highly invaded sites from all habitat types. The increase in nitrogen and phosphorus levels with increase in *Lantana* intensity could be due to de-

*Table 4* Summary of regression analysis of different sites for soil parameters and its relation with shrub's measured and calculated attributes

| **Measured and calculated parameters** | **Source of variation** | ***SS*** | ***df*** | **MS** | ***F*** | ***P*** |
|---|---|---|---|---|---|---|
| Organic Carbon (%) *Vs* Avg. Plant height (cm) | Between groups | 337346.06 | 1 | 337346 | 90.7557 | 0.032 |
| | Within groups | 52039.074 | 14 | 3717.08 | | |
| | Total | 389385.14 | 15 | | | |
| Nitrogen (%) *Vs* Avg. Plant height (cm) | Between Groups | 341657.79 | 1 | 341658 | 91.9226 | 0.001 |
| | Within Groups | 52035.19 | 14 | 3716.8 | | |
| | Total | 393692.98 | 15 | | | |
| Avg. Height (cm) *Vs* Avg. Crown Diameter | Between Groups | 67606.5 | 1 | 67606.5 | 17.5285 | 0.091 |
| | Within Groups | 53997.22 | 14 | 3856.94 | | |
| | Total | 121603.72 | 15 | | | |
| Nitrogen (%)*Vs* Avg. Plant height (cm) | Between Groups | 105301.87 | 1 | 105302 | 750.756 | 0.102 |
| | Within Groups | 1963.6553 | 14 | 140.261 | | |
| | Total | 107265.53 | 15 | | | |
| Organic Carbon (%)*Vs* Avg. Crown Diameter | Between Groups | 102914.24 | 1 | 102914 | 732.285 | 0.001 |
| | Within Groups | 1967.5395 | 14 | 140.539 | | |
| | Total | 104881.78 | 15 | | | |
| Organic Carbon (%)*Vs* Avg. Shrub Canopy Area ($m^2$) | Between Groups | 0.6102344 | 1 | 0.61023 | 1.45873 | 0.024 |
| | Within Groups | 5.8566423 | 14 | 0.41833 | | |
| | Total | 6.4668767 | 15 | | | |
| Nitrogen (%)*Vs* Avg. Shrub Canopy Area ($m^2$) | Between Groups | 8.5195394 | 1 | 8.51954 | 60.47 | 0.0000 |
| | Within Groups | 1.9724423 | 14 | 0.14089 | | |
| | Total | 10.491982 | 15 | | | |
| Nitrogen (%)*Vs* Canopy Coverage ($ha^{-1}$) | Between Groups | 633273.41 | 1 | 633273 | 134.029 | 0.001 |
| | Within Groups | 66148.655 | 14 | 4724.9 | | |
| | Total | 699422.06 | 15 | | | |
| Organic Carbon (%)*Vs* Canopy Coverage ($ha^{-1}$) | Between Groups | 627398.29 | 1 | 627398 | 132.778 | 0.021 |
| | Within Groups | 66152.539 | 14 | 4725.18 | | |
| | Total | 693550.83 | 15 | | | |
| Organic Carbon (%) *Vs* Phytovolume ($m^3ha^{-1}$) | Between Groups | 5.669324 | 1 | 5.74352 | 55.1941 | 0.011 |
| | Within Groups | 1.438345 | 14 | 1.26653 | | |
| | Total | 7.107233 | 15 | | | |
| Nitrogen (%)*Vs* Phyto-volume ($m^3ha^{-1}$) | Between Groups | 5.669234 | 1 | 5.73442 | 55.1958 | 0.021 |
| | Within Groups | 1.438455 | 14 | 1.22371 | | |
| | Total | 7.107366 | 15 | | | |
| Organic Carbon (% )*Vs* Biomass $m^{-2}$ (Kg) | Between Groups | 10.800708 | 1 | 10.8007 | 28.7303 | 0.011 |
| | Within Groups | 5.2630903 | 14 | 0.37594 | | |
| | Total | 16.063798 | 15 | | | |

crease in nutrient impounding followed by the displacement of native species or reduction in their recruitment and growth rates, also *Lantana* drops a large amount of litter beneath it, this could probably the reason for elevated nitrogen and phosphorus levels in all invaded sites (findings of this study). These findings are consistent with some findings where an increase in soil nitrate followed by *Lantana* invasion was recorded. According to this result nitrogen mineralization and nitrification commonly increase in response to invasions (Ehrenfeld, 2003); this could further explain the increase in available nitrogen that was recorded from the different study sites. N availability in soil is often increased under invasive plants, but reduced N availability has also been found, for example *Bromus tectorum* in arid grassland in the western USA (Evans et al., 2001). The latter effect was typically attributed to the production of nutrient poor litter, leading to slower N mineralization (Drenovsky and Batten, 2007).

The highest SOC (%) was recorded from riparian areas with highest average *Lantana* height, average stem diameter and the lowest was recorded from shrub grassland type habitat which was from 0.98 (±0.47) to 1.28 (±0.23) with an average *Lantana* height of (210cm). These two attributes were found very strong factors in the biomass calculation of shrub (r=0.88) when analysed in the regression model in some studies (Mandal and Joshi, 2014). Plant height was not found significantly correlated with the availability of SOC (%) and total N (%) (r=0.47) and (r=0.57) respectively, but when biomass as a whole taken into account these two soil parameters gave a strong positive correlation (r=0.91) and (r=0.92) respectively (Mandal and Joshi, 2014).

In forest habitat the height of the shrub was found unexpectedly higher than other habitats, this was explained due to the enormous power of *Lantana* to compete with the native species for natural resources like sunlight, as *Lantana* is a photophilous (growing best in strong light) plant, and in closed canopy forest areas it competes with the native trees in order to get more sunlight, this finding was also supported by the earlier study conducted by Sharma and Raghubanshi (2011). Both SOC (%) and total N (%) showed very strong positive correlation while taken as a variable to measure the crown diameter of *Lantana* (r=0.94) and (r=0.98) respectively. Not all the soil carbon is associated with organic material; there is also an inorganic carbon component in soils which is of particular relevance to dry lands because calcification and formation of secondary carbonates is an important process in arid and semi arid regions. Dynamics of inorganic carbon pool are poorly understood although it is normally quite stable.

Differences in litter fall mass interact with differences in the litter decomposition rate to affect the net flux of C into the soil. Many exotic plants have more rapidly decomposing litter than the natives. Decomposition rate may vary with plant tissue, so that differences in plant morphology ultimately control litter dynamics. These results clearly indicates that soil attributes like SOC, total N, P, K and soil textures play a vital role in the growth of *Lantana* in a subtropical deciduous condition like Doon valley. However, the present results clearly revealed that riparian habitat recorded maximum coverage and biomass of *Lantana* followed by grass land and forest habitat. The reason for riparian habitat receiving more coverage and biomass is probably due to the significant change in the soil attributes, open areas and heavy tourist activities. Soil moisture, potassium, nitrogen, soil organic carbon and phosphorus levels varied significantly among these habitats from control to heavy infested areas. Soil nitrogen, soil organic carbon, phosphorus and potassium levels increased with increase in *Lantana* density. Altitude, soil texture and soil depth are unlikely to change significantly following *Lantana* invasion. As a result, the insignificant difference in these variables among the two categories would indicate the homogeneity of the environment. This was supported by the study where disturbance by gophers can be the important factor in the invasion of serpentine grassland by *Bromus mollis* and other non-native annual grasses following years of above average rainfall (Hobbs and Mooney, 1991).

In some studies it was found that soil texture is a useful indicator of soil permeability, soil water retention capacity, and soil capacity to retain cations and influences plant available moisture and plant available nutrients (White, 1997). Some workers considered clay content as an index of nutrient availability (Scholes and Walker, 1993). The greatest influence of pH on plant growth is its effect on nutrient availability. Since the result for moisture and nutrients (soil depth, and texture) did not vary significantly with increase in *Lantana* intensity. It follows that changes in nutrient levels observed could be attributed to *Lantana* invasion effects. Differences in plant species composition reflect difference in soil water and nutrient availability (Scholes, 1990a), and changes caused by *Lantana* in the soil can be translated into plant composition. The increase in nitrogen and phosphorus levels with increase in *Lantana* intensity could be due to decrease in nutrient sequestration following native species displacement or reduction in their recruitment and growth rates. Decrease in soil moisture with increase in *Lantana* intensity shown by this study could be accounted for by the fact that *Lantana* is a short rooted plant, which maximises use of moisture on top layers of the soil, from which soil samples were collected. Furthermore, *Lantana* is very efficient in moisture sequestration leading to reduction in the soil availability of moisture. With increased growth rate, lantana propagates splendidly, which, as verified in this study results into changes in species composition and soil properties.

The structural design of *Lantana* growth is such that it prevents light penetration to the ground. Resulting in noticeable heterogeneity in terms of light availability beneath the *Lantana* bush and affects species diversity underneath its canopy (Fig. 5). Light availability on the forest floor has already been recognized by many researchers as a key factor that influences

fundamental character in propagating exotic species (Jones et al., 1994; Walters and Reich, 1996). The dense cover created by upright stratification of *Lantana* may reduce the strength or duration of light under its canopy and thus decrease the cover of plants specially the herbs. This could be explained due to the formation of a light regime which is photosynthetically inactive and situated at ground level (Fetcher et al., 1983; Turton and Duff, 1992). It is most likely that herbs are directly influenced by the amount of light reaching to the forest floor, and due to the non availability of light to the ground level because of heavy *Lantana* invasion in many habitats especially the riparian habitat the herbaceous cover is declined. This could also be the possible reason in the decline of tree seedlings and the herb flora, this finding was advocated by the findings of Sharma and Raghubanshi (2006, 2007). The current results are also in agreement with (Ehrenfeld, 2003) who documented that soil moisture can either increase or decrease following invasion. These findings where *Lantana* was foundreducing moisture levels are also consistent with the findings by Hiremath and Sundaram (2005) who found that *Lantana* affects water supply negatively.

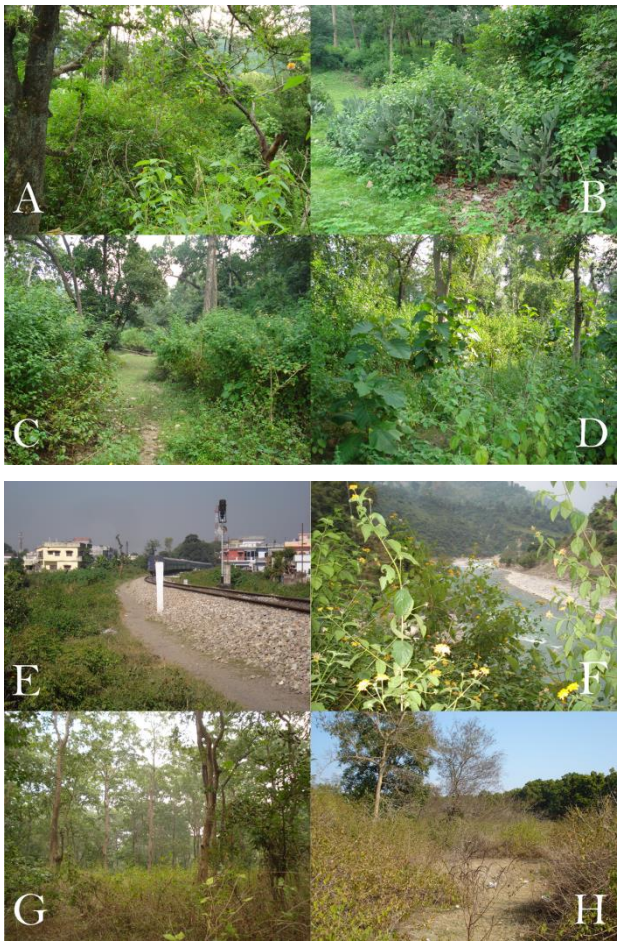


*Fig. 5* Photos of *Lantana camara* taken from the different habitats chosen for this study. [The letters represent different habitat types, such as A, B & C= Forest peripheries, D & E = Shrub grassland and F, G & H = Riparian habitat]

## CONCLUSIONS

The present study had provided strong evidence that *Lantana* invasion is reducing biodiversity and negatively affecting other ecosystem processes in Doon valley and possibly in other nearby areas of its occurrence. In conclusion it is clear from the present findings of this study and the past literature that the invasion of all three habitats including forest communities, riparian areas and the shrub grassland by woody plant invaders, such as *Lantana camara*, adversely affects the vascular plant species diversity by reducing species richness and abundance, in turn altering species compositions. There is also a remarkable change in the soil nutrient property in all the highly invaded areas of Doon valley from its adjacent areas which are either moderately invaded or not invaded by *Lantana*, this change is not only maximizing the uptake of these soil macronutrients by other opportunistic species but also favouring the further utilization of these nutrients by *Lantana* for its own growth. Administration and management of *L. camara* can diminish such adverse effects by facilitating the establishment of native juvenile species to increase species richness. However, management cannot restore species compositions, at least in the short term unless we understand the right factors that influence the distribution of *Lantana* and also initiate continuous monitoring of native forest regeneration following plant invader management, which can prevent secondary weed invasion and indicate whether long term habitat restoration can occur.

### Acknowledgements

We are thankful to the department of Botany and National forest library, ICFRE, Dehradun for providing both laboratory and library facilities. We extend our thanks to the Department of Botany, DAV (PG) College, Dehradun for providing the laboratory and statistical facility. We also thank APEX laboratory services, Dehradun, India for assisting in the soil analysis.

### References

Agrawal, A. A., Kotanen, P. M., Mitchell, C.E., Power, A. G., Godsoe, W., Klironomos, J. 2005. Enemy release? An experiment with congeneric plant pairs and diverse above – and below ground enemies. *Ecology* 86, 2979–2989. DOI: 10.1890/05-0219

Bhagwat, S.A., Breman, E., Thekaekara, T., Thornton, T.F., Willis, K.J. 2012. A Battle Lost? Report on Two Centuries of Invasion and Management of *Lantana camara* L. in Australia, India and South Africa. *PLoS ONE* 7(3), e32407. DOI: 10.1371/journal.pone.0032407

Bone, R., Lawrence M., Magombo, Z. 1997. The effect of a *Eucalyptus camaldulensis (*Dehn) plantation on native woodland recovery on Ulumba Mountain, southern Malawi. *Forest ecology and management* 99, 83–99. DOI: 10.1016/S0378-1127(97)00196-5

Bray, S.R., Kitajima, K., Sylvia, D.M. 2003. Micorrhizae differentially alter growth, physiology and competitive ability of an invasive shrub. Ecological Application 13, 565–574. DOI: 10.1890/1051-0761(2003)013[0565:MDAGPA]2.0.CO;2

Brooks, M.L., D'Antonio, C.M., Richardson, D.M., Grace, J.B., Keeleu, J.E., DiTomaso, J.M., Hobbs, R.J., Pellant, M., Pyke, D. 2004. Effects of Invasive Alien Plants on Fire Regimes. *Bio Science* 54, 677–688. DOI: 10.1641/0006-3568(2004)054[0677:eoiapo]2.0.co;2

Chatanga, P. 2007. Impact of alien invasive species *Lantana camara* L. on native vegetation in northern Gonarezhu National Park, Zim-

babwe. MSc Thesis, Department of Biological sciences, University of Zimbabwe. pp. 22

Cheal, D., Coman, B., Robley, A. 2006. Pest plants and animals. In: Attiwell, P., Wilson, B. (ed.) Ecology: An Australian Perspective, Oxford University Press, South Melbourne. pp. 416–432.

Clegg, S. 1999. Effects of perennial water on soil vegetation and wild herbivore distribution in Southern – eastern Zimbabwe. M.Sc. Thesis submitted to University of Natal, Pietermaritzburg, 80–115.

Cronk, Q.B., Fuller, J.L. 1995. Plant invaders. Chapman and Hall, London. pp. 241

D'Antonio, C.M., Mahall, B.E. 1991. Root profiles and competition between the invasive, exotic perennial, *Carpobrotusedulis*, and two native shrub species in California coastal scrub. *American Journal of Botany* 78, 885–894. DOI: 10.2307/2445167

D'Antonio, C.M., Vitousek, P.M. 1992. Biological invasions by exotic grasses, the grass/fire cycle, and global change. *Annual Review of Ecology and Systematics* 23, 63–87. DOI: 10.1146/annurev.es.23.110192.000431

Davis, M.A., Grime, J.P., Thompson, K. 2000. Fluctuating resources in plant communities: a general theory of invasibility. *Journal of Ecology* 88, 528–34. DOI: 10.1046/j.1365-2745.2000.00473.x

Day, M., Wiley, C.J., Playford, J., Zalucki, M.P. 2003. *Lantana*: Current management status and future prospects. *ACIAR Monograph* 102, 1–125.

Drenovsky, R.E., Batten, K.M. 2007. Invasion by *Aegilops triuncialis* (barb goat grass) slows carbon and nutrient cycling in serpentine grassland. *Biological Invasion* 9, 107–116. DOI: 10.1007/s10530-006-0007-4

Duda, J.J., Freeman, D.C., Emlen, J.M., Belnap, J., Kitchen, S.G., Zak, J.C., Sobek, E., Tracy, M., Montante, J. 2003. Differences in native soil ecology associated with invasion of the exotic annual chenopod, *Halogeton glomeratus*. *Biology and Fertility of Soils* 38, 72–77. DOI: 10.1007/s00374-003-0638-x

Ehrenfeld, J.G. 2003. Effect of exotic plant invasions on soil nutrient cycling processes. *Ecosystems* 6, 503–523. DOI: 10.1007/s10021-002-0151-3

Evans, R.D., Rimer, R., Sperry, L., Belnap, J. 2001. Exotic plant invasion alters nitrogen dynamics in arid grassland. *Ecological Application* 11, 1301–1310. DOI: 10.1890/1051-0761(2001)011[1301:epiand]2.0.co;2

Ferreira, R.L., Marques, M.M. 1998. Litter fauna of arthropods of areas with monoculture of Eucalyptus and heterogeneous secondary forest. *Anais da SociedadeEntomológica do Brasil* 27, 395–403.

Fetcher, N., Strain, B.R., Oberbauer, S.F. 1983. Effects of light regime on the growth, leaf morphology, and water relations of seedlings of two species of tropical trees. *Oecologia* 58, 314 – 319. DOI: 10.1007/bf00385229

Fickbohm, S.S., Zhu, W.X. 2006. Exotic purple loosestrife invasion of native cat tail freshwater wetlands: effects on organic matter distribution and soil nitrogen cycling. *Applied Soil Ecology* 32, 123–131. DOI: 10.1016/j.apsoil.2004.12.011

Gentle, C.B., Duggin, J.A. 1997a. *Lantana camara* L. invasion in dry rainforest ecotones: the role of disturbance associated with fire and cattle grazing. *Australian Journal of Ecology* 22(3), 296–304. DOI: 10.1111/j.1442-9993.1997.tb00675.x

Gordon, R.D. 1998. Effects of invasive, non-indigenous plant species on ecosystem processes.Lessons from Florida. *Ecological Application* 8(4), 975–989. DOI: 10.1890/1051-0761(1998)008[0975:eoinip]2.0.co;2

Guangwei, C. 2002. Biodiversity in the Eastern Himalayas: Conservation through dialogue. Summary reports of the workshops on Biodiversity Conservation in the Hindu Kush-Himalayan Ecoregion.ICIMOD, Kathmandu, Nepal.

Haubensak, K.A., D'Antonio, C.M., Alexander, J. 2004. Effects of nitrogen fixing shrubs in Washington and coastal California. *Weed Technology* 18, 1475–1479. DOI: 10.1614/0890-037x(2004)018[1475:eonsiw]2.0.co;2

Hawkes, C.V., Wren, I.F., Herman, D.J. 2005. Firestone MK; Plant invasion alters nitrogen cycling by modifying the soil nitrifying community. *Ecology Letters* 8, 976–985. DOI: 10.1111/j.1461-0248.2005.00802.x

Heneghan, L., Fatemi, F., Umek, L., Grady K., Fagen, K., Workman, M. 2006. The invasive shrub European buckthorn (*Rhamnus cathartica* L.) alters soil properties in Midwestern US woodlands. *Applied Soil Ecology* 32, 142–148. DOI: 10.1016/j.apsoil.2005.03.009

Hill, S.J., Peter, J.T., Leishman, M.R. 2005. Relationships between anthropogenic disturbance, soil properties and plant invasion in endangered Cumberland Plain Woodland, Australia. *Austral Ecology* 30, 775–788. DOI: 10.1111/j.1442-9993.2005.01518.x

Hiremath, A.J., Sundaram, B. 2005. The fire *Lantana camara* cycle hypothesis in Indian forests.*Conservation and Society* 3(1), 26–42. DOI: 10.1007/s10530-011-0144-2

Hobbs, R.J., Mooney, H.A. 1991. Effects of rainfall variability and gopher disturbance on serpentine annual grassland dynamics in N. California. *Ecology* 72, 59–68. DOI: 10.2307/1938902

Hulme, P.E. 2009. Trade, transport and travel: managing invasive species pathways in an era of globalization. *Journal of Applied Ecology* 46, 10–18. DOI: 10.1111/j.1365-2664.2008.01600.x

India State Forest Report.2013. State Forest Report of 2013, Forest Survey of India, Ministry of Environment and Forests Government of India, Dehra Dun, India.

Jones, R.H., Sharitz, R.R., Dixon, P.M., Segal, D.S., Schneider, R.L. 1994. Woody plant regeneration in four floodplain forests. *Ecological Monograph* 64, 345–367. DOI: 10.2307/2937166

Khuroo, A.A., Reshi, Z.A., Malik, A.H., Weber, E., Rashid, I., Dar, G.H. 2012. Alien flora of India: taxonomic composition, invasion status and biogeographic affiliations. *Biological Invasions* 14, 99–113.

King, S.A., Buckney, R.T.G. 2002. Invasion of exotic plants in nutirent-enriched urban bushland. *Austral Ecology* 27,573–583. DOI: 10.1046/j.1442-9993.2002.01220.x

Kohli, R.K., Batish, D.R., Singh, H.P., Dogra, K. 2006. Status, invasiveness and environmental threats of three tropical American invasive weeds (*Parthenium hysterophorus* L., *Ageratum conyzoides* L. and *Lantana camara* L.). *Biological Invasions* 8, 1501–1510. DOI: 10.1007/s10530-005-5842-1

Kourtev, P., Ehrenfeld, J., Häggblom, M. 2002. Exotic plant species alter the microbial community structure and function in the soil. *Ecology* 83, 3152–3166. DOI: 10.1890/0012-9658(2002)083[3152:epsatm]2.0.co;2

Kourtev, P., Ehrenfeld, J., Häggblom, M. 2003. Experimental analysis of the effect of exotic and native plant species on the structure and function of soil microbial communities. *Soil Biology and Biochemistry* 35, 895–905. DOI: 10.1016/s0038-0717(03)00120-2

Lake, J.C., Leishman, M.R. 2004. Invasion success of exotic plants in natural ecosystems: the role of disturbance, plant attributes and freedom from herbivores. *Biological Conservation* 117, 215–226. DOI: 10.1016/s0006-3207(03)00294-5

Le Maitre, D.C., Van Wilgen, B.W., Chapman, R.A., McKelly, D.H. 1996. Invasive plants and water resources in the Western Cape Province, South Africa: modelling the consequences of a lack of management. *Journal of Applied Ecology* 33, 161–172.

Leishman, M.R., Thomson, V.P. 2005. Experimental evidence for the effects of added water, nutrients and physical disturbance on invasive plants in low fertility Hawkesbury Sandstone soils, Sydney, Australia. *Journal of Ecology* 93, 38–49. DOI: 10.1111/j.1365-2745.2004.00938.x

Leishman, M.R., Hughes, M.T., Gore, D.B. 2004. Soil phosphorus enhancement below storm water outlets in urban bushland: spatial and temporal changes and the relationship with invasive plants. *Australian Journal of Soil Research* 42, 197–202. DOI: 10.1071/sr03035

Mandal, G., Joshi, S.P. 2014. Biomass calculation and carbon sequestration potential of *Shorea robusta* and *Lantana camara* from the dry deciduous forests of Doon Valley, western Himalaya, India. *International Journal of Environmental Biology* 4(2), 157–169. DOI: 10.1016/j.japb.2014.07.006

Myers, N., Mittermeier, R.A., Mittermeier, C.G., Da Fonseca, G.A.B., Kent, J. 2000. Biodiversity hotspots for conservation priorities. *Nature* 403(24), 853–858. DOI: 10.1038/35002501

Ogle, S.M., Ojima, D., Reiners, W.A. 2004. Modelling the impact of exotic annual Brome grasses on soil organic carbon storage in a northern mixed grass prairie. *Biological Invasion* 6, 365– 377. DOI: 10.1023/b:binv.0000034629.68660.28

Okalebo, R.J., Gathua, W.K., Woomer, L.P. 2002. Laboratory manual of soil and plant analysis: A working Manual, second Edition, Nairobi, Kenya: Soil Science Society East Africa Publication. pp. 58–60.

Olson, D.M., Dinerstein, E. 2002. The Global 200; Priority ecoregions for global conservation.*Annals of Missouri Botanical Garden* 89, 199–224. DOI: 10.2307/3298564

Olson, D.M., Dinerstein, E., Wikramanayke, E.D., et al. 2001. Terrestrial ecoregions of the world: A new map of life on earth. *Bio Science* 51(11), 993–1038. DOI: 10.1641/0006-3568(2001)051[0933:teotwa]2.0.co;2

Piper, C.S. 1944. Soil and Plant Analysis. Interscience Publication, New York.

Ridenour, W.M., Callaway, R.M. 2001. The relative importance of allelopathy in interference: the effects of an invasive weed on a native bunchgrass. *Oecologia* 126, 444–450. DOI: 10.1007/s004420000533

Ross, I.A. 1999. Medicinal plants of the world. Chemical constituents, traditional and modern medical uses. Humana Press, New Jersey, USA.

Saggar, S., McIntosh, P., Hedley, C., Knicker, H. 1999. Changes in soil microbial biomass, metabolic quotient and organic matter turnover under *Hieracium pilosella* L. *Biology and Fertility of Soils* 30, 232–238. DOI: 10.1007/s003740050613

Scholes, R.J. 1990a. The influence of soil fertility on the ecology of Southern African Dry Savannas.*Journal of Biogeography* 17, 415–419. DOI: 10.2307/2845371

Scholes, R.J., Walker, B.H. 1993. An African Savanna: Synthesis of the Nysvley Study. Cambridge University Press, Cambridge. pp. 33 – 77

Schwartz, M.W., Porter, D.J., Randall, J.M., Lyons, K.E. 1996. Impact of non indigenous plants. Sierra Nevada Ecosystem Project: Final Report to Congress. Volume 2. Assessments and scientific basis for management options. Centers for Water and Wild and Resources, University of California, Davis, California, USA, pp. 1203–1218.

Sharma, G.P., Raghubanshi, A.S. 2011. *Lantana camara* L. invasion and impact on herb layer diversity and soil properties in a dry deciduous forest of India. *Applied Ecology and Environmental Research* 9(3), 253–264. DOI: 10.15666/aeer/0903_253264

Sharma, G.P, Raghubanshi, A.S. 2006. Tree population structure, regeneration and expected future composition at different levels of *Lantana camara* L. invasion in the Vindhyan tropical dry deciduous forest of India. *Lyonia* 11(1), 25–37.

Sharma, G.P., Raghubanshi, A.S. 2007. Effect of *Lantana camara* L. cover on plant species depletion in the Vindhyan tropical dry deciduous forest of India.*Applied Ecology and Environmental Research* 5(1), 109–121. DPO_ 10.15666/aeer/0501_109121

Shinwari, Z.K., Qaisar, M. 2011. Efforts on conservation and sustainable use of medicinal plants of Pakistan.*Pakistan Journal of Botany* 43(Special Issue), 5–10.

Shinwari, Z.K., Gilani, S.A., Khan, A.L. 2012. Biodiversity loss, emerging infectious diseases and impact on human and crops. *Pakistan Journal of Botany* 44(Special Issue), 137–142.

Turton, S.M., Duff, G.A. 1992. Light environments and floristic composition across an open forest-rainforest boundary in north eastern Queensland. *Australian Journal of Ecology* 17, 415–423. DOI: 10.1111/j.1442-9993.1992.tb00824.x

Van Wilgen, B.W., Richardson, D.M. 1985. The effects of alien shrub invasion on vegetation structure and fire behaviour in South African fynbos shrubland: A simulation study. *Journal of Applied Ecology* 22, 455–466. DOI: 10.2307/2403243

Vitousek, P.M., Walker, L.R. 1989. Biological invasion by *Myricafaya* in Hawaii: Plant demography, nitrogen fixation, ecosystem effects. *Ecological Monographs* 59, 247–265. DOI: 10.2307/1942601

Vitousek, P.M., D'Antonio, C.M., Loope, L.L., Rejmanek, M., Westbrooks, R. 1997.Introduced species: a significant component of human caused global change. *New Zealand Journal of Ecology* 21, 1–16.

Vranjic, J.A., Woods, M.J., Barnard, J. 2000. Soil mediated effects on germination and seedling growth of coastal Wattle (*Acacia sophorae*) by the environmental weed bitou bush (*Chrysanthemoides monilifera* subsp. *rotundata*). *Austral Ecology* 25, 445–453. DOI: 10.1046/j.1442-9993.2000.01086.x

Walkley, A.J., Black, I.A. 1934. Estimation of soil organic carbon by the chromic acid titration method. *Soil Science* 37, 29–38

Walters, M.B., Reich, P.B. 1996. Are shade tolerance survival and growth linked? Low light and nitrogen effects on hardwood seedlings. *Ecology* 77, 841–853. DOI: 10.2307/2265505

White, R.E. 1997. Principles and Practices of Soil Sciences: The Soil as a Natural Resourece. Blackwell Science, Oxford, 44–88

Yelenik, S.G., Stock, W.D., Richardson, D.M. 2004. Ecosystem level impacts of invasive *Acacia saligna* in the South African fynbos. *Restoration Ecology* 12, 44–51. DOI: 10.1111/j.1061-2971.2004.00289.x

Yurkonis, K.A., Meiners, S.J., Wachholder, B.E. 2005. Invasion impacts diversity through altered community dynamics. *Journal of Ecology* 93, 1053–1061. DOI: 10.1111/j.1365-2745.2005.01029.x

JOURNAL OF ENVIRONMENTAL GEOGRAPHY
*Journal of Environmental Geography* 7 (3–4), 43–51.
DOI: 10.2478/jengeo-2014-0011
ISSN: 2060-467X

# DROUGHT SEVERITY AND ITS EFFECT ON AGRICULTURAL PRODUCTION IN THE HUNGARIAN-SERBIAN CROSS-BORDER AREA

**Károly Fiala[1*], Viktória Blanka[2], Zsuzsanna Ladányi[2], Péter Szilassi[2], Balázs Benyhe[1], Dragan Dolinaj[3], Imre Pálfai[1]**

[1] Lower-Tisza Water Directorate, Stefánia 4, H-6720 Szeged, Hungary
[2]Department of Physical Geography and Geoinformatics, University of Szeged, Egyetem u. 2-6, H-6722 Szeged, Hungary
[3] Climatology and Hydrology Research Centre, Faculty of Science, University of Novi Sad, Dositeja Obradovića 3, 21000 Novi Sad, Serbia
*Corresponding author, e-mail: FialaK@ativizig.hu

Research article, received 20 July 2014, accepted 15 October 2014

**Abstract**

Several environmental and economic consequences of drought and the accompanying water shortage were observed in the plain area of the Carpathian Basin in the last decades. This area is mostly used for agriculture, thus it is a key problem in the future to maintain food safety in the changing circumstances. Therefore, involvement and identification of areas affected by drought hazard and revealing steps of efficient adaptation are of high importance. In this study influence of drought severity on agricultural production is investigated in the Hungarian-Serbian cross-border area. The tendency in drought severity was analysed by PaDI and MAI drought indices. The effect of drought on agricultural production is evaluated on maize yield data as the most drought sensitive crop in the region. Increasing drought frequency and severity was indicated for the study area for the period of 1961-2012. The spatial assessment of annual PaDI maps revealed the higher exposure of the north and north-eastern part of the study area to drought, where drought frequency was also experienced to be the highest. Increased sensitivity was detected based on maize yield loss after the early 1990s and annual yields were in strong connection with drought severity. In spite of the technological development of agriculture, environmental factors still substantially affect crop yields. The observed unfavourable changes in the region mean that water management and spatial planning faces conceptual challenges to prevent and mitigate the damages of drought.

**Keywords:** climate change, drought, PaDI, agriculture, yield loss

## INTRODUCTION

Drought is one of the most important environmental hazards in Southern and Eastern Europe. The lack of water during drought periods have effect on many sectors (e.g. agriculture, energy production, industrial water use, health care, tourism) (Warrick et al., 1975; Maracchi, 2000; Svoboda et al., 2002; Zeng, 2003; Lei et al., 2011; Ye et al., 2012; Lin et al., 2013 Wisner et al., 2004) and also on ecology (Poiani et al., 1995, Winter, 2000, Parmesan, 2003, Normand et al., 2007, Beierkuhnlein et al., 2011, Pitchford et al., 2012).

Drought is a complex phenomenon influenced by the quantity and temporal distribution of precipitation, temperature, air humidity etc. In Hungary, due to climate change a 0.8°C rise in surface temperatures and a 60–80 mm decrease in precipitation were detected in the Carpathian Basin in the last century (Rakonczai, 2011) and increasing rate and occurrence of drought was described in the last decades (Bihari, 2006; Bartholy et al., 2007). Spasov et al. (2002) also reported that drought is also a quite often natural hazard in Serbia; dry years were particularly frequent in the last two decades of the 20th century. The strength of drought in South-eastern Europe shows different spatial distribution year by year. The map constructed from the 10% probability of Pálfai Drought Index (PaDI) occurrence showing the spatial pattern of drought inside the South-Eastern Europe (SEE) region (Pálfai and Herceg, 2011) clearly confirms the fact that the Hungarian-Serbian cross-border area is seriously affected by drought.

In the last decades several environmental and economic consequences of drought and the accompanying water shortage were observed in the plain area of the Carpathian Basin. Environmental consequences of drought are the decreasing groundwater table (Major and Neppel, 1988; Szalai, 2011; Rakonczai et al., 2012), reduction surface water cover (Kovács, 2008), alteration of soil properties (Ladányi et al. 2009; Puskás et al., 2012) and vegetation changes (Biró et al., 2008; Molnár et al,. 2008; Ladányi et al., 2010). The Great Plain is highly important in agricultural aspects for its countries, since it is mostly covered by high fertility soils and the fields are used as arable lands. Droughts stress due to water scarcity and heat

waves cause significant yield loss. In drought years, 40-50% loss is observed in the southern Great Plain, and in plot scale, total crop loss is experienced.

In spite of the dramatic technological development of agriculture (e.g. irrigation systems, new seeds for sowing, genetic modification), environmental factors such as climate, ecology and soil attributes still substantially affect crop yields. It is a key problem in the future to maintain food safety in the changing circumstances, therefore involvement and identification of areas affected by drought hazard and revealing steps of efficient adaptation are of vital importance. In this study the influence of drought severity on agricultural production is investigated in the Hungarian-Serbian cross-border area of the SEE region. Drought severity is calculated by two indices mostly used in Hungary and Serbia, and its effect on agricultural production is evaluated.

## STUDY AREA

The study area, South Hungary and the plain areas of Vojvodina, is situated in the southern part of the Carpathian Basin (Fig. 1). Similar physical-geographical features describe the area, where annual mean temperature is around 11 °C and the annual amount of precipitation is between 500-600 mm. In July the mean temperature is around 21 °C and 23 °C, the precipitation in the summer half-year is at about 300 mm (Smailagic et al., 2013; OMSZ, 2014). The dominant soil type is chernozem and its subtypes both in the Hungarian and the Serbian areas; furthermore meadow and sandy soils can also be found. The dominant land use type in the area is arable land based on Corine Land Cover 2006, thus the effect of drought on the agricultural production has high importance on the economy of the region.

## METHODS

*Calculation of drought severity*

Meteorological factors play a significant role in the formation of drought, thus by their assessment, drought severity can be quantified. Pálfai Drought Index (PaDI) (Pálfai and Herceg, 2011) and the Moisture Availability Index (MAI) (Hargreaves, 1975) were used to describe droughts of the past decade for the right bank-side catchment of Tisza and in Vojvodina.

The PaDI uses monthly temperature and precipitation data for the calculation and it characterises the drought with one numerical value that is associated with one agricultural year. The index is calculated as follows:

$$PaDI = \frac{\left[\sum_{i=apr}^{aug} T_i\right] \;/\; 5}{\sum_{i=oct}^{sept} \left(P_i * w_i\right)} * 100 * k_t * k_p * k_{gw}$$

where $T_i$ is the mean monthly temperature from April to August, $P_i$ is the monthly sum of precipitation from October to August, $w_i$ is a weighting factor expressing

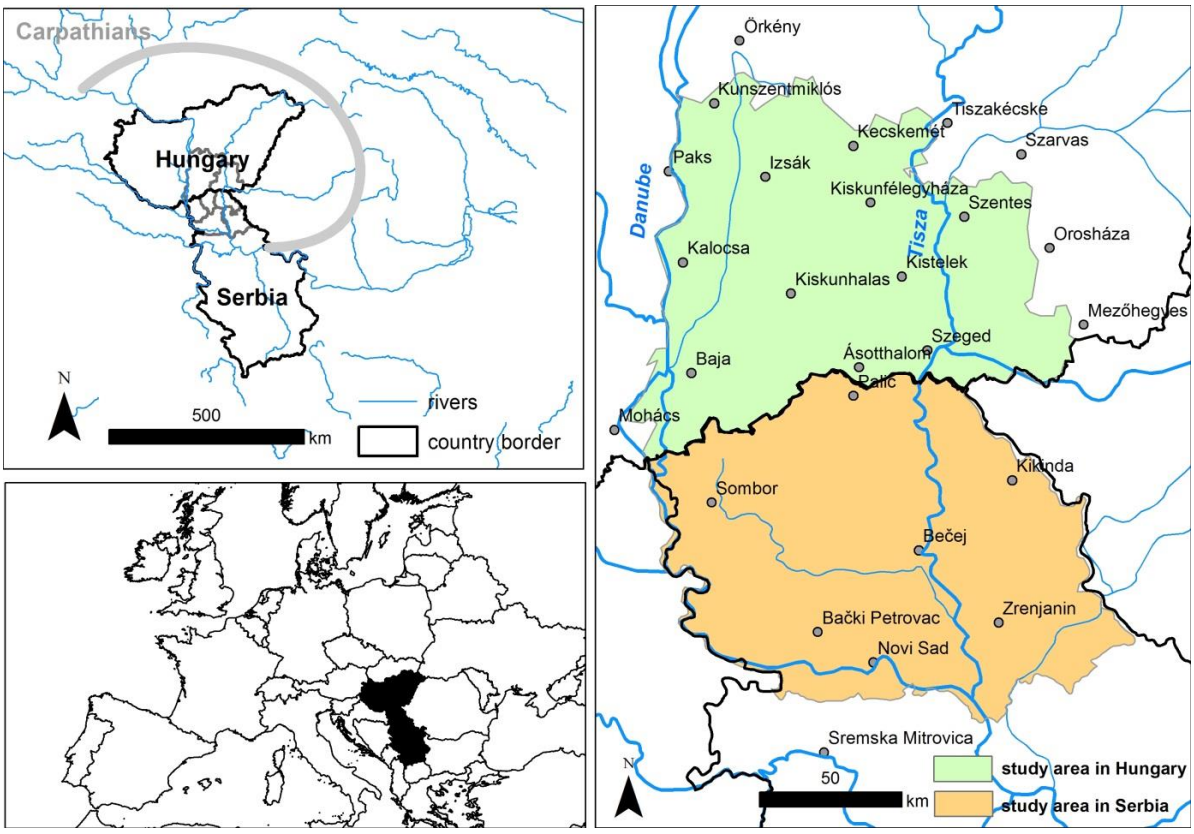


*Fig. 1* Location of the study area and the meteorological stations

the importance of the months in the evolution of drought, while $k_t$, $k_p$, and $k_{gw}$ are correction factors assessing the temperature, precipitation and groundwater conditions in the preceding years.

PaDI was calculated for each year in the period of 1961-2012. The tendency in drought severity was analysed by dividing the full period into two parts (1961-1987 and 1988-2012) calculating the average index value for both period. The changes of drought frequency were analysed by yearly drought index based on the average value of all stations. Spatial analysis of drought severity was also carried out by producing drought maps for each year.

The Moisture Availability Index (MAI) is a relative measure of the adequacy of precipitation in supplying moisture requirements (Hargreaves 1975). The MAI is suitable to evaluate the climate resource for agricultural production. The index is the ratio between monthly precipitation and reference evapotranspiration and this takes into account water requirements too (Hargreaves and Keller 2005). The MAI can be calculated at different time scales (monthly, seasonal, and annual). The MAI is calculated as:

$$MAI = \frac{AE}{PE}$$

where AE is the actual evapotranspiration and PEis the potential evapotranspiration.

*Analysis of the effects on agricultural production*

For analysing the effect of drought on agricultural production maize yield data were evaluated as the most drought sensitive crop in the region. To assess the spatial differences in yield loss, county level yield data were used for Hungary in the year 2012, which was the most recent serious drought in the region. The rate of yield loss compared to the mean value of the 2000-2012 was calculated in percentage for each Hungarian county.

In the study area the yearly anomalies of maize yield between 2000 and 2009 were calculated and compared to the mean value of the 2000-2012 for the south-eastern Hungarian counties (Bács-Kiskun and Csongrád) and for Vojvodina to assess the effect of drought in the different years and to identify the years when yield loss was significant. Moreover by the analysis of the data of the two countries, it can also be identified, whether the variability of yield is similar in both countries, meaning that the changes are irrespective of the different cultivation practices.

Finally the yearly yield data were compared to the yearly PaDI values between 1961 and 2012 to reveal the connection between the drought severity and maize yields.

## RESULTS

*Analysis of past and present droughts*

Analysis of Pálfai Drought Index in the study area

Based on the calculated Pálfai Drought Indices (PaDI) drought severity show increasing tendency in the region. A significant increase of the average PaDi value was observed between the two analysed period (1961-1987 and 1988-2012) on nearly all stations (Fig. 2). In the first period the average PaDI values varied between 4 and 5.5 °C/100 mm. The highest average value was observed on northern part of the area (Örkény station), while the lowest average value was detected on the southern part (Bečej station). In the second period PaDI values varied between 4.6 and 7.1 ° C/100 mm. In this period the drought severity was higher in the eastern part of the area, the highest average value occurred on north-eastern part (Tiszakécske) also in this period. The highest increase between the periods was identified and Tiszakécske station (north-eastern part), where PaDI value increased by 2 °C/100 mm, while a slight decrease in drought severity was observed at one station (Paks on the western part).

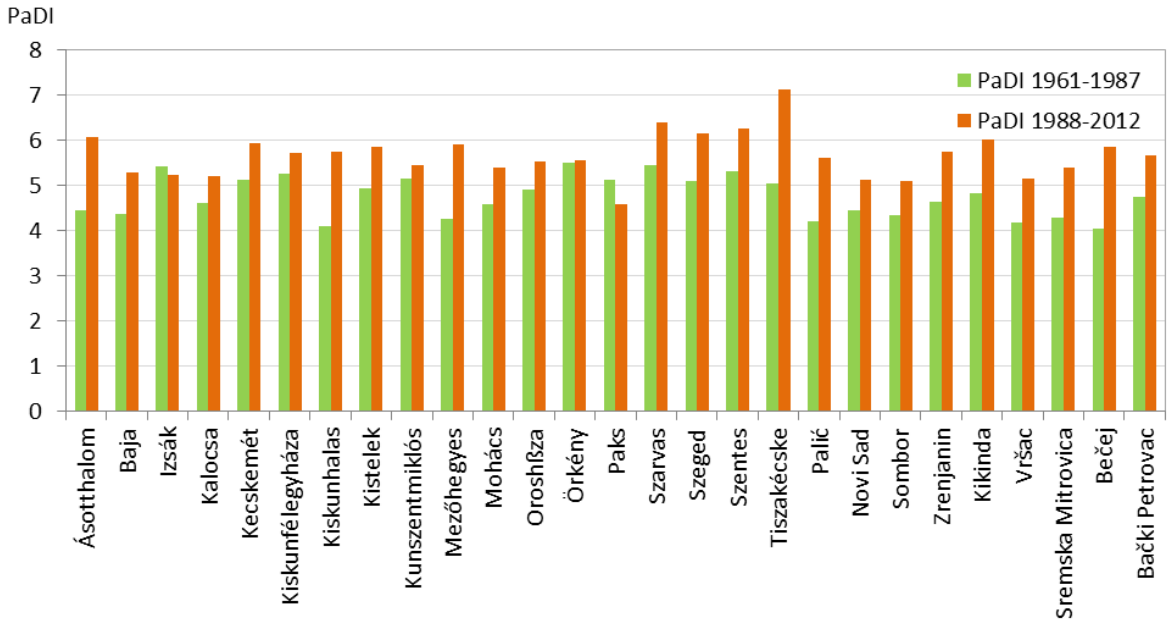


*Fig. 2* Changes of PaDI mean values in the studied stations in Hungary in the two partial periods

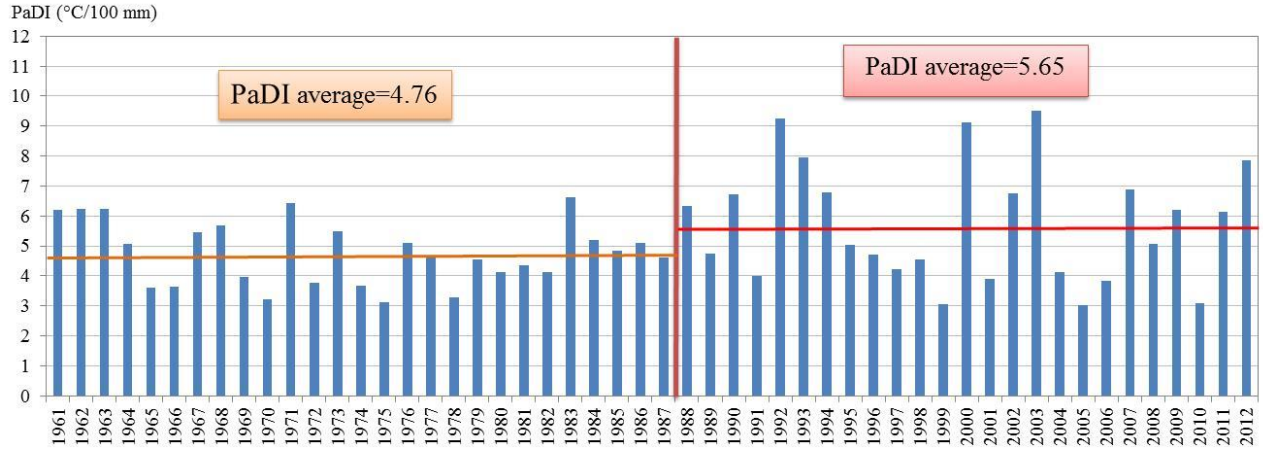


*Fig. 3* Mean PaDI values at the studied stations between 1961 and 2012

Drought severity can be defined by the degree of water scarcity, though sometimes this parameter is not considered appropriate for the affected sectors. Agriculture, ecology, industry and society have completely different water needs. Because of these various needs this question can be approached with reference to the average precipitation of the affected area. Precipitation amounts compared to the long-term average are suitable to describe the water shortage. Several researchers dealt with this issue (e.g. Szalai, 2009; Bartholy and Pongrácz, 2005) and maps of the areas with water deficiency were produced. According to these studies, water deficiency is between 100 mm and 200 mm in drought periods on the catchment area, which could be even higher in extreme circumstances. The problem can be increased when drought occurs on the same area for consecutive years since water shortage becomes more and more pronounced if no significant water refill is taken place.

Besides drought severity, frequency also has to be assessed to assess the importance of drought problem in the area. For assessing drought frequency regional averages were calculated for each years based on data of all stations. Fig. 3 shows that not only severity, but frequency also increased. In the first period (1961-1987), the annual drought index had reached the value of 6 °C/100 mm only in 5 years (moderate drought) in the 27-year long period. The most severe drought occurred in 1983, when the PaDI value was 6.6, which also means only moderate drought.

A more considerable change could be observed in the second period (1988-2012). Drought years occurred more frequently, the annual drought index exceeded the value of 6 °C/100 mm in 12 years in the 25-year long period. Moreover in this period more serious droughts occurred than in the first period. Heavy droughts also evolved in the region, PaDI value exceeded the value of 8 °C/100 mm in 3 years. The most severe drought occurred in 2003, when the PaDI value was 9.5 °C/100 mm. Data have pointed out that the area is affected at least by moderate drought in every 2 years, and heavy droughts are also recorded, causing serious damages. Beside the increasing severity, the variability of droughts between the years was also higher in the second period. The lowest PaDI value of the whole studied period (1961-2012) occurred in the second period.

In the studied region, considerable spatial differences can also be observed. Drought sensitivity is quite different, thus areas can be allocated where drought years occurred more frequently. Drought occur most frequently on the northern, north-eastern part of the study area, thus this area is the most effected. The average drought severity, calculated for the two periods, also indicated this area as the most affected.

Obviously, consecutive years differ from each other; therefore the spatial pattern of drought severity is different from year to year. Some characteristic example of the spatial differences is shown on Fig. 4. In 1983,

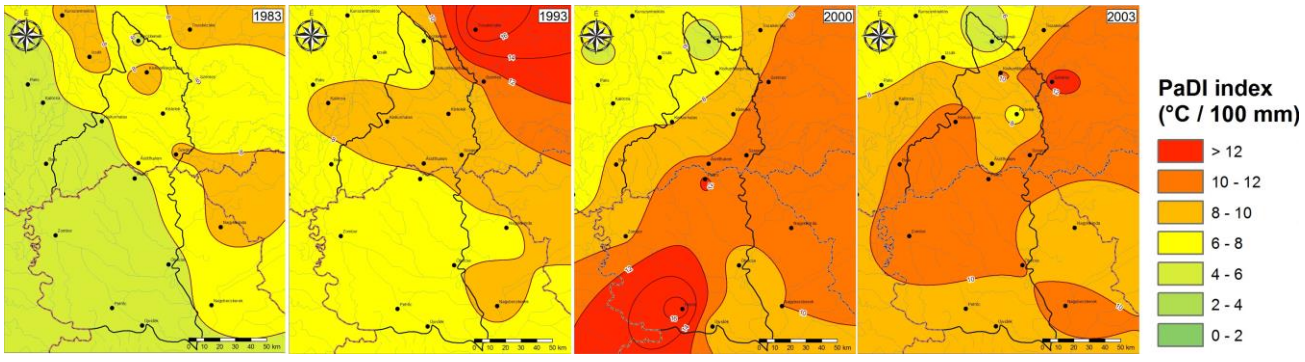


*Fig. 4* Distribution of PaDI values in 1983, 1993, 2000 and in 2007 (4-6: slight drought; 6-8:moderate drought; 8-10: heavy drought; 10-12: serous drought; 12-14: very serious drought; >14: extreme drought)

which was the most severe drought year in the period of 1961-1987, the north-eastern part of the area was more affected. This drought was evolved due to the warmer weather from winter to August and this warm period was associated with precipitation lower than average in almost every months. The dry autumn and snowless winter of the year 1989 contributed to the formation of droughts for the next years. In 1990 the low level of groundwater, followed by a hot July and August with no rainfall, resulted in huge losses in maize yield. The same causes could be determined the development of drought in 1992 and 1993 with similar severity to that of 1990. Based on the temperature data for 1992, the annual mean temperature for the April-August period was 18.8°C, which was not extreme, however the mean monthly temperature in August exceeded 25 °C, which meant new records since observations. The number of heat days in the three summer months was over 37 days, which is twice as much as the average value. The last quarter of the previous year precipitation exceeded the long-term average. After December, the monthly sums were below the long-term average, except June. During the warmest period there was no precipitation, the dry period without precipitation was more than 30 days on the affected area. The PaDI values were between 11-14 °C/100 mm.

The drought in 2000 was preceded by huge inland excess water inundations as a result of the precipitation in November and December in 1999, which was twice the amount of the average precipitation of these months. January and February was characterised by few precipitation, and then March and April were slightly more humid. However, after 7th April, an extremely long dry period started lasting until the first week of July then it went on after a short break. 216 mm precipitation was recorded for the whole calendar year in Szeged. Most stations in the Danube-Tisza Interfluve measured less than 300 mm. The precipitation did not reach 60 mm from April to August. The number of heat days was extremely high. These both contributed to severe drought, PaDI values exceeded 10 °C/100 mm (Fig. 4). The drought affected the area of Vojvodina much more seriously, here the PaDI values reached 12-14 °C/100 mm.

Prior to the drought in 2007, the area was affected largely by inland excess water inundations and a record-size flood in 2006. In spring time of 2007 water scarcity could be expected since a long arid period was experienced in the autumn and winter of 2006. The 3-month precipitation sum was only half of the long-term average. Besides these, winter months were unusually warm. The monthly mean temperature was around 4–5°C, while the long-term average is -1-1.5°C. Accordingly, evaporation was higher, which further increased the water shortage. An average amount of precipitation fallen at the beginning of spring, and then in April hardly any rain could be measured. The situation slightly moderated during the period starting in May defined by heavy rains, however, serious drought evolved as the summer heat arrived. The daily maximum temperature from mid-July exceeded 36°C. There were 50-60 heat days on the Great Hungarian Plain. The precipitation was half of the long-term average. Precipitation further decreased in August – one third of the amount typical for the area fell, which resulted in extreme drought (Fig 4). In 2007 moderate and mild drought could be observed in Vojvodina according to the values of Pálfai Index.

The most severe drought of the past 50 years evolved in 2012. Considering the national average, scarcely more than 400 mm precipitation was measured in 2011, which is two-thirds of the long term average. The annual precipitation was 325-400 mm in the study area (Fig. 4). The dry period continued in the first half of 2012. The precipitation on the catchment area was 30% less, while at certain places there was a decrease of 50% compared to the long-term average. On average, 225 mm precipitation was recorded until August (only about 5 mm fell in August), while the long-term average was 380 mm. The entire catchment area, especially the NE part of the area, was extremely dry (Fig. 4). The extremely high temperature in July and August intensified the unusual aridity. The monthly mean temperature was 3-4°C over the long-term average and there were 60 heat days in this year. Due to the superponation of the extreme weather elements, extreme and severe droughts developed on 80% of the catchment area.

Further analysis of drought indices in the Vojvodina part of the study area

Dry years were particularly frequent in the last two decades of the 20$^{th}$ century in Serbia as well (Spasov et al., 2002; Gocic and Trajkovic, 2013). Gocic and Trajkovic (2014) allocated North Serbia as a region with precipitation values under the average value of Serbia. The demonstration of the results was based on the meteorological station Rimski Sancevi, which is located 15 km from Novi Sad, because its statistics are exceedingly similar to the average meteorological values throughout Vojvodina. Measuring precipitation throughout critical months such as July and August for the period of 88 years (1924-2012) shows that 84.27% of the years July, and 84.27% of the years August were arid. The amount of the precipitation evidently was not sufficient to satisfy crop water requirements, which was above 100 mm from June to August (Table 1). The moisture Availability index (MAI) in the region very low, particularly in August (Table 2), and there are some spatial differences (Table 3). Regions where MAI index is under 0,33 are very deficient, 0,34-0,66 moderately deficient, 0,67-0,99 somewhat deficient, 1,0-1,33 adequate moisture and above 1,34 excessive moisture. According to analysis the climate circumstances in Vojvodina are semi arid, and semi humid.

The period 1924-2003 was analysed in terms of sufficient amount of water, specified by the precipitation that crops need for regular growth consistent with Hardgrave's' model and index. Model is based on the analysis of 75% precipitation (P) and potential evapotranspiration (ETo). Based on the assessment, the area of Vojvodina has semi arid or arid climate during summer, which is not favourable for successful crop production, thus irrigation has high importance in the region.

*Table 1* Percentage of the arid periods for all precipitation amounts in July and August, in Vojvodina (HMS Novi Sad), from 1924 to 2012

| precipitation (mm) | July | | August | | drought severity |
|---|---|---|---|---|---|
| | Nr of years | % | Nr of years | % | |
| 0-25 | 13 | 14.6 | 21 | 23.6 | extremely drought |
| 26-50 | 33 | 37.1 | 24 | 27.0 | very drought |
| 51-75 | 19 | 21.4 | 19 | 21.3 | drought |
| 75-100 | 10 | 11.2 | 11 | 12.4 | moderately drought |
| | 75 | 84.3 | 75 | 84.3 | total drought |
| 101-125 | 7 | 7.9 | 10 | 11.2 | moderately rainy |
| >126 | 7 | 7.9 | 4 | 4.5 | pluvial |
| total | 89 | 100 | 89 | 100 | |

*Table 2* Moisture Availability index (MAI) in Vojvodina

| Parameter | Months | | | | |
|---|---|---|---|---|---|
| | V | VI | VII | VIII | IX |
| P (mm) | 46 | 68 | 50 | 40 | 32 |
| ETP (mm) | 77 | 118 | 139 | 130 | 61 |
| MAI | 0.60 | 0.58 | 0.36 | 0.31 | 0.52 |

*Table 3* Potential evapotranspiration (ETo), and precipitation with probability of 75% and moisture availability index (MAI)

| Months | | VI | VII | VIII | VI-VIII |
|---|---|---|---|---|---|
| ETo | | 100 | 100-120 | 100-120 | 300-340 |
| P (mm) | Subotica | 52 | 44 | 44 | 140 |
| | Novi Sad | 70 | 44 | 39 | 165 |
| | Sremska Mitrovica | 70 | 44 | 32 | 174 |
| MAI | Subotica | 0.52 | 0.44-0.37 | 0.44-0.37 | 0.46-0.41 |
| | Novi Sad | 0.70 | 0.44-0.37 | 0.39-0.32 | 0.55-0.48 |
| | Sremska Mitrovica | 0.70 | 0.44-0.37 | 0.32-0.26 | 0.58-0.51 |

*Analysis of the effects on agricultural production*

Yield loss

According to the wheat and maize yield data of Hungarian Central Statistical Office, the most dominant field crops, in the period of 2000-2012 yields in 2000, 2002, 2003, 2007, 2009 and 2012 were below the average of the period, and maize showed the greater anomalies. The highest decrease of crop yield was seen due to the drought in 2012 (Fig. 5). In this year, the study area was highly affected, the maize yield was decreased by over 50% in Csongrád County, while in Bács-Kiskun County the crop yield dropped by 44% as compared to the average. The crop yield map for 2012 (Fig. 5) shows that the southern counties experienced the most substantial reduction. How-

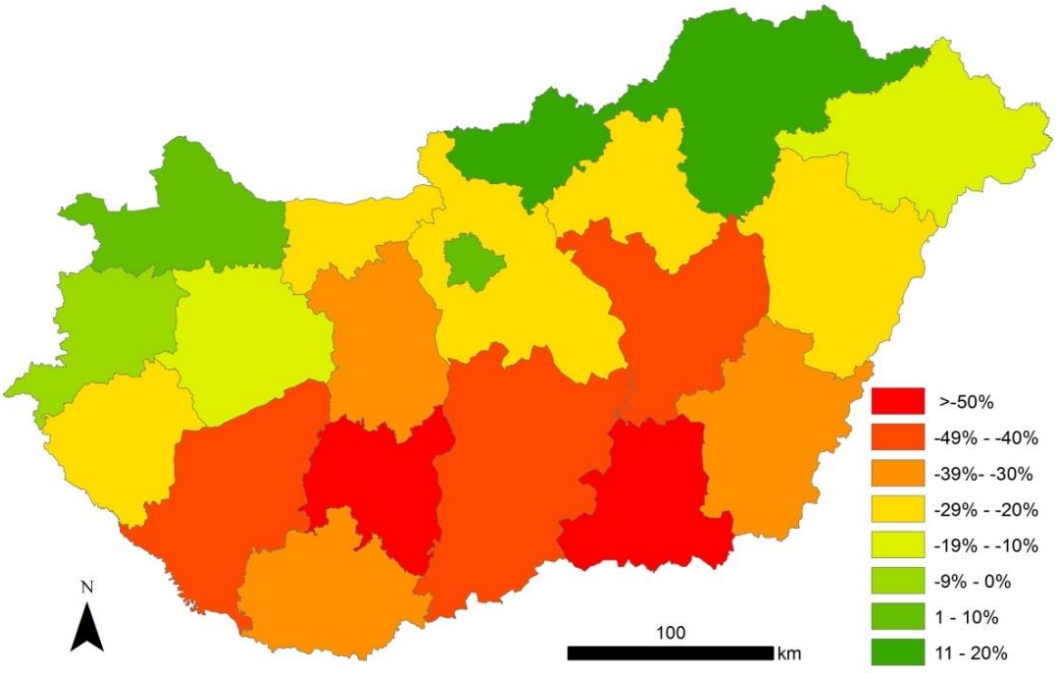


*Fig. 5* Impact of drought in 2012 on the maize crop yield in the Hungarian counties (with reference to the mean value for 2000-2012)

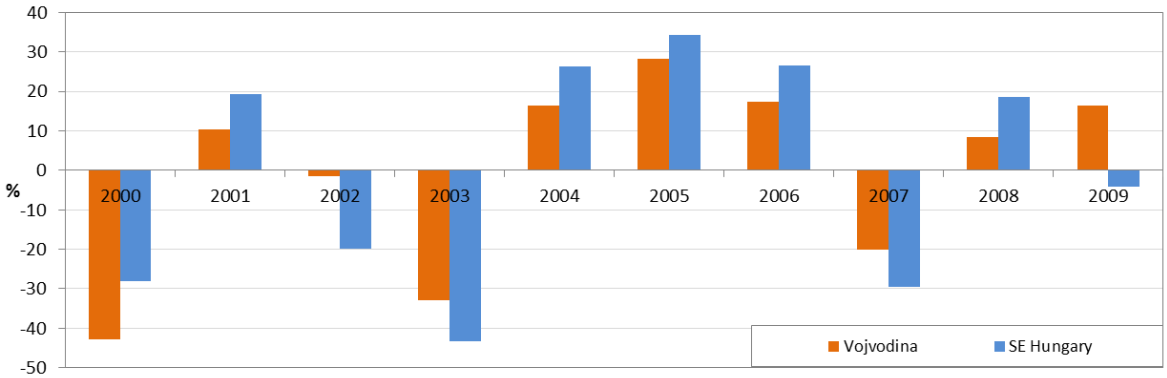


*Fig. 6* Changes of maize yield in the study area (Vojvodina and south-eastern Hungary) compared to the multiyear average between 2000-2009 (Source: Research Institute of Agricultural Economics, Hungary and Banski et al. 2010)

ever, there were some Hungarian counties where, in the same year, farmers could harvest maize with yield exceeding the long term average values.

In Vojvodina in 2012 remarkable yield loss could be observed, similarly to the southern Hungarian counties. There was a 50% decrease in maize yield in 2012 compared to 2011, furthermore reduced yields for less sensitive cereals were also observed (wheat: 8%, sugarbeet: 30%, sunflower: 11% , soy: 35%, potato: 30%, beans: 40%, clover: 30%, tobacco: 25%) (Mészáros et al., 2013).

Figure 6 illustrates the changes in maize yield, as the most drought sensitive plant in the region between 2000 and 2009. The variation of yields are similar in both countries. The most remarkable decrease occurred in 2000, 2003 and 2007, while the best crop yields were recorded for the years 2004, 2005 and 2006. The highest yield loss in Vojvodina occurred in 2000, when the yield loss exedded the loss experienced in the southern Hungarian counties. In the other years strongly affected by drought (2003, 2007) the Hungarian part suffered bigger damage owing to the sandy soils typical for the Bács-Kiskun County area (due to the better water retention capacity of chernozem, meadow and alluvial soils in Csongrád County and Vojvodina). The greatest changes both in positive and negative directions were found in the Hungarian part.

Analysis of the connection between drought and crop yields

To reveal the connection between the drought severity and maize yields, yearly yield data were compared to the yearly PaDI values between 1961 and 2012. In the first analysed period (1961-1987) the yearly yield data and PaDI index value do not show connection. In this period serious droughts do not occurred, while the yield data show continuous development of the maize production. In the second period the yearly maize yields have higher variability. This higher variability is caused by production changes after the political system change, because the transformation of plot structure was disadvantageous for unified irrigation, thus the rate of irrigation was greatly decreased and agro-technology is also changed. The decreased irrigation and changed agro-technology caused that the area became more sensitive to environmental hazards. Due to this increased sensitivity annual yields are in strong connection with drought sensitivity.

## DISCUSSION AND CONCLUSION

Based on the temporal changes of the Pálfai Drought Indices (PaDI) it can be stated that drought severity considerably increased in the region. A significant increase of the average PaDI value was observed between

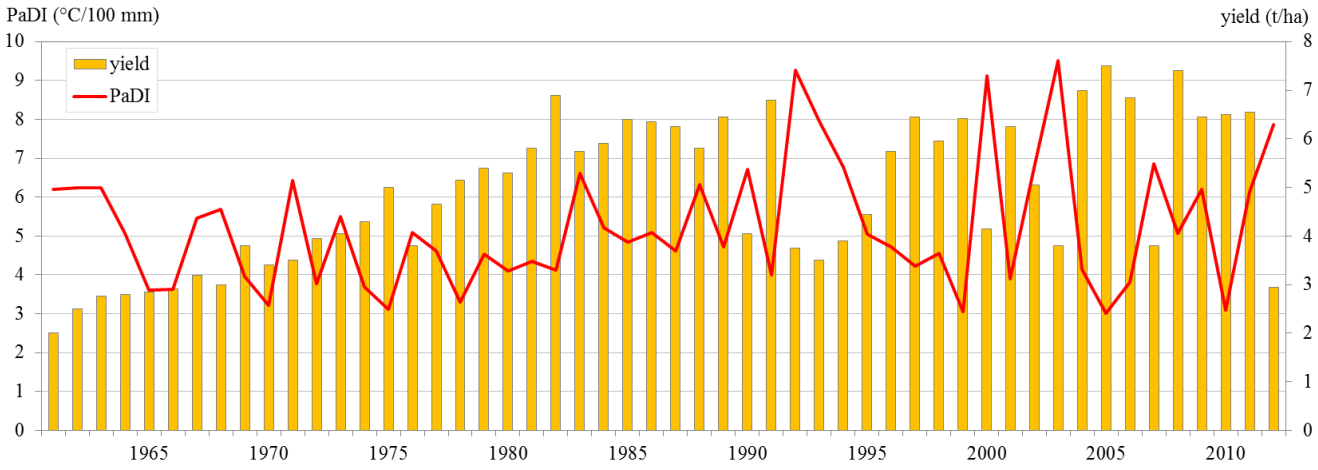


*Fig. 7* The Pálfai Drought Index (PaDI) annual values and the annual average maize yield for 1961-2012

the two analysed period (1961-1987 and 1988-2012) in the case of nearly all stations. On some stations the rate of increase reached 30-40 %, which is mainly caused by the apparent temperature increase. Moreover, in the 1988-2012 period more serious droughts occurred than in the previous period, thus heavy droughts also evolved from the 1990s. Besides drought severity, frequency has also increased in the area. If the tendency continues in the future, the 30-year average value of PaDI is expected to be around the value of 8 until the end of the 21st century (Blanka et al. 2014).

Drought severity in consecutive years can be significantly different; therefore, the spatial pattern of drought severity is different from year to year. At several times no drought occurred in subsequent years on a certain location. On the other hand consecutive years with drought also occurred, especially from the 1990s. These significant changes in drought characteristics also had serious economic consequences.

The damages caused by drought could be indicated by the rate of agricultural yield loss, since this reflects the impact of this phenomenon most visibly. The damages caused by drought are also influenced by the tolerance of cultivated crops, soil properties and the presence of irrigation. The most sensitive plants are maize, legumes, vegetables and cereals. On the areas of Kecskemét, Kiskőrös, Tiszaalpár, Csongrád and Szeged, yield losses of some crops and the consequent economic losses were determined (Table 4) to revel the effects of drought on different types of crops with different sensitivity. The data clearly shows that water shortage has an impact on all cultivated crops. The financial value of lost yield is incredibly high where the added work is greater, thus the damages of the given sector are especially severe.

Yield loss data in Hungary demonstrated the intensifying damages as a result of the more frequent droughts from the 1990s (Fig 7). Because of the considerable spatial differences in drought severity in Hungary, the yields losses are also distributed unevenly. Based on statistical data the southern Hungarian counties experienced the most substantial reduction, as it was shown also in 2012. Based on the analysis of the 2000-2009 period the effect of droughts on crops in Vojvodina is similar to the southern Hungarian counties.

In Hungary the economic losses due to the drought in 1990 were estimated to reach 50 billion HUF, for 1992 the damages arising from the drought may have been 30 billion HUF (Rátky, 1992; Csizmadia, 1992). In 2003 the damage due to drought was estimated at 40 billion HUF (Láng et al., 2007). Yield loss as a result of drought in 2012 reached 400 billion HUF (Kerpely, Tripolszky, 2013). In Serbia the damages resulting from yield loss reached 600 million EUR in 2007 (Popov and Frank, 2013), and in 2012 damage at 2000 million EUR was reported (Mészáros et al., 2013).

In Hungary in the Danube-Tisza Interfluve, considering that the groundwater level had considerably decreased, the damages caused by yield loss due water shortage reached 11 billion HUF on average on the catchment of Tisza River (almost 5000 $km^{2)}$. A special feature of the study area is the important tradition of vegetable and fruit cultivation that makes it sensitive to water deficit and drought. It is also important to mention that the mostly affected sectors are linked to smallholders, whose financial stability is much worse than that of large agricultural farms, where cereal production is typical. Consequently, damage can be expressed in numbers but has a lot more serious long-term impact on the farms.

The observed unfavourable changes in the region mean that water management and spatial planning faces conceptual challenges to prevent and mitigate the damages of drought, since the changing climatic and hydrological conditions generate new and increasing environmental and consequently social hazards in the future. Planning sustainable development requires the integration of economic, social, and environmental considerations as a key to maintaining basic living standards and protecting ecosystems. To reach these aims all the possibilities of agro-technological development, changing production structure, land use changes, development of irrigation technology, new concept in water management (water retention, reuse of water resources) and dynamic approach in nature conservation should be considered.

*Table 4* Yield losses of some crops on the study area

| | Kecskemét | Kiskőrös | Tiszaalpár | Csongrád | Szeged | |
|---|---|---|---|---|---|---|
| Area [ha] | 123 768 | 97 592 | 49 752 | 18 701 | 106 197 | |
| Gold crown value | 11.4 | 8.5 | 19.7 | 17.7 | 9.1 | |
| Crops | Yield loss (t/ha) | | | | | yield loss [million HUF/ha] |
| Cereals | 0.3 | 0.3 | 0.3 | 0.3 | 0.3 | 20 |
| Maize | 0.9 | 0.9 | 0.8 | 0.8 | 1.0 | 70 |
| Potato | 2.0 | 2.0 | 2.0 | 2.0 | 2.0 | 240 |
| Vegetables | 2.5 | 2.5 | 2.0 | 2.0 | 2.2 | 360 |
| Pasture | 1.5 | 1.5 | 1.3 | 1.4 | 1.2 | 6 |
| Fruit | 3.3 | 3.4 | 3.5 | - | 3.8 | 5000 |

## Acknowledgements

This research was supported by the IPA Cross-border Cooperation Programme of the European Union under the project WAHASTRAT (HUSRB/1203/121/130).

## References

Banski, J, Bednarek-Szczepańska, M. , Ł. Czapiewski, K., Mazur, M. 2010. Perspectives for agriculture of Vojvodina in the light of scenarios and models elaborated in the framework of the research projects of the European Union. Project Report prepared for Centre for Strategic Economic Studies "Vojvodina-CESS. Warsaw, 2010. Online at: https://www.igipz.pan.pl/tl_files/igipz/ZGWiRL/Projekty/Raport_Vojvodina.pdf

Bartholy, J., Pongrácz, R. 2005. Tendencies of extreme climate indices based on daily precipitation in the Carpathian Basin for the 20th century. *Időjárás* 109, 1–20.

Bartholy, J, Pongrácz, R., Barcza, Z., Haszpra, L., Gelybó, Gy., Kern, A., Hidy, D., Torma, Cs., Hunyady, A., Kardos, P. 2007. A klímaváltozás regionális hatásai: a jelenlegi állapot és a várható tendenciák. *Földrajzi közlemények* 131/4, 257–269.

Beierkuhnlein, C., Thiel, D., Jentsch, A., Willner, E., Kreyling, J. 2011. Ecotypes of European grass species respond differently to warming and extreme drought. *Journal of Ecology* 99, 703–713. DOI: 10.1111/j.1365-2745.2011.01809.x

Bihari, Z., Lakato,s M., Mika, J., Szalai, S., Szentimrey ,T. 2006. Hazánk éghajlatának néhány jellemzője az 1956-2005 időszakban, kitekintéssel a globális tendenciákra. In: „50 éves a Légkör" *Légkör* 51, különszám 24–28.

Biró, M., Révész, Á., Molnár, Zs., Horváth, F., Czúcz, B. 2008. Regional habitat pattern of the Danube-Tisza Interfluve in Hungary II The sand, the steppe and the riverine vegetation, degraded and regenerating habitats, regional habitat destruction. *Acta Botanica Hungarica* 50/1–2, 19–60. DOI: 10.1556/abot.50.2008.1-2.2

Blanka ,V., Ladányi, Zs., Mezősi, G. 2014. Climate change in the 21th century. In. Blanka V, Ladányi Zs. (Eds.) Drought and Water Management in South Hungary and Vojvodina. Szegedi Tudományegyetem, Természeti Földrajzi és Geoinformatikai Tanszék, Szeged, 152–157.

Csizmadia K. (1992). Országos vízrendezési, -hasznosítási és társulati szakágazatiértekezlet. *Vízpart* 1 (12), 1.

Gocić, M., Trajković, S. 2013. Analysis of precipitation and droguht data in Serbia over the period 1980-2010. *Journal of Hydrology* 494, 32–42. DOI: 10.1016/j.jhydrol.2013.04.044

Gocic, M., Trajkovic, S. 2014. Spatio-temporal patterns of precipitation in Serbia. *Theoretical and Applied Climatology* 117/3-4, 419–431. DOI: 10.1007/s00704-013-1017-7

Hargreaves, G.H. 1975. Water requirements manual for irrigated crops and rainfed agriculture. Agricultural and Irrigation Engineering, Utah State University, Logan, Utah, 1–44.

Hargreaves, G., Keller, A. 2005. Global Mapping of the Moisture Availability Index: Using the World Water and Climate Atlas. Impacts of Global Climate Change, 1–9. DOI: 10.1061/40792(173)533

Kerpely, K., Tripolszky, S. 2013. Változó Vizeken - Vállalatok vízfüggősége és felelős vízhasználata. WWF Hungary. Online at: http://www.wwf.hu/media/file/1369810200_Felelos_vallalati_vizgazdalkodas.pdf

Ladányi, Zs., Rakonczai, J., Kovács, F., Geiger, J. , Deák, J. Á. 2009. The Effect of Recent Climatic Change on the Great Hungarian Plain. *Cereal Research Communications* 37 Suppl. 4, 477–480.

Ladányi Zs., Deák J. Á., Rakonczai, J. 2010. The effect of aridification on dry and wet habitats of Illancs microregion, SW Great Hungarian Plain, Hungary. *AGD Landscape & Environment* 4 (1), 11–22.

Láng, I., Csete, L., Jolánkai, M. 2007. A globális klímaváltozás - hazai hatások és válaszok - A VAHAVA jelentés. Szaktudás Kiadó Ház Rt., 2007

Lei, Y.D., Wang J.A., Luo L.L. 2011. Drought risk assessment of China's mid-season paddy. *International Journal of Disaster Risk Science* 2 (2), 32–40.

Lin, Y.Z., Deng, X.Z., Jin, Q. 2013. Economic effects of drought on agriculture in North China. *International Journal of Disaster Risk Science* 4 (2), 59–67. DOI: 10.1007/s13753-013-0007-9

Major, P., Neppel, F. 1988. A Duna–Tisza közi talajvízszint süllyedések. *Vízügyi Közlemények* 70/4, 605–626.

Maracchi, G. 2000. Agricultural drought – A practical approach to definition, assessment and mitigation strategies. In Vogt J.V., Somma F (ed.) Drought and drought mitigation in Europe. *Advances in natural and technological hazards research* 14, 63–78. DOI: 10.1007/978-94-015-9472-1_5

Mátyás, Cs. 2010. Forecasts needed for retreating forests. *Nature* 464/7293, 1271. DOI: 10.1038/4641271a

Mészáros, M., Pavić, D., Stankov, U. (2013). The social aspects of drought in Vojvodina (Serbia). Opening conference of WAHASTRAT, 14 June 2013, Szeged, oral presentation.

Molnár, Zs, Bölöni, J., Horváth, F. 2008. Threatening factors encountered: actual endangerment of the Hungarian (semi-) natural habitats. *Acta Botanica Hungarica* 50 (Suppl), 199–217. DOI: 10.1556/abot.50.2008.suppl.10

Normand, S., Svenning, JC., Skov, F. 2007. National and European perspectives on climate change sensitivity of the Habitats Directive characteristic plant species. *Journal for Nature Conservation* 15, 41–53. DOI: 10.1016/j.jnc.2006.09.001

OMSZ (2014): Országos Meteorológiai Szolgálat http://www.met.hu/en/eghajlat/ magyarorszag_eghajlata

Pálfai, I., Herceg, Á. 2011. Droughtness of Hungary and Balkan Peninsula. *Riscuri si Catastrofe*, An X 9/2 145–154.

Parmesan, C., Yohe, G. 2003. A globally coherent fingerprint of climate change Impacts across natural systems. *Nature* 421, 37–42. DOI: 10.1038/nature01286

Pitchford, J.L., Wu, C., Lin, L.S., Petty, J.T., Thomas, R., Veselka, W.E., Welsch, D., Zegre, N., Anderson, J.T. 2012. Climate Change Effects on Hydrology and Ecology of Wetlands in the Mid-Atlantic Highlands *Wetlands* 32/1, 21–33. DOI: 10.1007/s13157-011-0259-3

Poiani, KA, Johnson, CW, Kittel, TGF 1995. Sensitivity of Prairie Wetland to Increased Temperature and Seasonal Precipitation Changes. *Water Resources Bulletin* 31, 283–294. DOI: 10.1111/j.1752-1688.1995.tb03380.x

Popov. S., Frank. A. (2013). Challenges of drought monitoring and risk assessment in Serbia. Opening conference of WAHASTRAT, 14 June 2013, Szeged, oral presentation.

Puskás, I., Gál, N., Farsang, A. 2012. Impact of weather extremities (excess water, drought) caused by climate change onsoils in Hungarian Great Plain (SE Hungary). In: Rakonczai J. , Ladányi Zs. (eds) Review of climate change research program at the University of Szeged,73–89

Rakonczai, J., Ladányi, Zs., Deák, JÁ., Fehér, Zs. 2012. Indicators of climate change in the landscape: investigation of the soil–groundwater–vegetation connection system in the Great Hungarian Plain. In: Rakonczai J, LadányiZs (Ed) Review of climate change research program at the University of Szeged (2010-2012). Institute of Geography and Geology, Szeged, 41–59

Rátky. P. 1992. Mezőgazdasági vízhasznosítás. Tavalyi mérleg. *Vízpart* 1 (2), 3.

Smailagic, J, Savovic, A, Markovic, D, Nesic, D. 2013. Climate characteristics of Serbia. Republic Hydrometeorological Service of Serbia.

Svoboda, M., D. Le Comte, M., Hayes, R. Heim, K. Gleason, J. Angel, B. Rippey, R. Tinker, et al. 2002. The drought monitor. *Bulletin of the American Meteorological Society* 83, 1181–1190. DOI: 10.1175/1520-0477(2002)083<1181:tdm>2.3.co;2

Szalai, S. 2009. Drought tendencies in Hungary and its impacts on the agricultural production, *Cereal Research Communications* 37: 501–504.

Szalai, J. 2011. Talajvízszint-változások az Alföldön. In: Rakonczai J. (ed.) Környezeti változások és az Alföld. Nagyalföld Alapítvány kötetei 7, 97–110.

Warrick, R.A., Trainer P.B., Baker E.J., Brinkman W. 1975. Drought hazard in the United States: A research assessment. NSF program on technology, environment and man monograph. Institute of Behavioral Science, University of Colorado.

Winter, T.C. 2000. The vulnerability of wetlands to climate change: a hydrologic landscape perspective. *Journal of the American Water Resources Association* 36, 305–311. DOI: 10.1111/j.1752-1688.2000.tb04269.x

Wisner, B., Blaikie, P., Cannon, T., Davis I. 2004. At Risk: Natural Hazards, People's Vulnerability and Disasters. London, Routledge p. 124.

Ye, T., P.J. Shi, J.A. Wang, L. Liu, Y. Fan, and J. Hu. 2012. China's drought disaster risk management: Perspective of severe droughts in 2009–2010. *International Journal of Disaster Risk Science* 3/2, 84–97. DOI: 10.1007/s13753-012-0009-z

Zeng, N. 2003. Drought in the Sahel. *Science* 302/5647, 999–1000. DOI: 10.1126/science.1090849

JOURNAL OF ENVIRONMENTAL GEOGRAPHY
*Journal of Environmental Geography* 7 (3–4), 53–59.
DOI: 10.2478/jengeo-2014-0012
ISSN: 2060-467X

# BRACKETING THE AGE OF FRESHWATER CARBONATE FORMATION BY OSL DATING NEAR LAKE KOLON, HUNGARY

**György Sipos[1*], Orsolya Tóth[1], Eszter Pécsi[1], Csaba Bíró[2]**

[1]Department of Physical Geography and Geoinformatics, University of Szeged, Egyetem u. 2-6, H-6722 Szeged, Hungary
[2]Directorate of Kiskunság National Park, Liszt F. u. 19, H-6000 Kecskemét, Hungary
*Corresponding author, e-mail: gysipos@geo.u-szeged.hu

Research article, received 02 September 2014, accepted 13 October 2014

**Abstract**

Freshwater carbonates are unique depositions in the centre of the Carpathian Basin, with debated origin and age. Their formation on the sand covered area of the Danube-Tisza Interfluve is mainly related to lakes appearing in low lying interdune areas from time-to-time. Carbonate deposition is governed by various processes, but in general it can be traced back to climatic and concomitant surface and subsurface hydrological variations. Therefore marl, limestone and dolomite layers can be a marker of environmental change. To identify the type of environmental change they may indicate absolute or numerical ages are needed. In previous studies this issue has been addressed by the means of radiocarbon dating. In the present study we attempted to bracket the age of freshwater carbonate formation with the help of optically stimulated luminescence dating and compared our results to radiocarbon data from the literature. In general, the luminescence properties of the investigated samples proved to be suitable for determining the age of the bedding and covering sediments. OSL dates confirmed previous interpretations that freshwater carbonate formation in the area could have a peak around 10,5 ka. However, the termination of the deposition could not be unambiguously determined at the present stage of the analysis. The compound geomorphology and sedimentology of the study area call for further investigations.

**Keywords**: OSL dating, freshwater carbonates, environmental change, blown sands

## INTRODUCTION

In the Carpathian Basin freshwater carbonate deposits may occur at various locations, but have mostly been reported from the blown sand covered area of the Danube-Tisza Interfluve (DTI). The extension and thickness of occurrences is highly variable as a consequence of the mosaic landscape and the complex formation of the deposits (Sümegi et al., 2011). The source of the carbonates, precipitating and accumulating in the form of hard and compact limestone and dolomite benches is debated (Fügedi et al., 2008; Sümegi et al., 2011). Nevertheless carbonate formation has been extensively studied and the major processes have been identified by Molnár et al. (1981). Deposition can traditionally be related: 1) to groundwater fluctuation and consequent precipitation of Ca/Mg rich salts from pore water above the fluctuation zone and 2) to shallow lakes where either $CO_2$ distraction by plants or time-to-time desiccation can lead to extensive carbonate formation (Molnár and Botz, 1996; Fügedi et al., 2008). However, based on palinological data, Sümegi et al. (2011) have shown that carbonate formation can also occur at deeper oligotrophic stages of lake evolution. Nevertheless, each interpretation underlines the importance of climatic changes and parallel alteration of the hydrological regime. Besides, they agree in that the Ca-content of lake carbonates is higher than those precipitating from groundwater (Molnár and Botz, 1996; Fügedi et al., 2008).

The time of carbonate formation has been also debated, as previously it was primarily related to drier and warmer periods of the Holocene, namely the Boreal Phase (Mucsi, 1963). Based on radiocarbon measurements on herbivorous gastropod shells enclosed by carbonate deposits at a typical limestone exposure, Jenei et al. (2007) have proved that major carbonate formation started at around 13,0-11,5 ka (9500-11000 cal BC) and terminated at 6,9 ka (4900 cal BC), thus they pushed the peak of carbonate formation to the colder climate of the Late Glacial. These results were reinforced by the extensive study of Sümegi et al. (2011) at another site in the basin of Lake Kolon, using also radiocarbon dating. Based on their study, carbonate rich marls were formed between 13.6 ka and 10.5 ka (11,393–11,621 cal BC and 8311–8455 cal BC) with a peak around 11 ka.

Freshwater carbonate formation cannot be restricted to the Late Glacial however, as it was already suggested by Jenei et al. (2007), who identified carbonate formation up till around 3.3 ka (1300 cal BC). A similar result can be deduced from the study of Sipos et al. (2009) from another site on the DTI where they dated the blown sand bedding of a carbonate rich lacustrine layer by using optically stimulated luminescence (OSL) to 3,8 ka and the organic rich cover of it by using radiocarbon to 3,5 ka (1500 cal BC).

The aim of the present research is to provide further data for the time of carbonate formation on the DTI by performing OSL measurements on sediments below and above freshwater carbonate layers. These measurements provide also the possibility to compare the results of different numerical dating methods and therefore to achieve a more robust interpretation for the timing and environment of carbonate formation in the Carpathian Basin.

## STUDY AREA

Lake Kolon is situated on the western edge of the sand hills of the DTI in a former channel of the Danube (Fig. 1). The elevated, central territory of the DTI had been the alluvial fan of the Danube throughout most of the Pleistocene (Pécsi, 1967). The shift of the river to its present day N-S direction is estimated to occur 30-40 ka ago, and generally explained by the subsidence of the Baja and Kalocsa depressions southwest of the area (Jaskó and Krolopp, 1991). The westward translation of the Danube was presumably continuous, and a final phase of this process could be the formation of a 5-6 km wide valley on the western edge of the alluvial fan (Fig. 1). Lake Kolon, and the study site is situated in this relatively deep lying area. The age of the channel and the termination of fluvial activity have not been determined yet, though radiocarbon dating of lake sediments led Sümegi et al. (2011) to the conclusion that lacustrine sedimentation started at around 27 ka (25 000 cal BC).

After the Danube had left the area, fluvial processes were overtaken mostly by eolian activity, especially intensive during the Last Glacial Maximum (Borsy, 1977; Borsy, 1987; Lóki et al., 1994). In these circumstances the basin was time-to-time covered by sand sheets. Consequently, a hummocky landscape appeared with wind blown depressions and residual

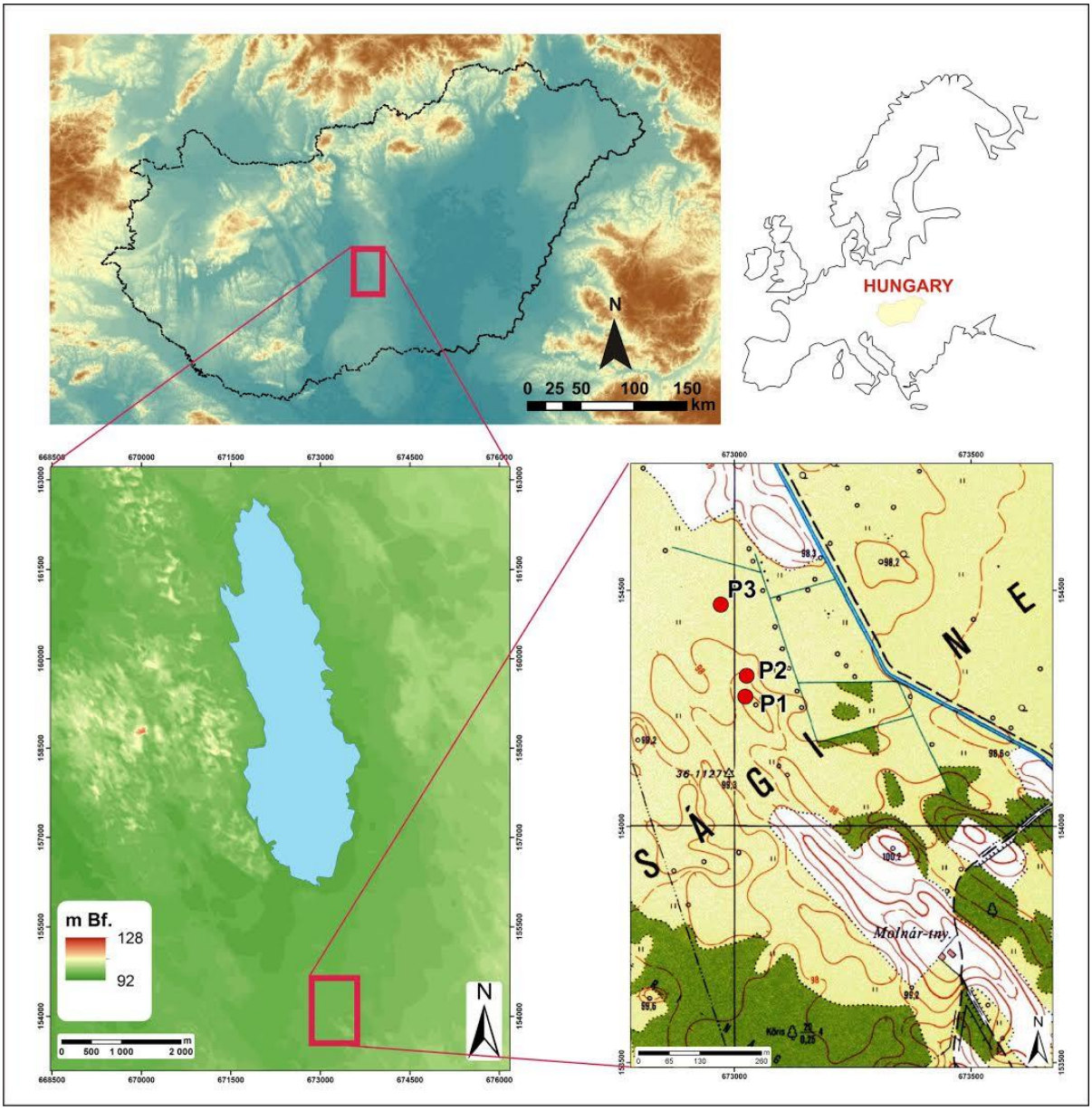


*Fig. 1* Location and topography of the study site near Lake Kolon

ridges, which favoured the development of a mosaic network of wetlands and shallow lakes, adequate for freshwater carbonate formation (Sümegi et al., 2011). However, as a result of height differences between sub-basins considerable spatial and temporal variations can be presumed in terms of carbonate formation. Spatial variability is reinforced by the study of Pécsi et al. (2014), when using high resolution drilling and ground penetrating radar for the delineation of dolomite platforms and carbonate rich layers in the area.

OSL dating was performed south of the present day lake (Fig. 1). At the study site 3 sampling points were identified, the lowest and the highest being at 97.5 m and 99.0 m asl., respectively. The geomorphology of the area is compound, a deflational basin can be seen at sampling point P3, while point P2 and point P1 are located at the foot and on the top of a NW-SE direction, relatively small positive form, interpreted as a left behind wing fragment of a larger parabolic dune, situated SE of the form (Fig. 1).

## MATERIALS AND METHODS

Sedimentary features were mapped at the study site as described by Pécsi et al. (2014) by using hand drills and a Pürckhauer soil sampler. After revealing the spatial extension of carbonate rich layers 2 drillings were made to collect OSL samples by using Eijkelkamp type undisturbed sampling cylinders (Fig. 2). At sampling point P3 the bedding of the freshwater dolomite was sampled from an artificial exposure, using the same cylinders. The aim of sampling was to collect sediments of relatively high sand content from below and above the very fine grained carbonate layers. In all, 9 samples were taken, each weighing about 200 g. From layers, in which only low sand content was presumed on the basis of orienteering drills, double samples were collected. The processing of these samples was started separately, however, in case it was necessary they were merged to receive an adequate amount of material for dating. In one case even the doubled sample did not yield enough datable grains (OSZ872/873).

Sample preparation was based on the techniques proposed by Aitken (1998) and Mauz et al. (2002) for coarse grain sample treatment. First the samples were wet sieved to separate the 90-150 μm grain size fraction, the typical grain size interval for blown-sand sediments. Subsequently, samples were subjected to repeated acid treatments (HCl and $H_2O_2$) to remove their usually high carbonate and moderate organic matter content. The quartz content was divided from other minerals by heavy liquid separation (2.62 and 2.68 $cm^3$). In order to clean quartz, and to remove any remaining feldspars a 45 min HF etching was applied. Grains were adhered to stainless steel sample holding discs by using silicone spray and a 4 mm mask, chosen as a compromise between signal intensity and the available low amount of material.

The absorbed dose since deposition, termed as the equivalent dose ($D_e$) was determined by using the single aliquot regenerative-dose (SAR) protocol (Murray and Wintle, 2000; Wintle and Murray, 2006), on a RISØ DA-15 automated TL/OSL system with a beta dose rate (Sr/Y) of 0.105±0.002 Gy $s^{-1}$ at the time of measurements. Preheat temperatures were set between 200-240 °C depending on the results of dose recovery preheat plateau tests, performed on each sample. Prior to the dose recovery aliquots were bleached by the blue LEDs of the RISØ reader at room temperature, and irradiated with a dose similar to the one determined through initial trial measurements.

During the evaluation of $D_e$ some of the aliquots were rejected mainly for the following reasons: the recycling ratio (the ratio of the sensitivity corrected OSL response to the first regeneration dose and that of an identical dose at the end of the measurement cycle) was outside 1.00±0.05, the error of $D_e$ (mainly related to the fitting of the dose response curve) was larger than 10%, or the recuperation signal (the OSL response given for zero irradiation as a matter of previous thermal treatment) was over 5% of the natural signal. The distribution of $D_e$ values usually had an overdispersion below 0.20, consequently, and by considering the decision procedure of (Bailey and Arnold 2006) the central age model was applied for most of the calculations, however in one case, at sample OSZ869 ($\sigma_{OD}$=0.27) the minimum age model was chosen (Galbraith et al., 1999; Galbraight and Roberts, 2012).

*Fig. 2* Sampling at the exposure beneath the carbonate bench by using steel cylinders

Environmental dose rate was determined by using high resolution, low-level gamma spectrometry. Dry dose rates were calculated using the conversion factors of Adamiec and Aitken (1998). Wet dose rates were assessed on the basis of in situ water contents. Samples below the fresh water carbonate layers were close to their saturation, consequently a lower variation was attributed to their water content in the past. Samples above had a water content between 12-15 %, in their case a much larger error was assumed (Table 1). The rate of cosmic radiation was determined on the basis of burial depth following the method of Prescott and Hutton (1994).

## RESULTS

Based on our preliminary investigations, we found that the quartz OSL signal is dominated by the fast component in general if compared to the decay curve of the RISØ calibration quartz (180-255 μm) (Fig. 3). Therefore, the eolian sand of Lake Kolon seems to be suitable for adequate OSL dating. Nevertheless, in case of some aliquots the presence of a later, possibly medium component can be seen. To resolve the effect of this issue on dating further analysis has to be made. In order to minimize the effect of the medium component the first 5 channels (0.8 s) were integrated and used as an OSL signal in later measurements. Background was calculated from the last 50 channels of the decay curve.

Regarding dose recovery preheat tests samples were performing the best between 200 °C and 240 °C, recovered doses were close to unity in this temperature region (Fig. 4). A full dose recovery test was not performed at this stage of the investigation. Another check on the suitability of the applied measurement protocol is the calculation of recycling ratios. Concerning this parameter values were also acceptable in the above temperature range, and most of the measured aliquots proved to be adequate for further evaluation (Fig. 4). The problem of recuperation, however, at one samples appeared to be significant during the tests (OSZ870/871). Therefore, the traditional SAR protocol was replaced by the one advised by Wintle and Murray (2006), including an elevated temperature OSL measurement (hot bleach) at the end of each regeneration cycle to decrease the effect of charge transfer (Fig. 4).

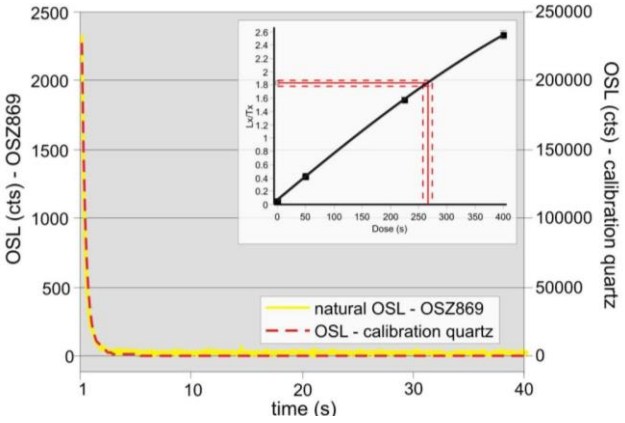


*Fig. 3* Natural decay curve of an aliquot compared to that of the RISØ calibration quartz and a typical dose response curve of the same sample

With the exception of one sample (OSZ875) 24 aliquots were subjected to the SAR protocol in order to determine equivalent doses. The turnout rate of well behaving aliquots, passing all internal checks, was 70-90 % in four cases and only sample OSZ875 proved to be problematic and has to be tested further (Table 2). This means that the applied settings and protocol was proper in most of the cases.

The distribution of equivalent doses, with the exception of sample OSZ869 was unimodal and unskewed, meaning that there was an adequate exposure to sunlight during sediment transport, just as it can be expected from eolian samples (Fig 5.). Conversely, the significant skewness of OSZ869 data may imply that exposure was not adequate and the sample experienced either a short transportation distance or it was deposited by water related processes (fluvial or lacustrine).

*Table 1* Sampling and radiometric data and the calculated dose rate of the samples

| ID | depth (cm) | W (%) | $^{238}$U (ppm) | $^{232}$Th (ppm) | K (%) | D* (Gy/ka) |
|---|---|---|---|---|---|---|
| OSZ867/868 | 180–190 | 11,0±5,0 | 2,07±0,20 | 6,51±0,96 | 0,85±0,09 | 1,75±0,08 |
| OSZ869 | 230 | 34,0±2,0 | 2,07±0,20 | 6,51±0,96 | 0,85±0,09 | 1,43±0,07 |
| OSZ872/873 | 75–85 | 34,0±2,0 | 1,19±0,12 | 3,54±0,35 | 0,17±0,01 | 1,99±0,06 |
| OSZ870/871 | 120–130 | 23,0±4,0 | 2,96±0,29 | 8,85±0,89 | 0,16±0,01 | 2,10±0,08 |
| OSZ874 | 100 | 26,6±4,0 | 2,99±0,30 | 10,33±1,03 | 0,17±0,01 | 1,71±0,06 |
| OSZ875 | 100 | 27,0±4,0 | 2,99±0,30 | 10,33±1,03 | 0,17±0,01 | 1,71±0,06 |

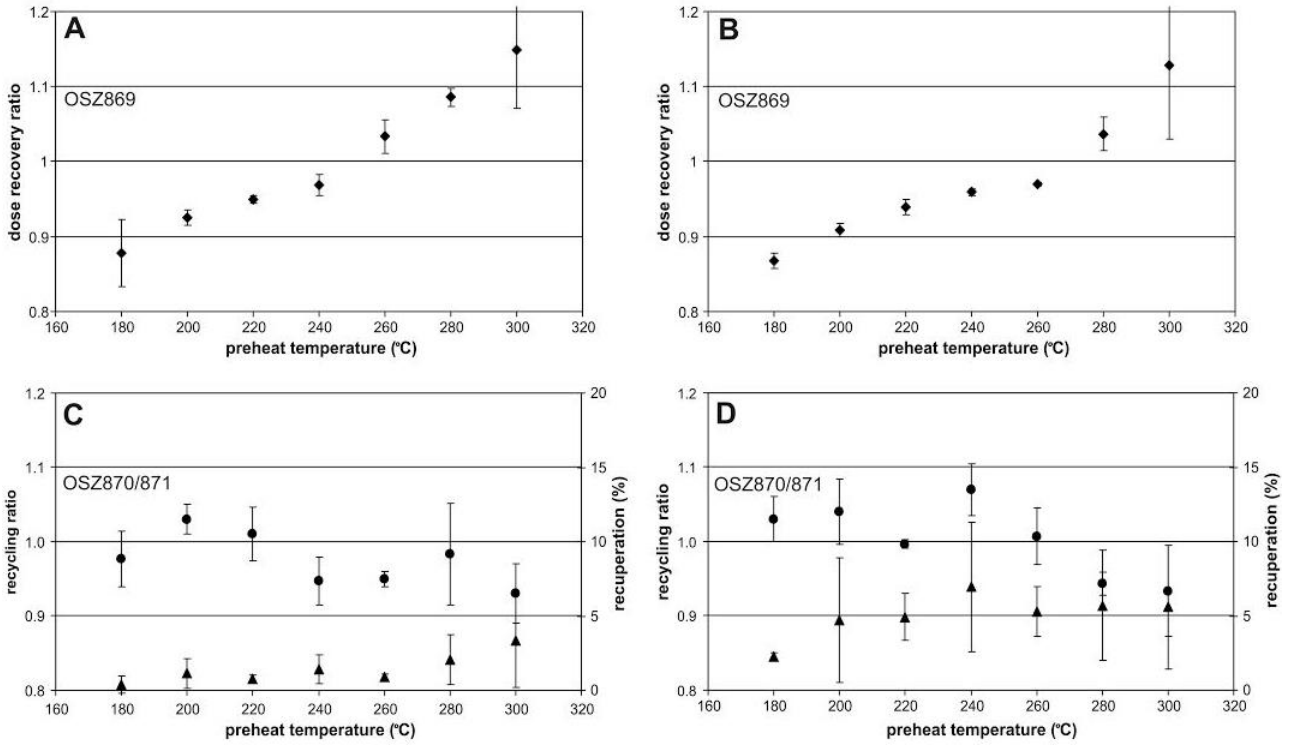


*Fig. 4* Results of dose recovery preheat tests (A and B) and SAR internal checks (C and D) in case of two samples (OSZ869 and OSZ870/871)

The results of gamma spectrocopical measurements and calculated dose rates are presented in Table 1. Ages, calculated as the quotient of equivalent doses and dose rates, have a 5-10 % relative error (Table 2) and show a good stratigraphic correlation (Fig. 6).

In case of sampling point P1 the bedding of the carbonate layer was dated to the Last Glacial Maximum (23.6 ± 1.2 ka), while the cover sediments to the beginning of the Holocene (10.2 ± 0.6 ka). Consequently, the timing of lacustrine freshwater carbonate formation can be assumed for a very broad time interval.

If the stratigraphy of P1 is compared to that of P2 then the cover layer in P1 corresponds well to the bedding of carbonate in P2 (Fig. 6). Accordingly, the age of the later is also dated to the beginning of the Holocene (10.8 ± 0.7 ka). Unfortunately the cover sediments at P2 did not yield enough coarse material to carry out a successful measurement, therefore the termination of the process could not be determined. Concerning P3 the bedding of the carbonate also had a similar age (Table 2, Fig.6) as before and confirmed previous measurements. In this case the two parallel samples were dated separately, and the two dates showed a good correspondence (10.9 ± 0.4 ka and 10.4 ± 0.7 ka) (Table 2 and Fig. 6). The mean of the ages representing the beginning of the Holocene is 10.6 ka.

*Table 2* Equivalent dose data and the calculated age of the samples

| ID | measured/rejected (pcs) | age model | $D_e$ (Gy) | D* (Gy/ka) | OSL age[1] (ka) |
|---|---|---|---|---|---|
| OSZ867/868 | 24 / 18 | CAM | 17,76±0,34 | 1,75±0,08 | 10,2±0,6 |
| OSZ869 | 24 / 22 | MAM3 | 33,67±0,29 | 1,43±0,07 | 23,6±1,2 |
| OSZ872/873 | – | – | – | 1,99±0,06 | – |
| OSZ870/871 | 48 / 40 | CAM | 22,82±1,09 | 2,10±0,08 | 10,8±0,7 |
| OSZ874 | 24 / 17 | CAM | 23,59±0,12 | 1,71±0,06 | 10,9±0,4 |
| OSZ875 | 18 / 8 | CAM | 22,49±1,47 | 1,71±0,06 | 10,4±0,7 |

[1] age is given by dividing $D_e$ and D*

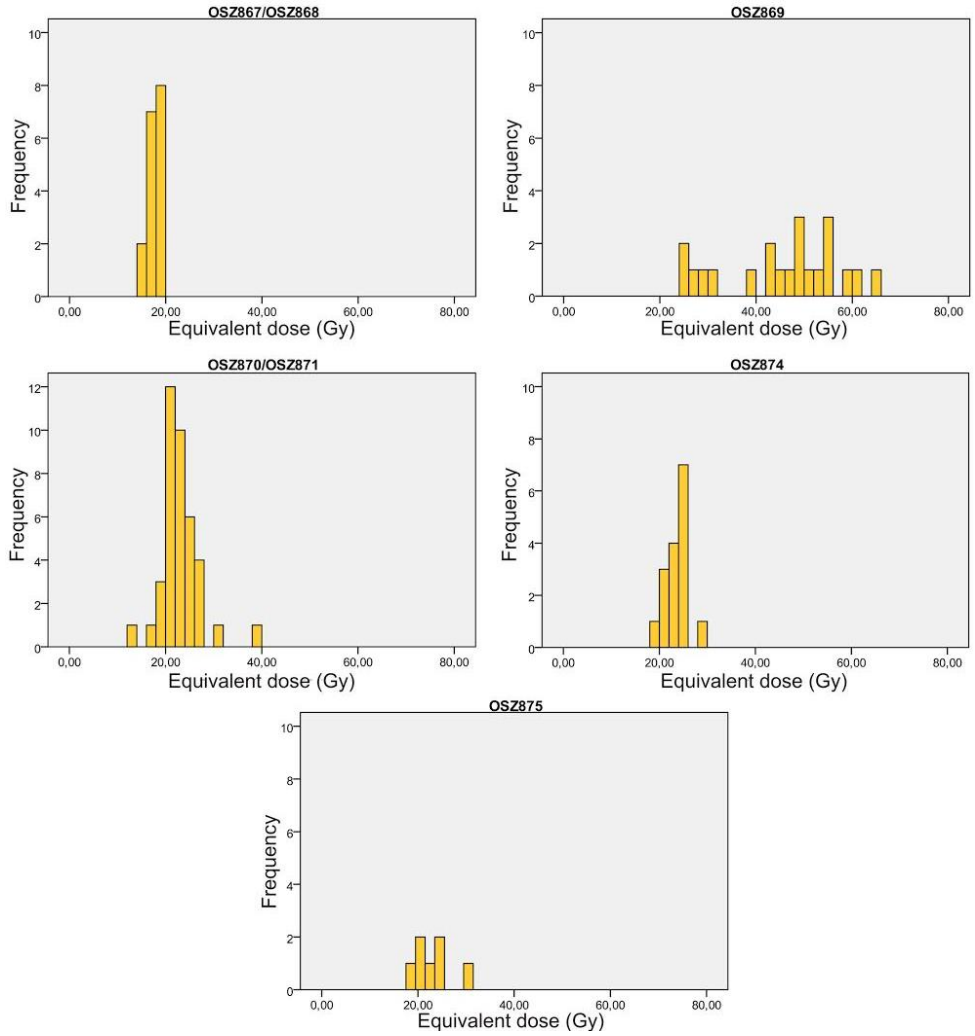


*Fig. 5* The distribution of equivalent doses in terms of the measured samples

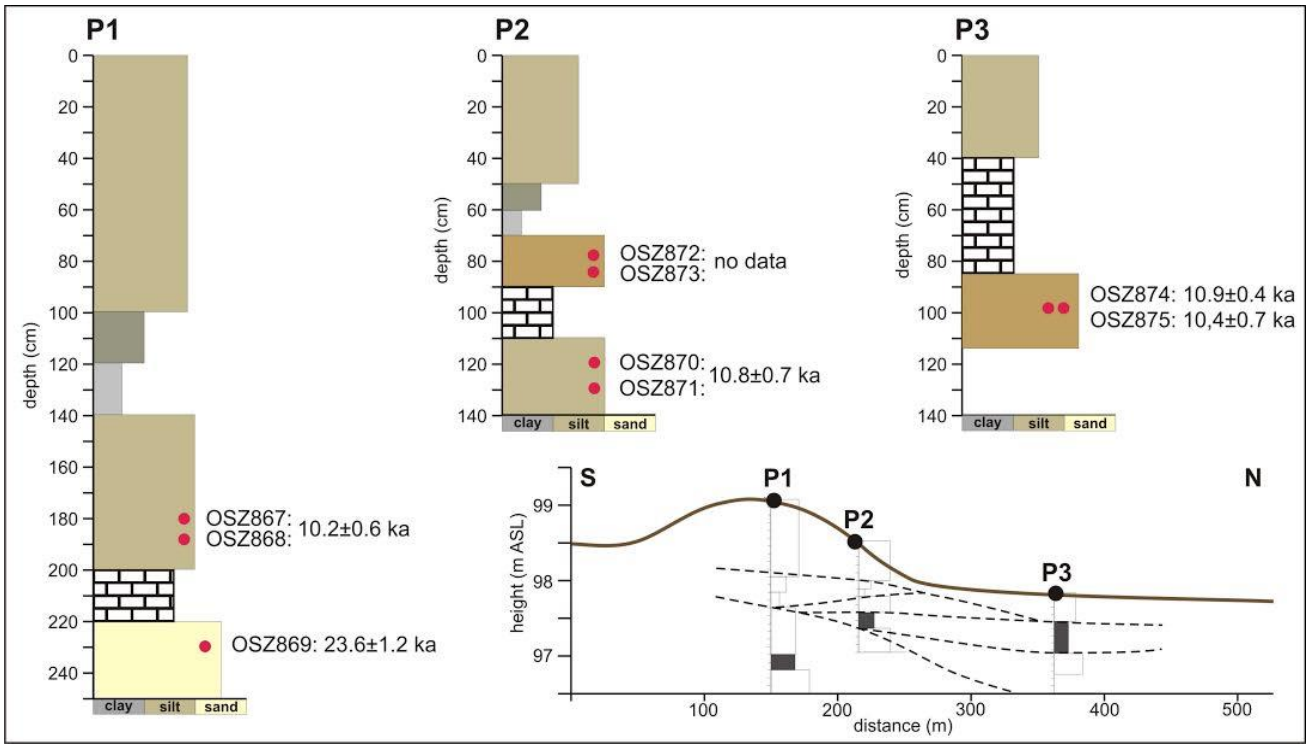


*Fig. 6* The stratigraphy of the profiles and the measured OSL ages. The absolute height of freshwater carbonate layers is indicated on the inset

## CONCLUSIONS

Based on various tests, the luminescence properties of the sediments originating from the Lake Kolon area are adequate for conducting a reliable dating study, only recuperation can be an issue which has to be considered especially when dating younger sediments.

The ages received at the present stage of analysis can be fitted to the radiocarbon data presented by Jenei et al. (2007) and Sümegi et al. (2011). The age of the sand layer at the base of the section is not identical to, but close to age of the earliest lacustrine layers identified by Sümegi et al. (2011) at the central part of the lake's basin. By considering the above and the dose distribution received for the material, we assume that this layer might represent the fluvial sand of the Danube.

Based on the stratigraphy and the OSL ages, it seems clear that there could be several phases of freshwater carbonate formation throughout the Late Pleistocene and Holocene. One phase is suggested to occur in the end, or after the LGM, however its precise timing needs further analysis, as there is a nearly 13 ka age difference between the layers below and above the carbonate platform. Another phase occurred after the topography had changed as a matter of blown sand movement, covering the carbonates of the first phase and forming a more pronounced topographical difference between the southern and northern part of the site. The bedding sediment of this phase is dated unambiguously to the onset of the Holocene. If the four dates corresponding to each other within their errors are averaged then a mean age of 10,6 ka is received for this event. Thus, carbonate formation occurred subsequently, though the termination of this phase could not be dated. However, based on the results of both Jenei et al. (2007) and Sümegi et al (2011) it is highly probable that there is a correspondence between the timing of carbonate formation on our site, at the centre of the Kolon Lake basin and at other sites of the DTI. Consequently, the peak of freshwater carbonate formation could be at around 10.5 ka in the region, and these deposits mark rather a relatively colder climate with variable water input, than a warm and dry environment.

### Acknowledgement

This research was supported by the European Union and the State of Hungary, co-financed by the European Social Fund in the framework of TÁMOP-4.2.4.A/ 2-11/1-2012-0001 'National Excellence Program'.

### References

Adamiec, G., Aitken, M. 1998. Dose-rate conversion factors: update. Ancient TL 16 (2), 37–49.

Aitken, M.J. 1998. An Introduction to Optical Dating. Oxford University Press, Oxford, 266 p.

Bailey, R.M., Arnold, L.J., 2006. Statistical modelling of single grain quartz De distributions and an assessment of procedures for estimating burial dose. *Quaternary Science Reviews* 25, 2475–2502. DOI: 10.1016/j.quascirev.2005.09.012

Borsy, Z. 1977. A Duna–Tisza köze homokformái és a homokmozgás szakaszai. *Alföldi tanulmányok* 345, 43–53.

Borsy, Z. 1987. Az Alföld hordalékkúpjainak fejlődéstörténete. *Acta Academiae Paedagogicae Nyiregyháziensis*. 11/H, 5–37.

Fügedi, U., Pocsai, T., Kuti, L., Horváth, I., Vatai, J. 2008. A mészfelhalmozódás földtani okai Közép-Magyarország talajaiban. *Agrokémia és Talajtan* 57 (2), 239–260.

Galbraith, R. F., Roberts, R. G. 2012. Statistical aspects of equivalent dose and error calculation and display in OSL dating: An overview and some recommendations *Quatermary Geochronology* 11, 1–27. DOI: 10.1016/j.quageo.2012.04.020

Galbraith, R.F., Roberts, R.G., Laslett, G.M., Yoshida, H., Olley, J.M., 1999. Optical dating of single and multiple grains of quartz from Jinmium rock shelter, northern Australia: Part I, experimental design and statistical models. *Archaeometry* 41, 339–364. DOI: 10.1111/j.1475-4754.1999.tb00987.x

Jaskó, S., Krolopp, E. 1991. Negyedidőszaki kéregmozgások és folyóvizi üledékfelhalmozódás a Duna-völgyben Paks és Mohács között. Földtani Intézet Évi Jelentése 1989-ről, 65–84.

Jenei, M., Gulyás, S., Sümegi P., Molnár M. 2007. Holocene lacustrine carbonate formation: old ideas in the light of new radiocarbon data from a single site in central Hungary. *Radiocarbon* 49 (2) 1017–1021.

Lóki, J., Hertelendi, E., Borsy, Z. 1994. New dating of blown sand movement in the Nyírség. *Acta Geographica Debrecina* 32, 67–76.

Mauz, B., Bode, T., Mainz, H., Blanchard, W., Hilger, R., Dikau, R., Zöller, L. 2002. The luminescence dating laboratory at the University of Bonn: equipment and procedures. *Ancient TL* 20, 53–61.

Molnár, B., Botz, R. 1996. Geochemistry and stable isotope radio of modern carbonates in natron lakes of the Danube–Tisza interfluve, Hungary. *Acta Geol. Hung.* 39 (2), 153–174.

Molnár, B., Szónoky, M., Kovács, S. 1981. Recens hiperszalin dolomitok diagenetikus és litifikációs folyamatai a Duna–Tisza közén. *Földtani Közlöny* 111, 119–144.

Mucsi, M. 1963. Finomrétegtani vizsgálatok a kiskunsági édesvízi karbonát-képzıdményeken. *Földtani Közlöny* 93 373–86.

Murray, A.S., Wintle, A.G. 2000. Luminescence dating of quartz using an improved single-aliquot regenerative-dose protocol. *Radiation Measurements* 32, 57–73. DOI: 10.1016/s1350-4487(99)00253-x

Pécsi, M. (ed.), 1967. A Dunai Alföld. Akadémiai Kiadó, Budapest.

Pécsi , E., Katona, O., Barta, K., Sipos, Gy., Biró, CS. 2014. Mapping possibilities of freshwater limestone around Lake Kolon with gorund penetrating radar. *Journal of Environmental Geography* 7 (3-4), 13–19. (in this issue)

Prescott, J. R., Hutton, J. T. 1994. Cosmic ray contributions to dose rates for luminescence and ESR dating: large depths and long-term time variations. *Radiation Measurements* 23, 497–500. DOI: 10.1016/1350-4487(94)90086-8

Sipos, Gy., Kiss, T., Nyári, D. 2009. Kormeghatározás optikai lumineszcenciával: homokmozgások vizsgálata a történelmi időkben Csengele területén. In: Kázmér, M. (ed.) Környezettörténet. Az elmúlt 500 év környezeti eseményei történeti és természettudományi források tükrében. Hantken Kiadó, Budapest 409–420.

Sümegi, P., Molnár, M., Jakab, G., Persaits, G., Majkut, P., Páll, D. G., Gulyási, S., Jull, T. A. J, Törcsik, T. 2011. Radiocarbon-dated paleoenvironmental changes on a lake and peat sediment sequence from the Central Great Hungarian Plain (Central Europe) during the last 25,000 years. *Radiocarbon* 53 (1), 85–97.

Sümegi, P., Mucsi, M., Fényes, J., Gulyás, S. 2005. First radiocarbon dates from the freshwater carbonates of the Danube-Tisza interfluve. In: Hum, L., Gulyás, S., Sümegi, P., (eds.) Environmental Historical Studies from the Late Tertiary and Quaternary of Hungary. Szeged,University of Szeged, Department of Geology and Paleontology, 103–18.

Wintle, A., Murray, A. S. 2006. A review of quartz optically stimulated luminescence characteristics and their relevance in single-aliquot regeneration dating protocols. *Radiation Measurements* 41, 369–391. DOI: 10.1016/j.radmeas.2005.11.001